SAND77-0270
Unlimited Release

Analysis, Scale Modeling, and Full Scale Tests of a Truck Spent-Nuclear-Fuel Shipping System in High Velocity Impacts Against a Rigid Barrier

Michael Huerta

Prepared by Sandia Laboratories, Albuquerque, New Mexico 87185 and Livermore, California 94550 for the United States Department of Energy under Contract AT(29-1)-789

Printed April 1978

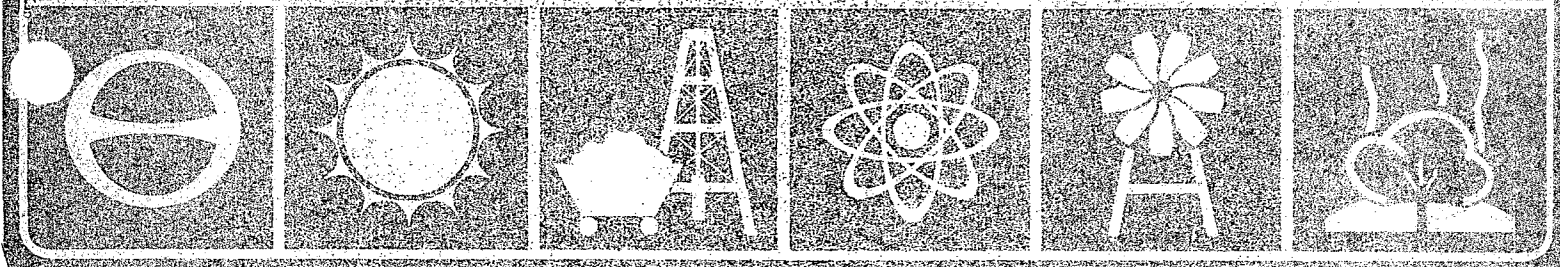

Issued by Sandia Laboratories, operated for the United States Department of Energy by Sandia Corporation.

NOTICE

Printed in the United States of America
Available from
National Technical Information Service
U. S. Department of Commerce
5285 Port Royal Road
Springfield, VA 22161
Price: Printed Copy $~~7.50~~ 9.00, Microfiche $3.00

Org.	Bldg.	Name	Rec'd by *	Org.	Bldg.	Name	Rec'd by *

* Recipient must initial on classified documents.

SAND77-0270

NOVEMBER 1977

Analysis, Scale Modeling, and Full Scale Tests of a Truck Spent-Nuclear-Fuel Shipping System in High Velocity Impacts Against a Rigid Barrier

M. Huerta
Applied Mechanics
Division 1282

ABSTRACT

This report describes analyses conducted to predict the response of a truck tractor-trailer system with a spent-nuclear-fuel shipping cask in very severe (98-135 kilometers per hour) head-on crashes into a rigid concrete structure. The analyses include both mathematical and physical scale modeling of the system. The results of the analyses are compared to the results of instrumented full-scale tests conducted as the last step in the research program described in the report.

ACKNOWLEDGMENTS

Numerous Sandia personnel were involved in the full-scale testing program described in this report. H. R. Yoshimura was the project engineer in charge of the overall program and made numerous contributions to the work described here. D. C. Bickel and R. L. Lucas designed the propulsion system and were responsible for conducting the full-scale tests. D. R. Stenberg provided much assistance in preparing the hardware for the test and in making measurements afterwards. M. E. Barnett and W. V. Hereford were responsible for the instrumentation. T. L. Leighley was responsible for the extensive photometrics provided for the tests. J. E. CdeBaca and W. W. Gravning made valuable contributions in obtaining data from the high-speed films. J. Puhara, G. M. Haines, and C. C. Bates provided valuable assistance in design definition and construction of the scale models. L. M. Ford assisted in designing the instrumentation plan. Zelma E. Beisinger was of great assistance with the finite-element model. T. G. Priddy, W. F. Hartman, J. T. Foley, and L. T. Wilson provided many valuable suggestions and discussions throughout the program.

The author wishes to thank all the individuals, some mentioned above and others, who were of assistance to him in the work described in this report and in the preparation of this document.

SUMMARY

This report describes mathematical and physical scale modeling of a highway spent-nuclear-fuel shipping system involved in a severe transportation accident at two separate velocities. The shipping system analyzed consists of a tractor-trailer system and a lead shielded cask container. Results of the analyses, which predict the response of the transportation system and cask to head-on crashes into a very rigid concrete target, are compared to the results of instrumented full-scale tests conducted as part of the program.

The mathematical analyses are accomplished in two steps. First, the overall system is modeled using a lumped-parameter computer program. This first step provides information regarding the response of the vehicle and the rigid body motion of the cask in the impact. A second step utilizes a finite element computer program to calculate the detailed deformation response of the cask. These analyses were done for system impact velocities of 97 and 129 kph (60 and 80 mph).

The lumped-parameter model indicated that the vehicular system would be completely destroyed at both velocities. At the lower velocity it predicted that the mitigating structures would prevent the cask from undergoing any deformation to its basic body structure. At the higher velocity, the lumped-parameter model predicted that the cask would impact the target sufficiently hard to undergo some deformation. This information was used as input to the

finite-element model, the second step in the mathematical analysis. The finite-element model predicted slight mushrooming of the cask body, but containment of the fuel.

A second phase in the accident analysis included scale modeling of the transport system. One-eighth scale models of the tractor, trailer, and cask were constructed. These were impact tested into scaled concrete targets at two different velocities. Results of these tests agreed well with the mathematical analyses. In both tests, the vehicular system was severely damaged. In the first low velocity test, the cask did not sustain any measurable deformations. In the second test, the impact end of the cask model was deformed much as was predicted by the mathematical finite-element analysis.

The last step in this study involved full-scale tests. Used but representative vehicular systems and a lead shielded cask were utilized. Two separate tests were conducted at velocities of 98 and 135 kph (61 and 84 mph). The results of the full-scale tests agreed well with the analyses. The vehicular systems were completely destroyed in each test. After the first test, the basic body structure of the cask was completely undeformed and the same cask was used in the second test. Damage to the cask in the second test agreed very well with results predicted by the mathematical analyses and the scale models. The impact end of the cask was slightly expanded. At its worst point, the diametral expansion was 3%. The cask very capably maintained its containment ability.

The full-scale tests provided much data regarding the response of a shipping cask in an accident environment. A number of conclusions have been drawn based on the findings of this study. These are included in the final section of the report.

CONTENTS

Contents (cont'd)

ILLUSTRATIONS

FIGURE

Illustrations (cont'd)

FIGURE

Illustrations (cont'd)

FIGURE

1.0 Introduction

The transportation phase of the nuclear fuel cycle requires that irradiated fuel elements (spent-nuclear-fuel) be shipped from a reactor site to a reprocessing plant or to permanent storage. This material is shipped in very massive radiation-shielded containers usually termed shipping casks. Casks are shipped either on a railroad car or a truck tractor-trailer system. Sandia Laboratories is currently involved in a full-scale testing program where, as a final step, casks together with their transport system are being tested to determine their ability to withstand extremely severe accident conditions.

This report describes the analysis and results of crash tests involving a cask and its truck transport system. These tests were conducted by Sandia Laboratories for the Environmental Control Technology Division of the U. S. Department of Energy. The two tests described in this report represent the first phase of the broader series. A description of the overall test program and its purposes can be found in Reference [1]*.

In the tests reported here, used truck tractor-trailer systems were impacted head-on into a very rigid and massive concrete target at respective velocities of 98 and 135 kph** (61 and 84 mph). Nearly identical transport systems

---

* Numbers in brackets indicate references at the end of the text.

** This abbreviation will be used to indicate kilometers per hour

carrying the same 20,500 kg (45,000 lb) cask were used. A schematic of this lead shielded cask container is shown in Figure 1.1.

In the tests described here, the cask was water filled and carried unirradiated fuel elements. It was mounted head forward on its normal shipping trailer, using the original tiedown system. The cask was equipped with conventional type balsa wood impact limiters on both ends. The tests were conducted on January 18 and March 16, 1977.

The overall program for the tests included an analysis effort aimed at predicting the response of the full-scale system and, in particular, the damage to the shipping cask. The analysis included independent mathematical and scale modeling of the full-scale test. The results of the analysis, including both mathematical and scale modeling, were first reported in [2] and [3]. The present report brings together in a concise, comprehensive manner, a description of the mathematical analysis, scale modeling, and results of the full-scale tests.

The mathematical analyses were accomplished with the use of two pre-existing computer programs. The first of these was used to analyze the overall system response with a lumped parameter model. A second step in the numerical analysis utilized a dynamic finite element model of the shipping cask. This model provided detailed information of the structural response of the cask, including possible permanent deformations and slump of the lead shielding material. Section 2 includes a description of the mathematical

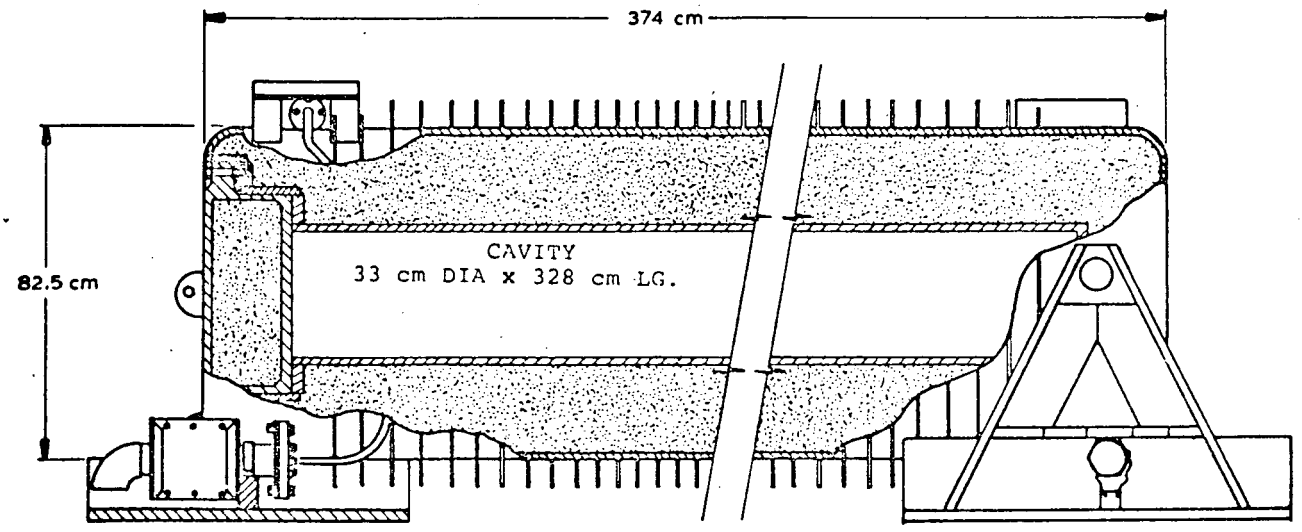

Figure 1.1 Schematic of the lead shielded cask used in the full-scale tests.

(numerical) work performed prior to conducting the full-scale tests as well as the results of the work.

A second phase in the analysis utilized scale modeling. Scale models of the system including the cask, trailer, and tractor structures were built and impact tested against model concrete targets. These experiments provided much information regarding the expected behavior of the full scale system and confirmed the mathematical analysis. The scale modeling work is described in detail in Section 3.

The full-scale tests were performed after the mathematical analysis and scale modeling were complete. For purposes of data acquisition, each of the full-scale tests had extensive high speed photocoverage as well as onboard instrumentation operating through a telemetry package bolted to the cask. A large amount of data were gathered in each case and used as a basis for comparing the pretest predictions with the actual response of the full-scale system.

Section 4 of this report describes the full-scale test procedure and results. Section 5 compares the pretest analysis predictions with results from the full-scale tests. Conclusions and recommendations based on observations made through this phase of the full-scale testing program are included in Section 6.

2.0 Mathematical Analysis

2.1 Introduction

Detailed mathematical analyses were performed prior to conducting the full-scale tests. These analyses were designed to predict the response of the full-scale system and in particular, of the shipping cask at system impact velocities of 97 and 129 kph (60 and 80 mph).

The mathematical analysis was accomplished in two steps. First, the entire transport system, including the vehicle and the cask, was analyzed using a lumped-parameter model. This model provided information regarding the behavior of the vehicular system. Also, using a lumped-parameter model and treating the cask as a rigid body, output from this model was used to determine the impact velocity input to a detailed dynamic finite element model of the container. This section describes both of these techniques and results of their application.

2.2 Lumped-Parameter Model

In the lumped-parameter model, the transport system was discretized into masses and couplings. The model was one-dimensional; therefore, each mass had one degree of translational freedom. The coupling definitions were based on structural analysis estimates of their load-displacement behavior. Once the model was constructed, the SHOCK [4] computer program was used to solve the system of equations associated with it. The displacement-time and velocity-time

histories computed for the mass elements provided estimates of the deformation and dynamic response of the full-scale system, including the rigid body dynamics of the cask.

The applicability of a one-dimensional model was determined by preliminary calculations based on the rotational moment of inertia of the cask and trailer and on the calculated strengths of the trailer and tiedown structures. These basic calculations indicated that no appreciable rotation of the system would occur as the vehicle system crushed during the impact. Hence, a one-dimensional model was judged to be appropriate.

Figure 2.1 is a schematic of the lumped parameter model which was formulated for this study. In this model, the system (including the target) was modeled with eight discrete masses and ten couplings. Mass 1 (the target) was held fixed and the remaining masses were given initial velocities equal to the impact velocity. In figure 2.1, coupling 3-4 represents the tractor-trailer fifth wheel connection. Couplings 5-6 and 6-7 simulate the cask tiedowns. Couplings 1-4 and 1-6 represent the interactions between the front end of the trailer and the target and the cask and the target. These were given appropriate amounts of displacement without loading. Coupling 1-6 included the effects of the impact limiter on the front end of the container. The remainder of the couplings represent frame elements.

In the model, extensive use was made of the hysteresis option available in the SHOCK program. This option was used to simulate large deformation plastic behavior. In this type of coupling, loading and unloading curves follow different paths simulating crush up and permanent deformation of a

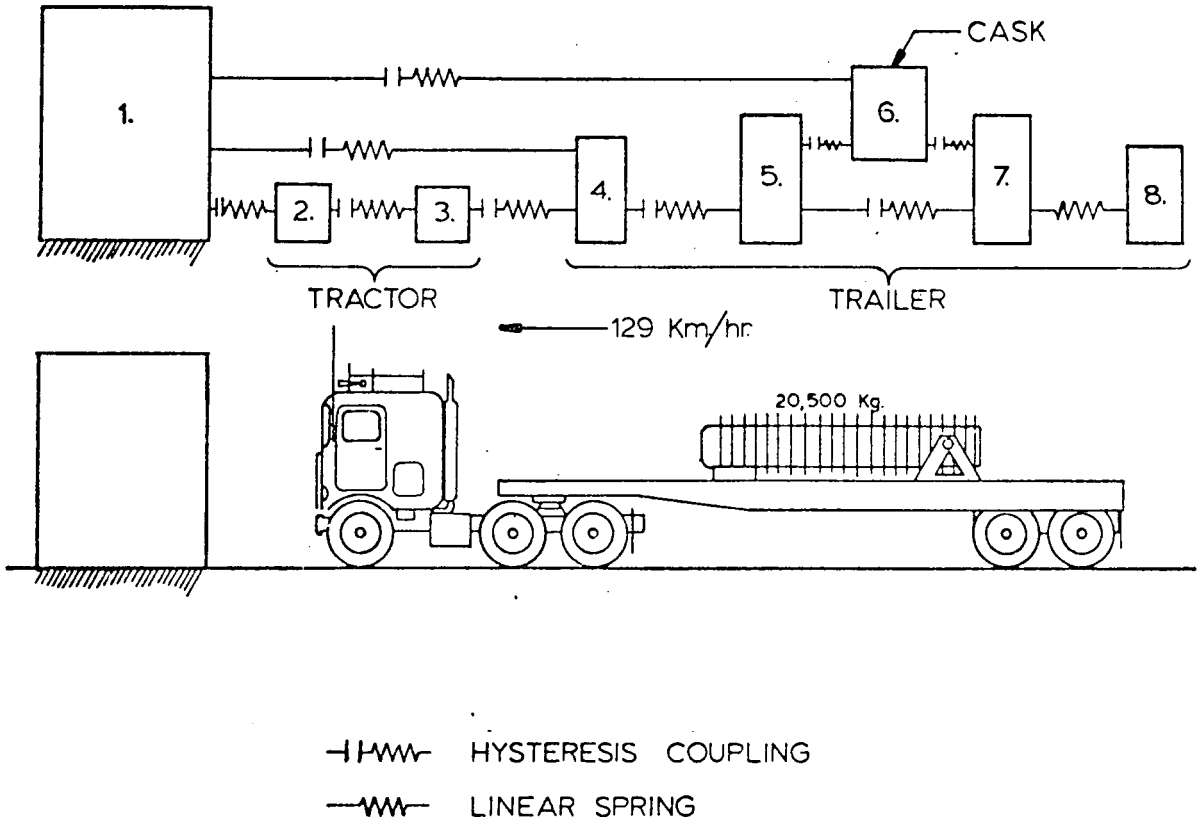

Figure 2.1 Schematic illustration of the lumped parameter model.

structure. Appendix A includes additional details of the lumped-parameter model.

Computer runs with this model at impact velocities of both 97 and 129 kph indicated that the tractor frame and cab would be completely crushed. Calculations also indicated that the front end of the trailer would plow through the cab, breaking the fifth wheel connection and crushing substantially. Regarding the dynamics of the cask, the SHOCK model indicated that it would impact the wall with a relatively high velocity directly related to the behavior of the tiedown system.

Because of uncertainties which exist in hardware (which are much greater in old, used equipment), parameters in the model described above were varied to obtain information regarding a possible range of system response. In particular, the strength of the cask tiedown system was varied. Results of the parametric study provided definitions of "favorable" and "unfavorable" cask responses. In the unfavorable case, the container broke free from the trailer structure very early in the impact with only a small reduction in velocity. In this case, calculations indicated that the container would impact the wall at a relatively high velocity and that the velocity change at target impact would be large and rapid. In the favorable case, the container remained attached to the trailer and continuously slowed as the front end of the trailer crushed. In this case, the container would impact the wall at a lower velocity.

Figure 2.2 illustrates the calculated displacement-time histories for the cask in the two extreme cases for the slower, 97 kph, impact. The condition where the tiedowns

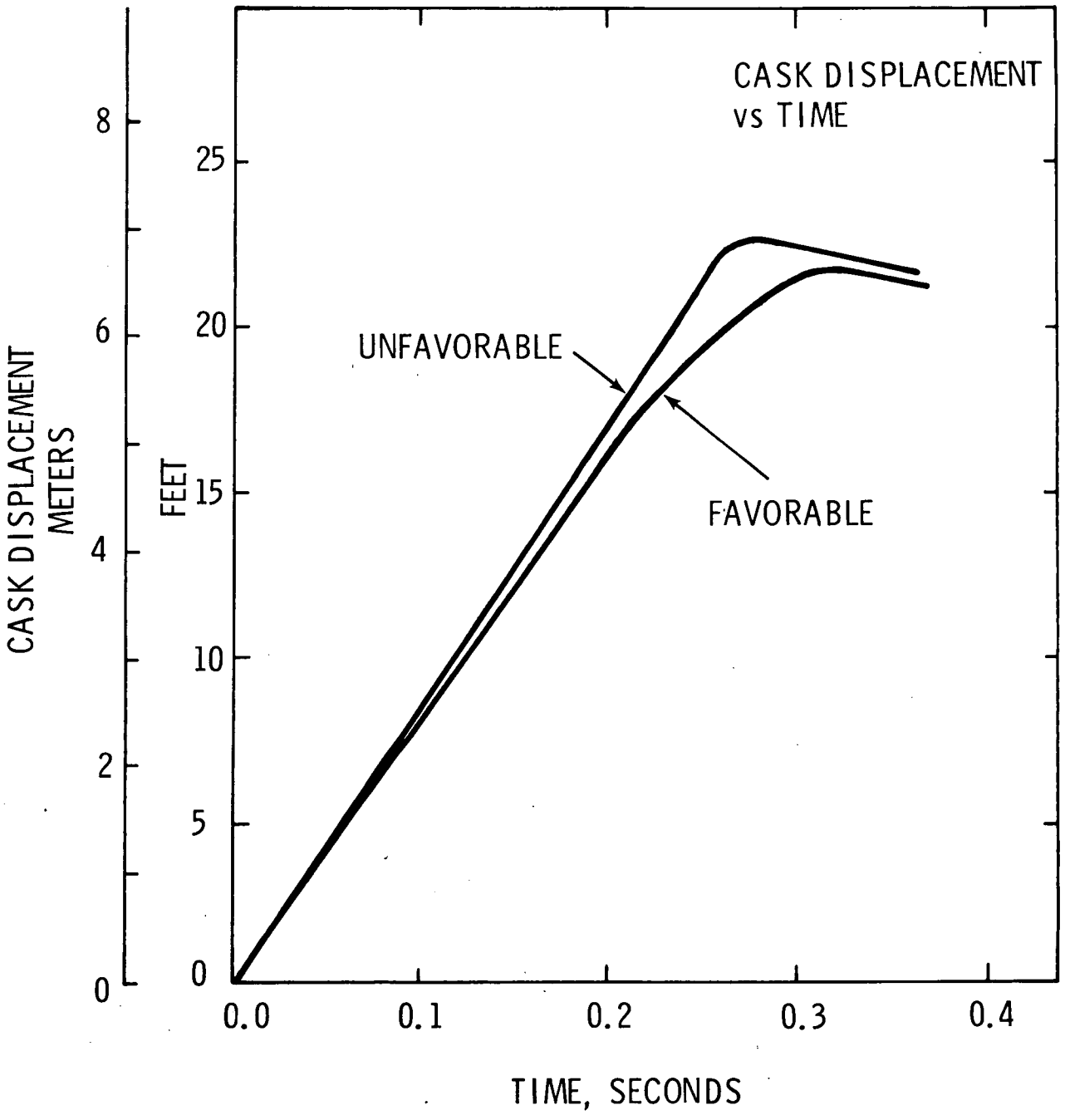

Figure 2.2 Calculated cask displacement as a function of time for a 97 kph impact.

fail produces a quicker impact of the cask into the wall and completely crushes the impact limiter. In the more favorable case it was calculated that the impact limiter would not crush completely, resulting in much smaller forces being transmitted to the cask. As can be seen from the figure, it was calculated that the container would bottom out against the target in about 0.3 second.

Figure 2.3 illustrates the velocity-time histories calculated for the cask in the two cases. As can be seen, when the tiedowns break early, it was calculated the cask would impact the wall with only a small reduction in velocity. The impact limiter in this case would be crushed completely, mitigating the impact somewhat. (The impact into target point is defined as that configuration where the impact limiter begins to crush.) The point at which the limiter crushes completely can be distinguished by the definite change in slope which occurs after this point. After bottoming the limiter, the cask would still have a velocity of about 75 kph (47 mph).

In the favorable condition, where the cask did not leave the trailer structure completely, a large amount of energy would go into deforming the trailer structure. The cask velocity would be greatly reduced by the time that it reached the wall. The model then indicated that the cask would not have enough velocity left to bottom out the limiter, and it would undergo a much milder shock. Such an impact would not result in forces sufficiently large to deform the cask.

The analysis of the full-scale test, conducted at 129 kph, was accomplished with essentially the same model. In order to reflect better the hardware available for this test,

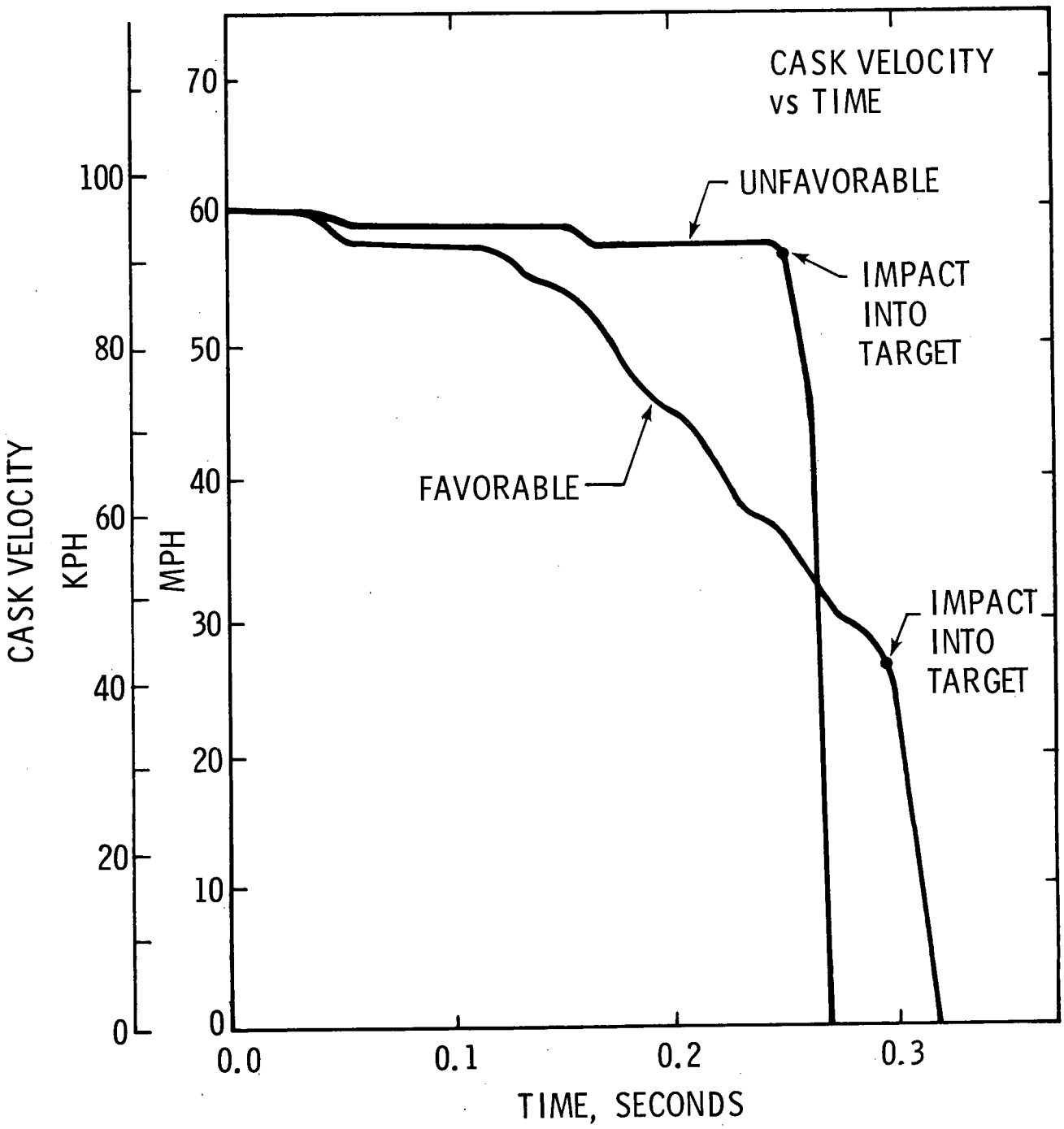

Figure 2.3 Calculated cask velocity as a function of time for a 97 kph impact.

coupling 1-6 was modified to more accurately model the distance between the front end of the cask and the wall. Figure 2.4 illustrates the displacements calculated for the higher impact velocity. As can be seen, the curve is quite linear to the point at which the cask bottoms against the wall. It was calculated that this event would occur in 0.2 second, and that the limiter would be completely crushed in each case. Figure 2.5 illustrates the velocity-time history calculated for the cask. Again a favorable and unfavorable case is depicted. In the worst case, it was calculated that the impact limiter would be completely compacted at 109 kph (68 mph). Under the most favorable conditions, it was calculated that this would occur at 84 kph (52 mph). The time required for the total horizontal velocity to be dissipated was calculated to be 0.2 seconds. For both the favorable and unfavorable cases it was calculated that the cask impact would be very severe and would completely crush the limiter, with the cask still maintaining a relatively high velocity.

The lumped-parameter model calculations for both velocities predicted cask deceleration levels during crush up of the structure, prior to the cask solidly hitting the wall, of less than 20 g's. This was used as a basis for determining whether the head bolts, which keep the cask cover in place, would be adequate to prevent the cover from being dislodged during crush up of the structure. Since the head was mounted towards the front of the truck, inertial loads from the head itself, fuel elements, impact limiter, and coolant water would act to stress the headbolts in tension. The closure system was carefully investigated and found to be adequate. Appendix C includes details of this calculation.

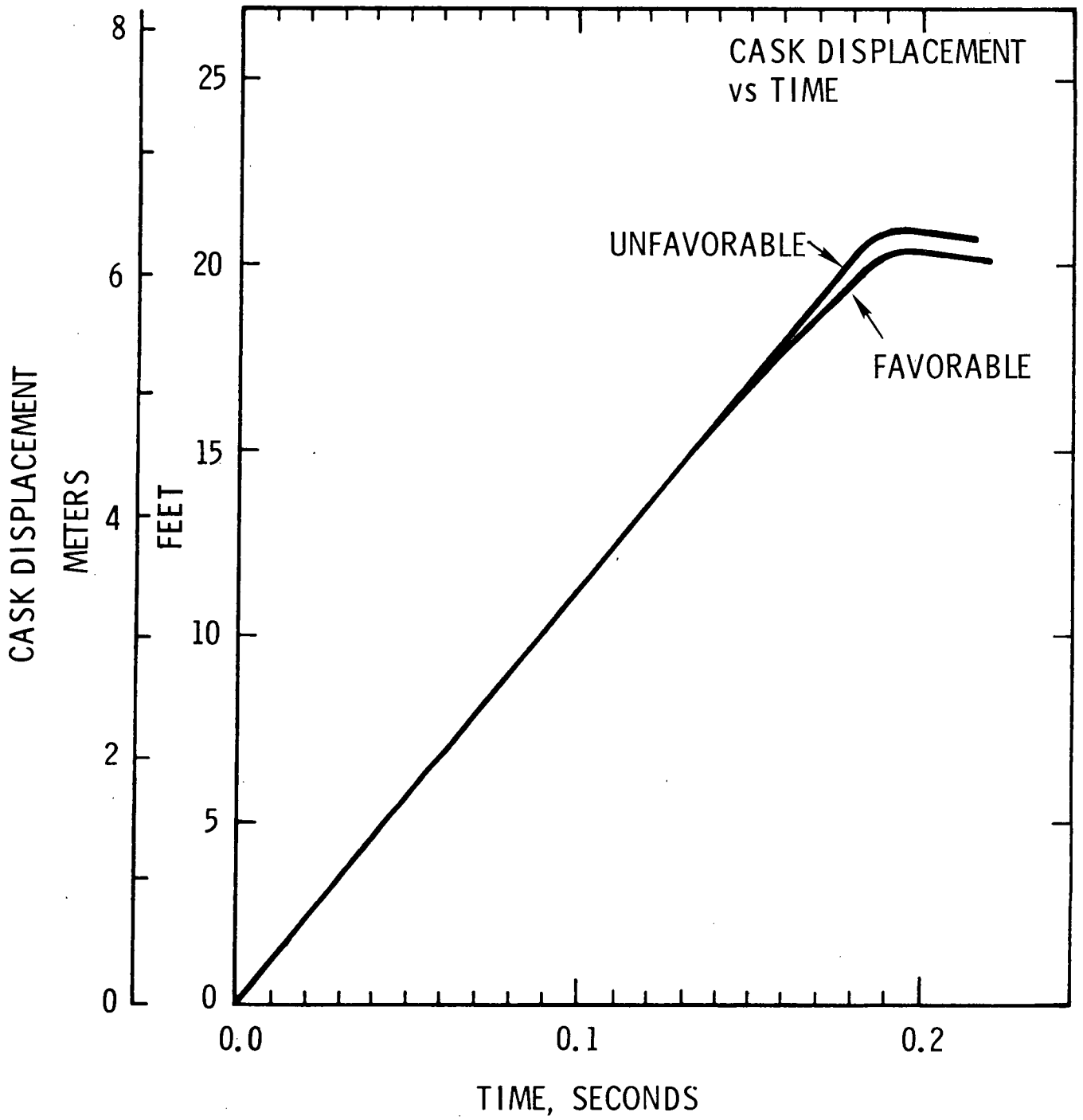

Figure 2.4 Calculated cask displacement as a function of time for a 129 kph impact.

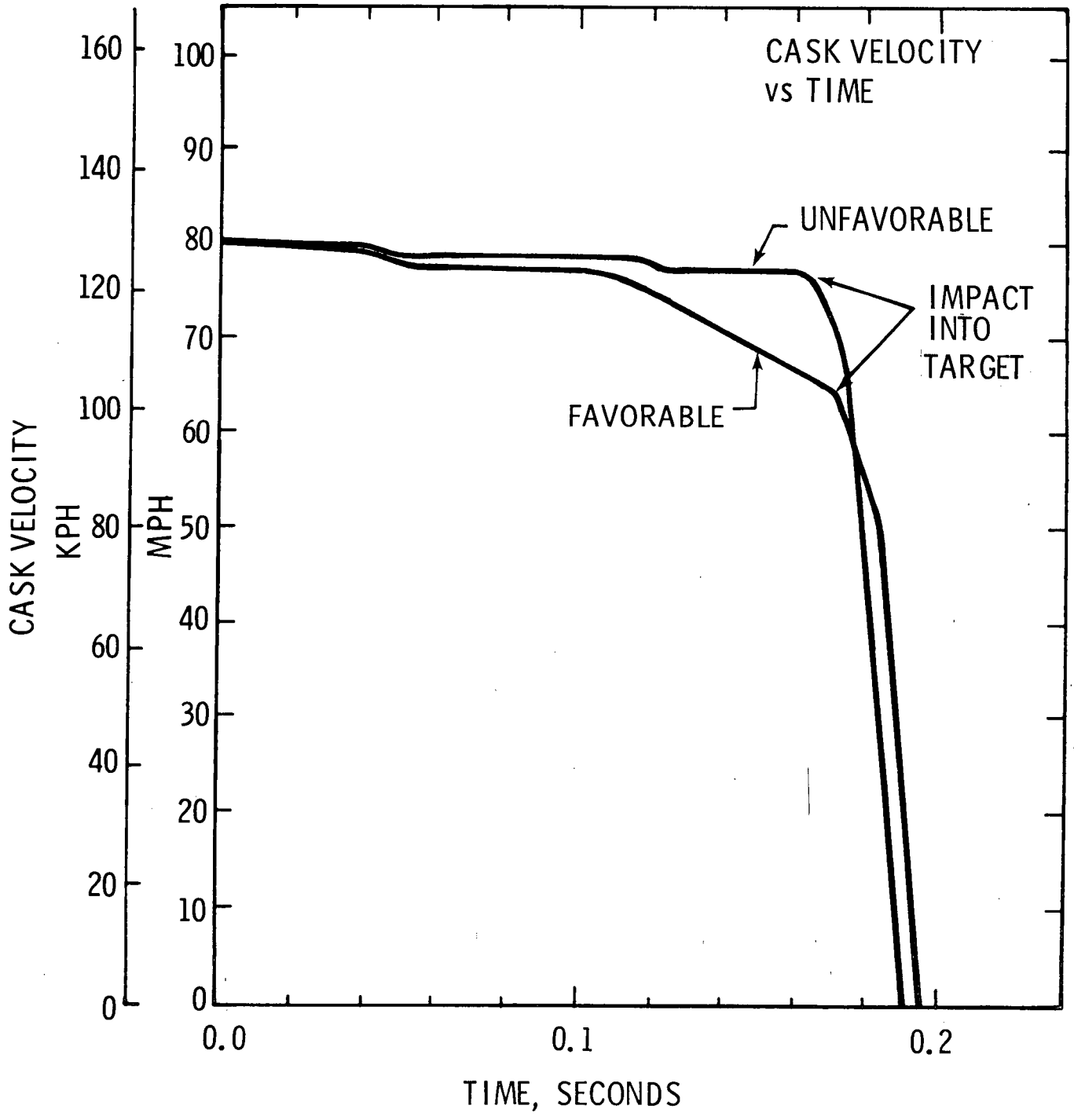

Figure 2.5 Calculated cask velocity as a function of time for a 129 kph impact.

The results described above indicated that the cask could be expected to impact the wall, with rubble from the cab in between, at a substantial velocity. In cases where calculations indicated that the impact limiter would be completely crushed, the cask would encounter a solid constraint and possibly deform. The extent and nature of the deformation was numerically investigated in detail by means of a dynamic finite element computer program.

2.3 Finite Element Model

The dymamic finite element model was designed to provide detailed information regarding the possible response of the shipping cask in an end-on axial impact. The HONDO [5] computer program was used with this model. Appendix B includes some details of the model, including material properties used.

Figure 2.6 illutrates the axisymmetric mesh for the cask. As can be seen, the mesh was made progressively finer towards the impact end, on the left, where the greatest deformation was expected. With this model, the body is given an initial velocity into a rigid plane which prevents node penetration. This effectively simulates an impact into an unyielding surface at the velocity input to the model.

The cask shells and the lead shielding material were modeled separately with a sliding interface between them. A frictionless condition was assumed at the interface. The stiffening effect of the cooling fins was neglected. Figure 2.6 shows an expanded view of the impact end. Here the steel and the lead shielding material can be very clearly distinguished.

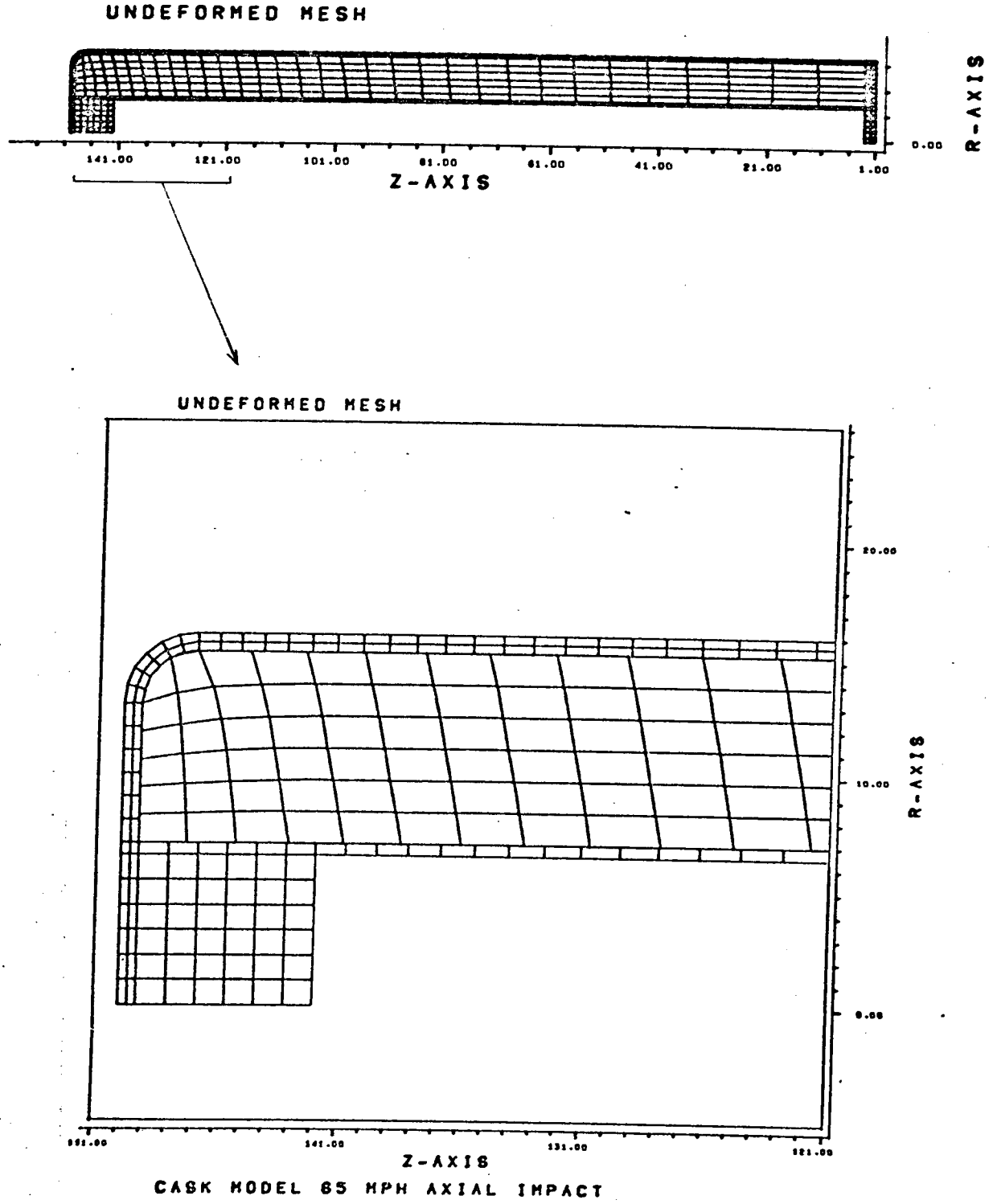

Figure 2.6 Illustration of the cask mesh for the dynamic finite element model.

Calculations with the finite element model were made for various impact velocities. For the full-scale truck, a 105 kph (65 mph) impact into an unyielding surface was considered to be a probable worst case, although calculations were also made for higher velocities. The calculated deformation results for this velocity are depicted in Figure 2.7. As can be seen, it was calculated that some bulging and hoop strains would occur on the impact end. The maximum hoop strain was calculated to be 9%. It was calculated that the cask body would be shortened by 2%, and that changes to the internal cavity dimensions would be extremely slight. Simulated computer runs at velocities up to 129 kph (80 mph) did not produce significantly different results.

2.4 Discussion

As has been described, a possible range of system response was calculated with the lumped parameter model. The inability to predict a single result was principally due to uncertainties in the used, out of service, equipment available for the full-scale tests. The model response was most sensitive to the strength of the cask tiedown system. Tiedowns which were given a strength greater than the crush strength of the trailer structure allowed the cask to remain with the vehicle, and take advantage of the vehicle's energy absorption potential. Tiedowns which were made weaker and broke loose when the front end of the trailer encountered a solid obstacle allowed the cask to come loose and impact at a higher velocity.

It is interesting to note that the possible range of cask response is broader as the transport system impact

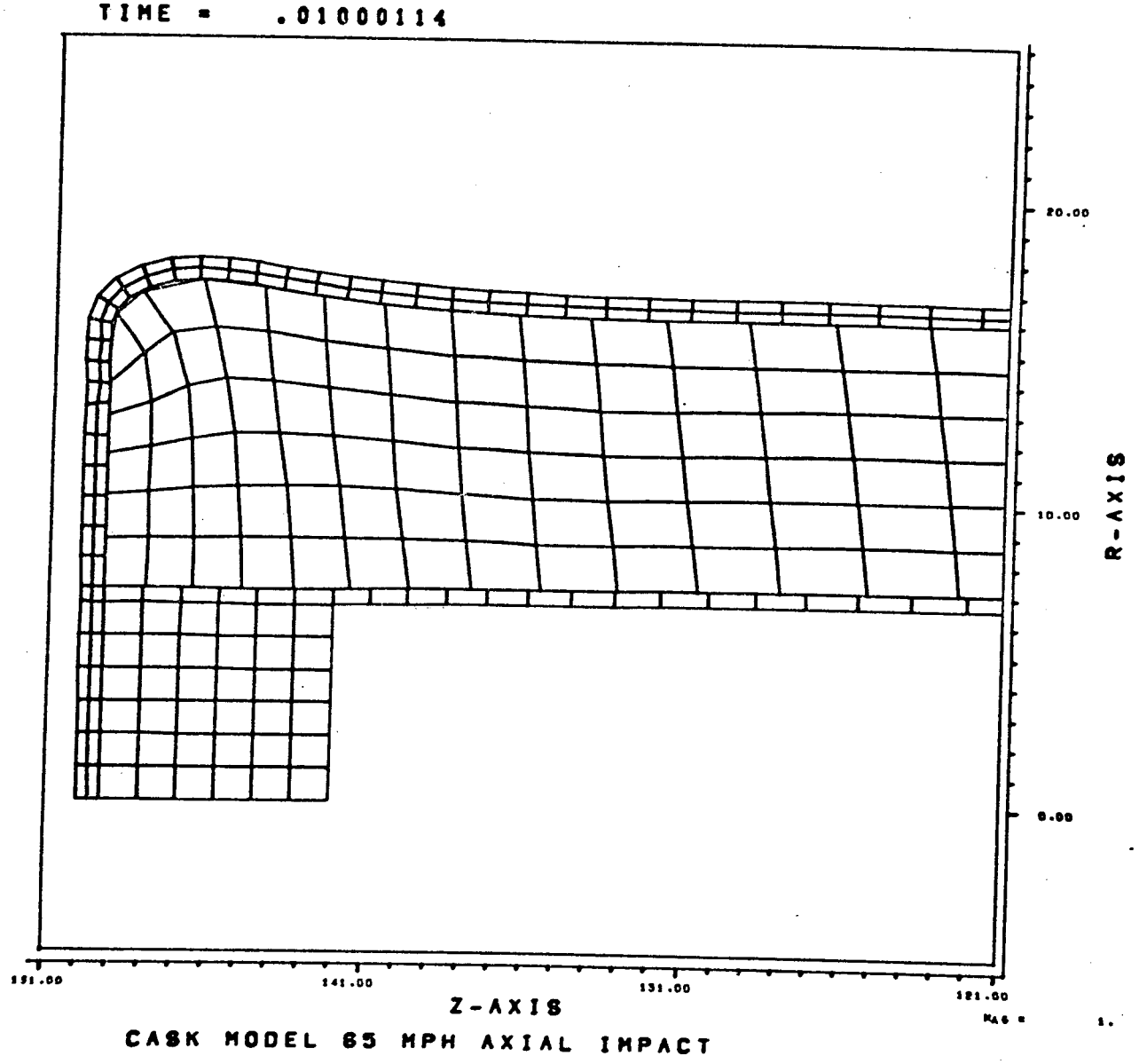

Figure 2.7 Deformed finite-element mesh for the cask.

velocity decreases. This can be seen by comparing Figures 2.3 and 2.5. At the higher velocity, the two velocity-time curves are closer together. This is due to the fact that the energy absorption capability of the trailer structure becomes less significant, as it remains constant, while the kinetic energy increases as the square of the velocity. This behavior has the effect of increasing the accuracy of the model as the test impact velocity increases.

With the system impact velocities considered, the highest possible cask impact velocity into the wall (after crushing the limiter) was calculated to be about 105 kph (65 mph) as is indicated in Figure 2.5. At this point, it is assumed that all material between the cask and the target had been completely crushed and the cask would encounter a stiff target. The response of the cask from this point on is calculated with the HONDO finite element model, which computes the deformations which will occur.

The results of the HONDO calculations are considered to be conservative for several reasons. First, the unyielding surface of the HONDO model is stiffer and absorbs less energy than the real target. Secondly, the hoop stiffening effects of the cooling fins were not included in the finite element model. Finally, it was assumed that there was no interface friction between the lead and the steel. These three factors tend to increase the calculated deformations to the cask body and lead motion within the steel shells. Therefore, these results were considered to be conservative in terms of cask deformations.

As has been mentioned, calculations indicated that the head bolts were sufficiently strong to prevent dislodgment of

the head during crush up of the vehicular structure. It should be pointed out that the cask undergoes higher decelerations when it reaches the target. However, in the final impact, the head is lodged between the cask body and the target. There is no mechanism for failing the head bolts or dislodging the head in this impact geometry. The cask head was therefore predicted to remain in place.

The analysis indicated that, even under the unfavorable impact conditions that might occur in a 129 kph (80 mph) impact, the cask would be only slightly deformed on the impact end and would not be breached. The calculated hoop strains of the outer shell were judged to be capable of initiating a crack in the outer shell if flaws were present. However, it was not anticipated that an external fracture would threaten containment of the fuel, but it was expected that the impact, in either case, might damage the head gasket leading to some slight seepage of cooling fluid.

In summary, the mathematical analysis indicated that in a 129 kph impact the cask would hit the target in an end-on condition causing some bulging of the impact end of the cask but not threatening its containment ability. Calculations also indicated that the inner cavity dimensions would change very slightly. In addition, the duration of the impacts was calculated to be 0.3 and 0.2 seconds respectively for the two impact velocities.

3.0 Scale Models

3.1 Introduction

Scale models of the full-scale system were built and tested to confirm and complement the mathematical analysis. Using a scale factor of 8 (linear dimensions 1/8 as large as the prototype full-scale system), models of the cask and vehicular system were designed and fabricated. The system scale models were tested at a sled track by impacting them into scaled concrete targets. Extra cask models were constructed for tests not involving the vehicular structure. These were tested by impacting them with a massive steel ram at a pneumatic actuator facility at velocities up to 129 kph (80 mph). High speed films were obtained from each test and analyzed to study the response of the models closely. This section describes the scale models and test results. First, some background information regarding scale modeling of a structural impact problem will be reviewed.

3.2 Modeling Theory

Scale modeling has previously been used to model structural impact problems [7,8]. In both of these referenced studies, a dimensional analysis of simple structures subjected to impacts severe enough to cause large plastic deformations was made. The targets in each case were essentially unyielding surfaces. In these studies, a number of pertinent parameters were identified and arranged into dimensionless groups called Pi terms. (Techniques for doing

this are described in References 9, 10, & 11.) In [7,8] it was assumed that the model and prototype were constructed of similar materials. The results indicated that, if material strain rate and gravity effects were insignificant, the Pi terms of an exact model could be kept equal to those of the prototype. This indicates that the response of the model system would be similar to the prototype and it was deduced that scale model test results could be directly related to the prototype. Both studies included experimental work, utilizing exact replica models, for verification of the analysis. In both cases, agreement between model and prototype was found to be excellent.

The pertinent parameters and the dimensional analyses of [7,8] are applicable to the problem of modeling the full-scale tests of this report. The structures in the current problem, however, are considerably more complicated and the additional assumption that a somewhat simplified structure will give valid results must be made. Substitution of an approximate (simplified) model, as opposed to an exact geometrical model, is often done due to practical considerations. Such a model is usually termed an "adequate" model [10]. The models of this study, described later, were designed according to this concept. For completeness, the relationships between the model and prototype will first be reviewed, following closely the results of [7].

Letting n be the scale factor (n = 8, in this case) and the subscripts m and p denote model and prototype, the following relationships exist when the impact velocities are equal for the model and prototype:

Deflection	$y_m = y_p/n$
Stress or Pressure	$s_m = s_p$
Force	$f_m = f_p/n^2$
Energy	$e_m = e_p/n^3$
Mass	$m = m_p/n^3$
Time	$t_m = t_p/n$
Acceleration	$a_m = na_p$

In particular, it can be seen that deformations (deflection) in the model and prototype are similar. From the time relation, it can be seen that events in the model occur faster by the scale factor. Thus accelerations in the model are higher by the scale factor.

As mentioned above, gravity effects have to be assumed to be insignificant. For complete similitude, the gravity field of the model has to be greater by the scale factor. This means that in a scale model test, where the gravity field cannot be altered, vertical motions will be exaggerated. The assumption that gravity effects can be neglected is valid in a horizontal impact where only insignificant vertical forces are generated. The principal impact will scale correctly and the dynamic behavior and deformations of the model structure will simulate the prototype according to the above relationships. However, the

rebound phase and the later time trajectories of fragments and separated components will not scale correctly.

The assumption that material strain rate effects can be neglected is considered quite valid [12]. This is in view of the relatively low difference in strain rates between model and prototype. In this case, the model structure will see strain rates which are higher by the scale factor, 8. It is generally agreed that strain rate effects may become significant only when they differ by several orders of magnitude.

3.3 Model Description

The scale model designed for this study included structural models of the tractor, trailer, impact limiter, cask, and the tiedown system. It was designed to run on a rail at a sled track. The model was pushed up to speed by a small rocket powered sled and allowed to coast into a scaled concrete target. Figure 3.1 is a photograph of the model and pusher system at the sled track. Construction details for the model are included in Appendix D.

The tractor and trailer structures were constructed from flat sheet metal formed into channel shapes and welded in place. They were designed to simulate the mass and stiffness of the full-scale prototype. The kingpin connection was simulated with a 1/4" steel pin. Because of the necessity of testing the model on a track, axle and wheel masses were simulated with shoes conforming to the shape of the rail, clearly visible in Figure 3.1. The flanges on the rail were removed from a section directly in front of the target to allow free vertical motion of the model at this point.

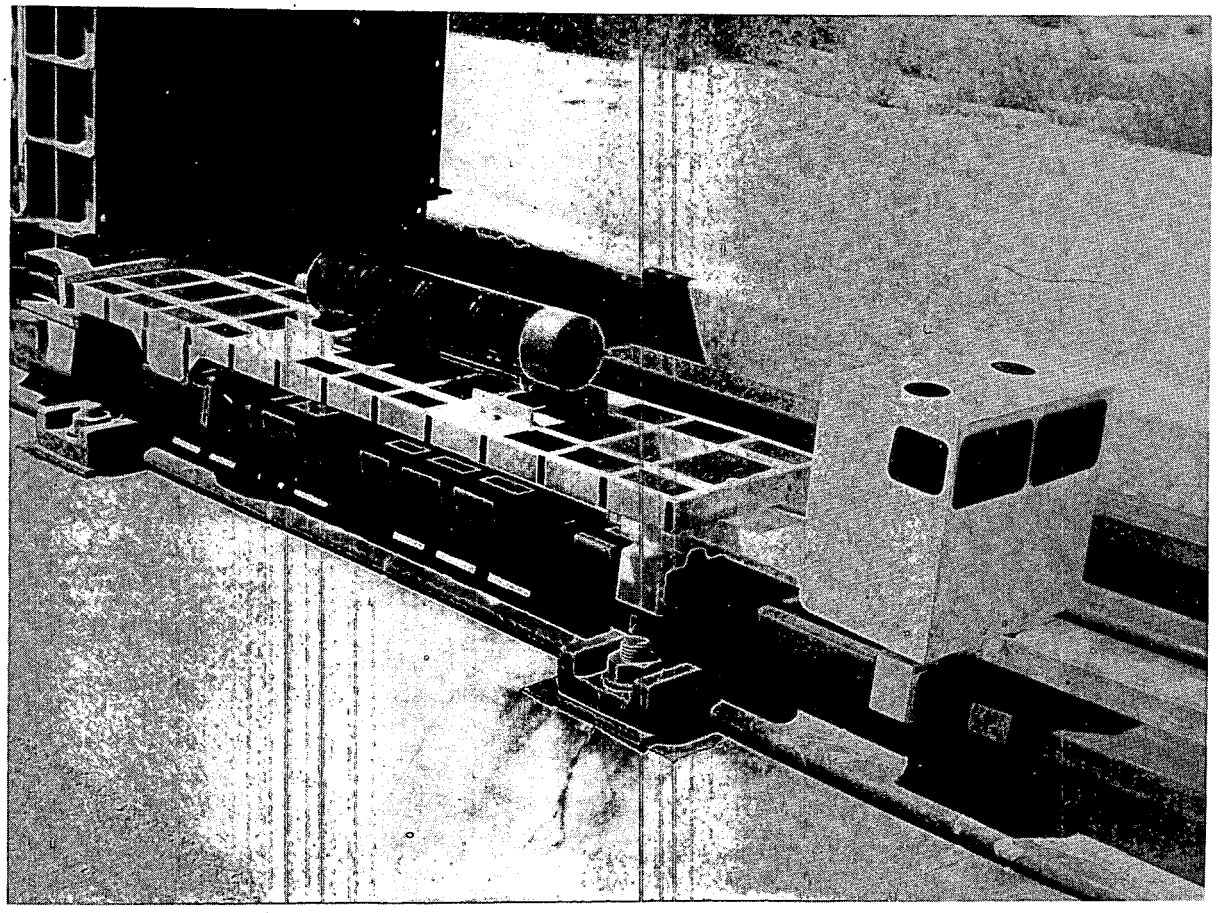

Figure 3.1 Scale model of the transport system.

The model impact limiter was constructed out of balsa wood encased in a sheet metal band spot welded at the joint. It was attached with adhesive to the front end of the cask. The cask model itself was quite detailed. The head and closure system were simulated very closely using scaled down bolts. The shells were made out of 304 stainless steel with chemical grade lead cast into the annular region. The model casks were always water-filled for testing. The cask tiedown system was modeled by scaling down the bolting stress areas and approximating the geometry with small steel plates, as can be seen in Figure 3.1

The models were believed to be structurally adequate since the cask and tiedown system were modeled in detail. Also, the major structural elements in the vehicle which could transmit forces to the components were carefully modeled. Since most of the prototype vehicle detail is essentially non-structural, its omission does not affect the dynamic response of the cask.

3.4 Model Tests and Results

Two transport system scale tests were conducted with resulting impact velocities of 98 and 123 kph (61 and 76 mph). Both tests were extensively covered with high speed photography, which allowed close observation of the response of the models. The dynamics of the model cask through the impact were closely analyzed by examining the films. Damage to the vehicular system and the cask models was also carefully examined.

The first test was intended to simulate a 97 kph (60 mph) impact. This test resulted in no damage to the cask.

After this test, it was decided to simulate the unfavorable response condition with a 127 kph (80 mph) impact. For this test, it was decided to use weaker bolts in the tiedown system to precipitate an early failure resulting in the more severe impact which the cask might experience. The impact velocity achieved in the test was 123 kph (76 mph). The tiedown system failed early as anticipated allowing the cask to go into the target at a very slight reduction in velocity. The cask sustained very minimal damage in this worst expected condition. Test results are described in more detail below.

Figures 3.2 and 3.3 illustrate the sequence of events in the first model test. In this test, the tractor model crushed completely at impact with the concrete. The pin connection between the tractor and trailer failed early in the impact allowing the front end of the trailer structure to crush the cab and solidly impact the target. At this time, the front end of the trailer crushed partially and buckled upwards along the face of the target. The cask model remained nearly horizontal moving forward through the cab structure and solidly impacted the target in nearly an end-on condition, partially crushing the impact limiter. Subsequent to the last frame in Figure 3.3, the container rotated somewhat with the rear portion moving upward.

Figure 3.4 shows the resultant damage to the model. As can be seen, the tractor was completely crushed and remained in front of the target. The front end of the trailer structure crushed partially and then buckled upwards coming between the cask and the target. The impact limiter crushed partially and came to rest behind the buckled up portion

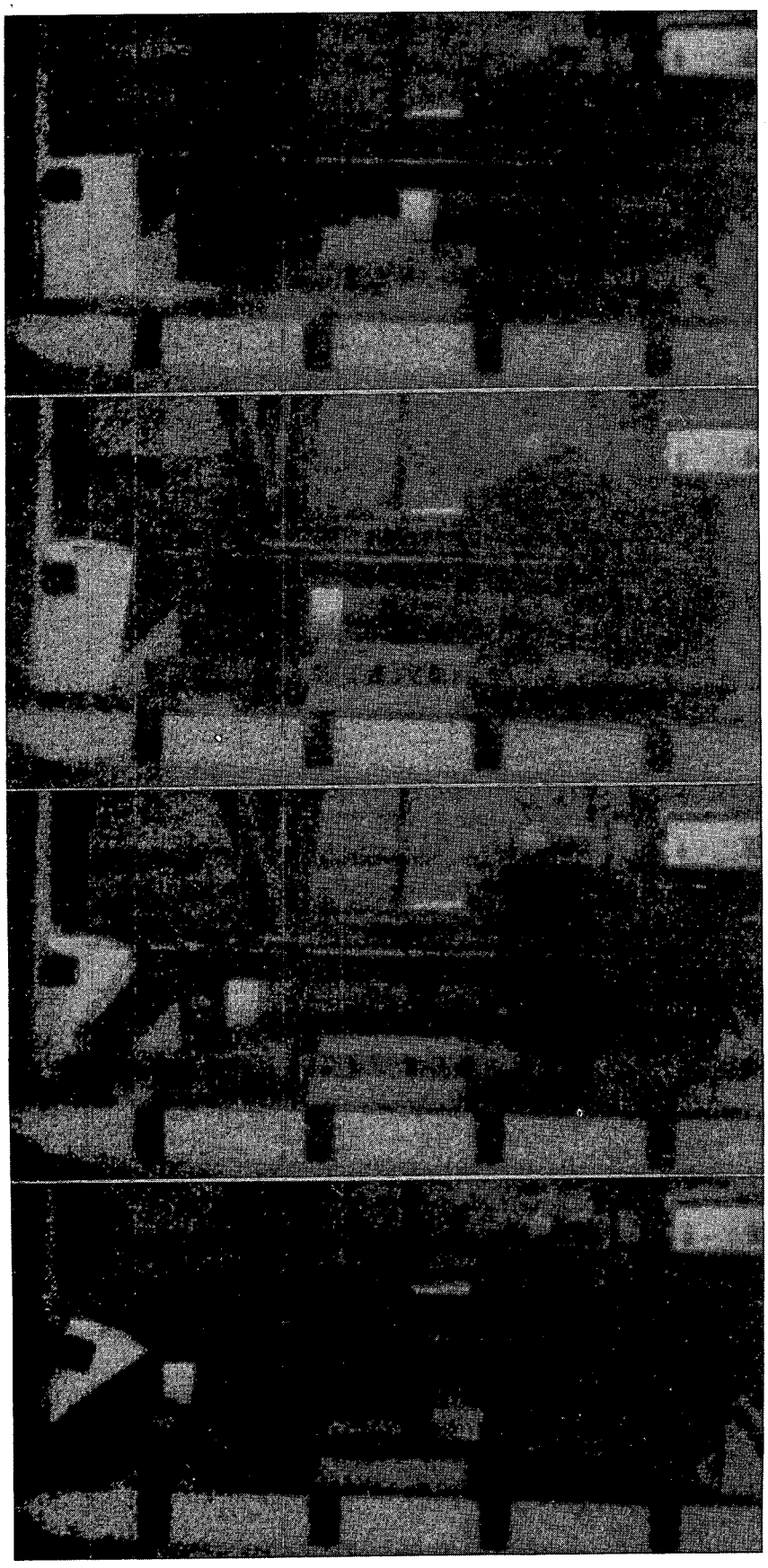

Figure 3.2 Early sequence of events in a scale model test.

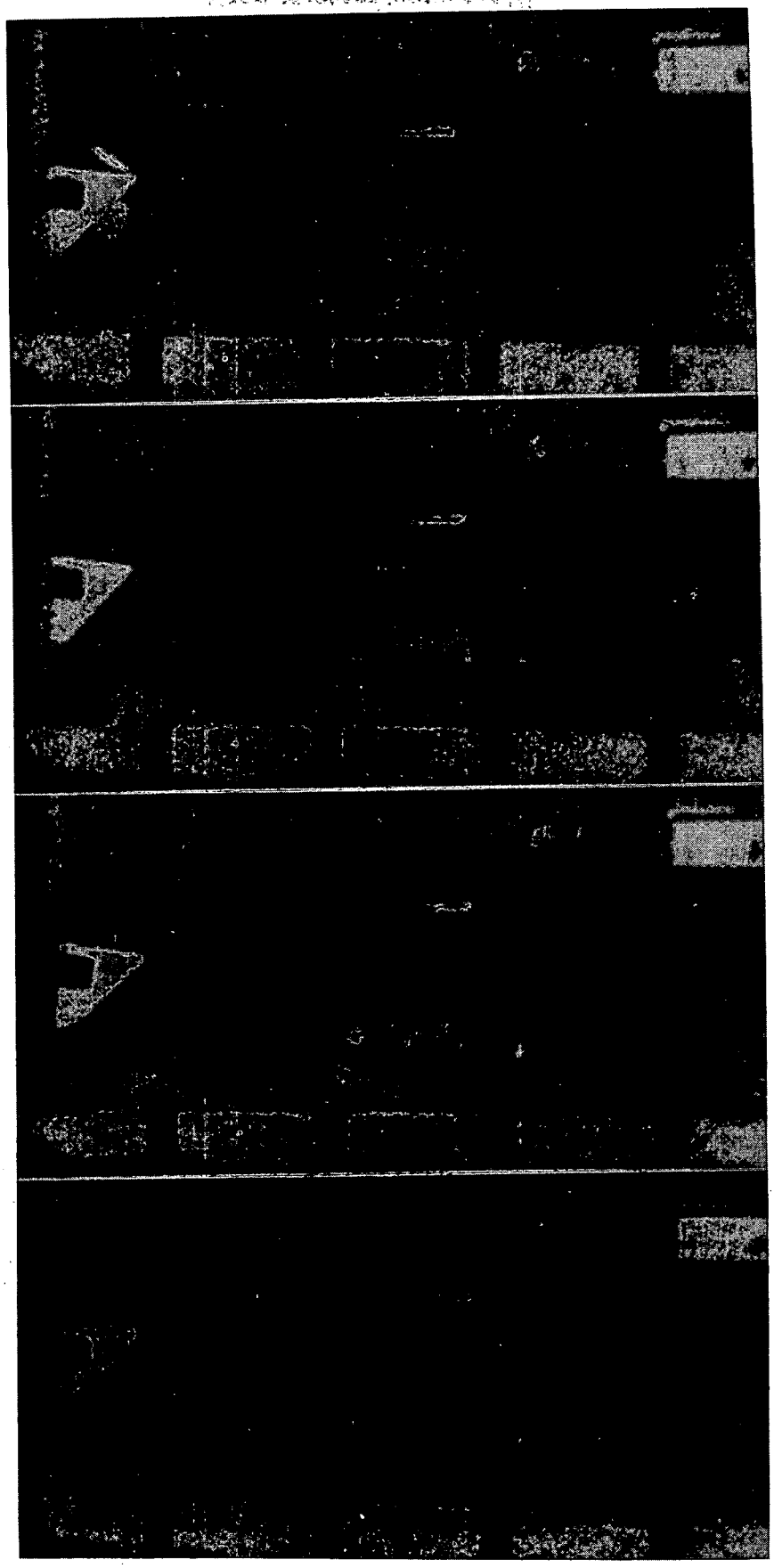

Figure 3.3 Late sequence of events in a scale model test.

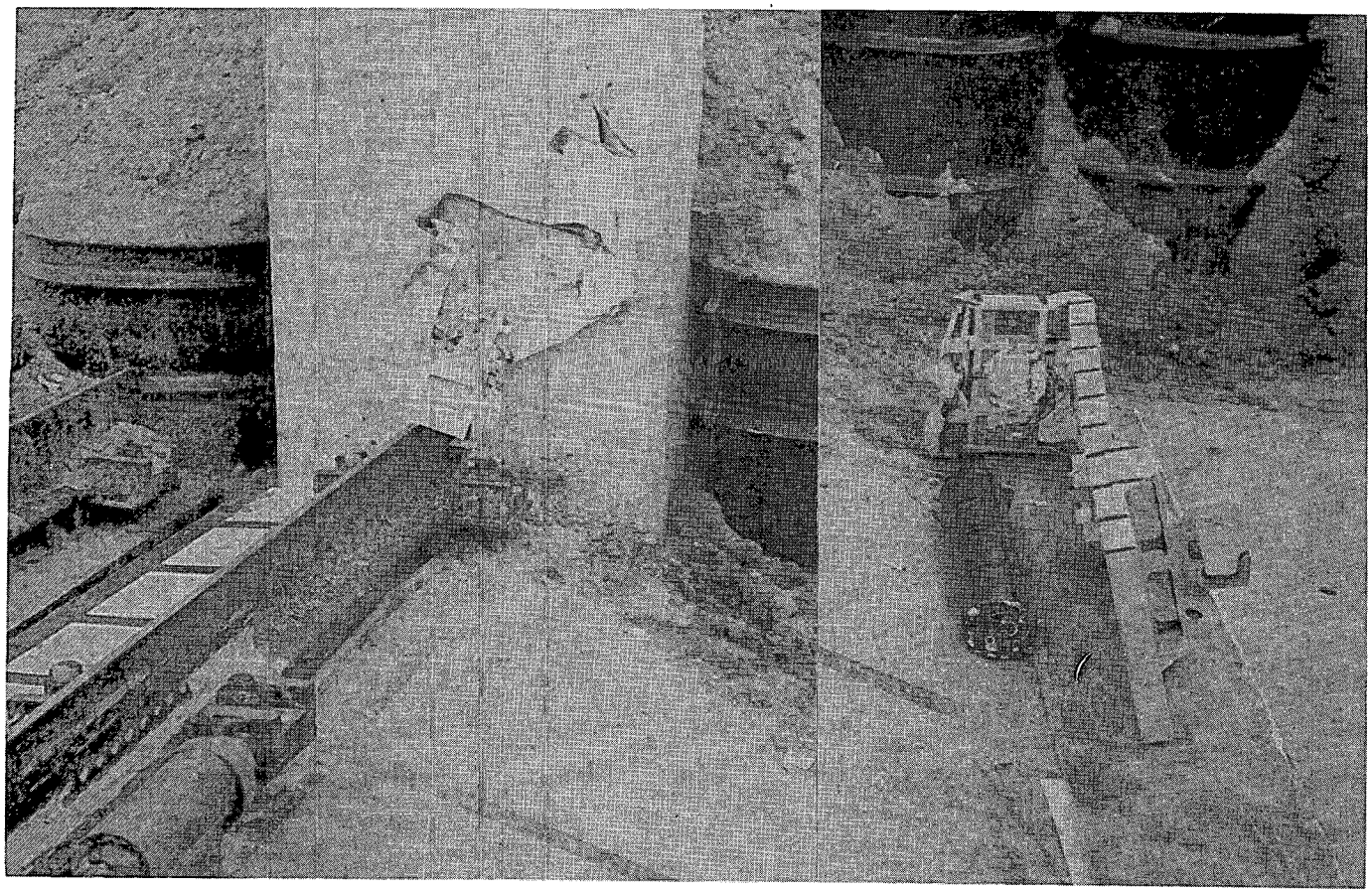

Figure 3.4 Scale model after an impact test.

of the trailer structure. The cask model was intact, without any measurable deformations. No leakage of water was detected.

The duration of the impact, from the time the front end of the tractor touched the target to the point in time when the cask bottomed out against the target, was 0.04 second. The velocity time curve was smooth with no abrupt changes. The displacement-time and velocity-time curves obtained from high speed films by following a point near the cask center of gravity are included in Appendix E. This data will be compared to results from the corresponding full-scale test in Section 5.

The model in the second test behaved in basically the same manner. Damage to the vehicular system was approximately the same as in the first test except that the front end of the trailer was crushed to a greater amount and did not buckle upward as clearly. The tiedowns in this test broke early in the impact, and the cask went into the target much harder at about 105 kph (65 mph).

Figure 3.5 is a close up view of the model cask after this second, more severe, test. The model did not exhibit a large amount of hoop strain on the impact end, with the maximum being 3%. Lead slump, measured on the opposite end, was 0.355 cm (.14 in.). The cover remained firmly in place and the containment integrity of the cask was not threatened. The duration of this model impact was 0.026 second. Figure 3.6 illustrates, in an exaggerated fashion, the deformation profile for the cask. The cask response in this scale model test will be compared with the results of the second full-scale test in Section 5.

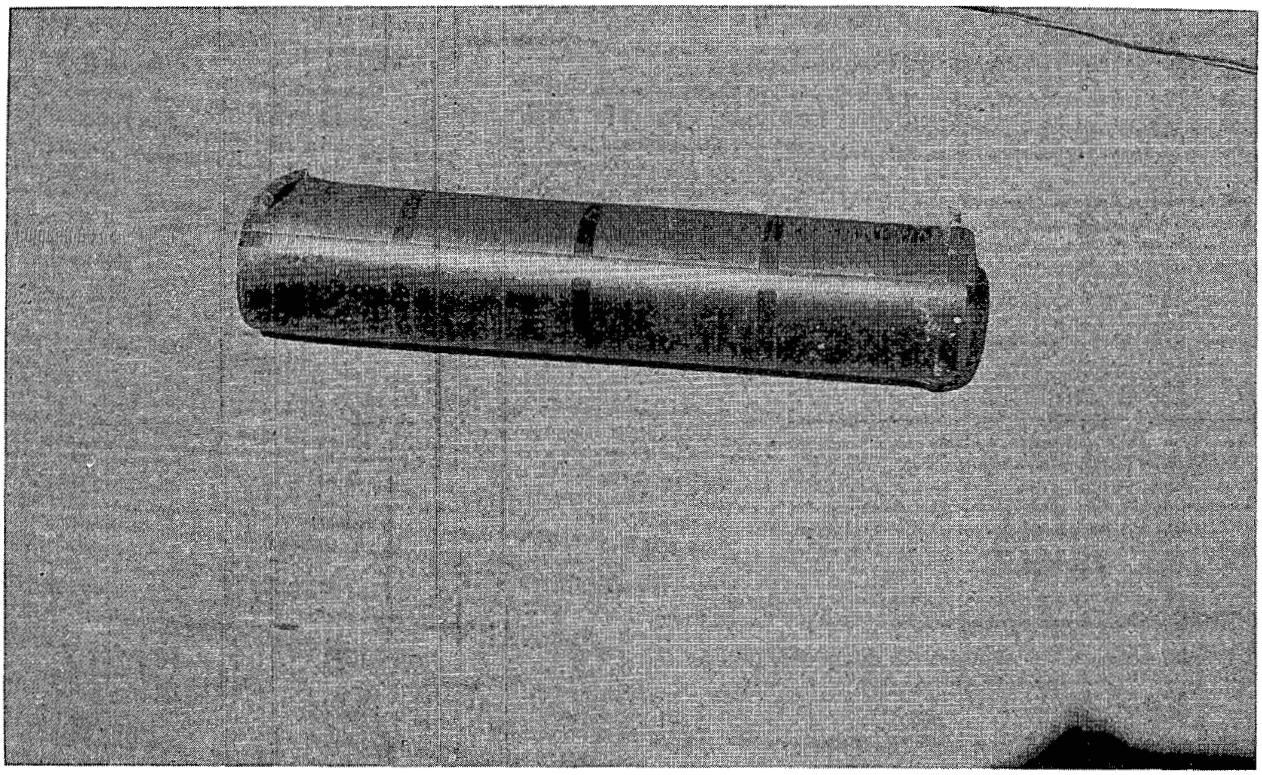

Figure 3.5 Scale model cask after the high velocity impact test.

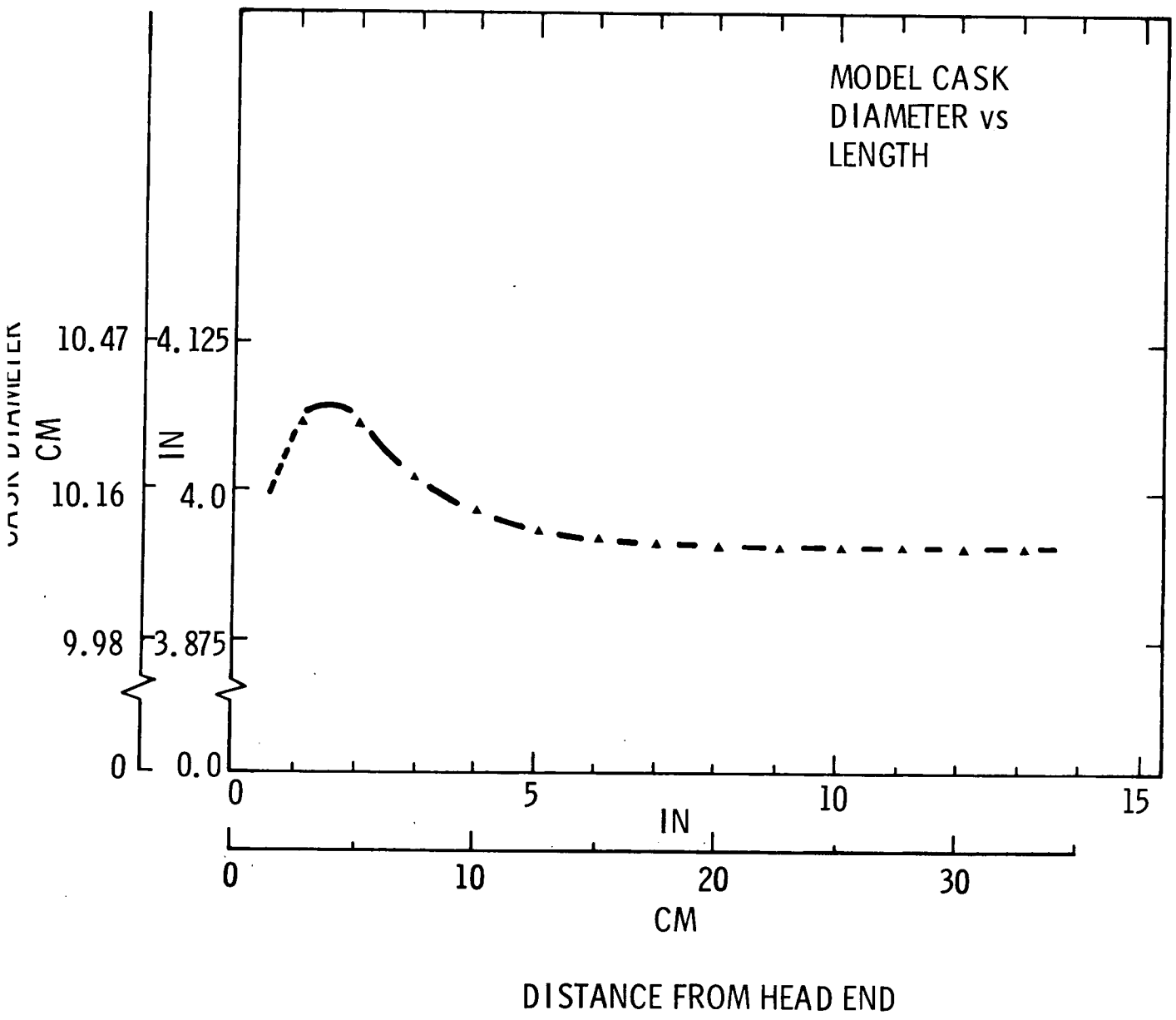

Figure 3.6 Magnified deformation pattern for a scale model cask.

As mentioned above, some cask models were tested in extra severe conditions without a vehicle structure. These were tested at an actuator facility by impacting them with a very massive steel ram weighing about 200 times as much as the cask model. These tests were conducted to further explore the possible response or failure modes of the cask in situations which were much more severe than the planned full-scale tests. The casks were end-impacted with impact limiters in place.

Figure 3.7 illustrates a model tested in this manner at 129 kph (80 mph). In this figure, the model has been sectioned in order to illustrate deformations to the container and lead motion within the shells more clearly. In this case, there was a maximum hoop strain of 13% near the impact end and a lead slump of 1.0 cm (.4 in.) on the back end. The cover remained firmly in place.

3.5 Discussion

The system scale model tests confirmed results obtained from mathematical analysis well. As had been predicted, the tractor was completely crushed. The trailer structure hit the wall solidly and crushed. The cask remained close to horizontal going forward through the truck cab and impacting the wall in an almost end-on configuration. At the lower velocity, it came through without measurable deformations. In the higher velocity test, the cask sustained only minor damage which was not viewed as a threat to the cask's integrity.

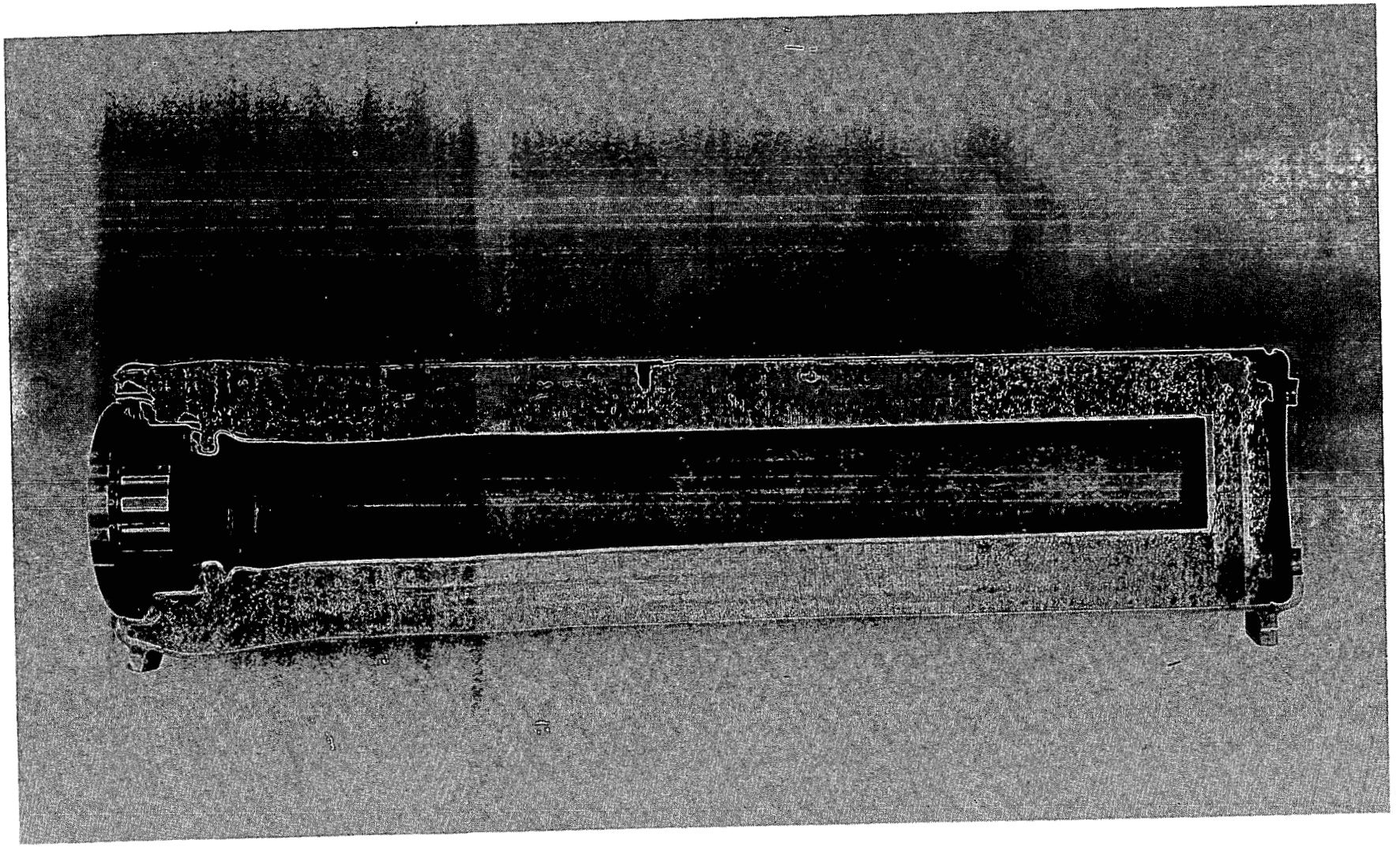

Figure 3.7 Cross section of a scale model cask after a 129 kph impact into an unyielding target.

The actuator tests showed that even at a condition which was much more severe than could be encountered in the full scale tests, the cask would not be grossly deformed nor would it be breached. On the basis of the scale model tests, it was predicted that, even in the more severe of the two full scale tests, the cask would come through with only minor deformations. The models indicated that the full-scale cask would not be breached.

4.0 Full Scale Tests

4.1 Introduction

Two full-scale tests were conducted using the same cask with different, but similar, vehicular systems. The impact velocities were 98 and 135 kph (61 and 84 mph). The vehicles and cask were impacted into a specially constructed rigid reinforced concrete target. The tests had extensive high speed film coverage as well as onboard instrumentation operating through a telemetry unit. This section describes the test procedure and presents results from both tests.

4.2 Test Descriptions

The tests were conducted at a sled track facility where a road was constructed to the level of the top of the rails. In the tests, the vehicle wheels bridged a trench and a section of track leading to the target. The system was guided by the rails but rolled on its tires. Rocket motors mounted on a sled attached to the track were fired in stages to accelerate the system up to speed at a controlled acceleration level of about 0.5 g. A sand brake was used to disengage the pusher sled, and the transport system was allowed to coast into the target.

Figure 4.1 illustrates the transport system used in the first test. To make it more representative of current day equipment, the cask was equipped with balsa wood impact limiters on each end, as can be seen in the figure. The 20,500 kg (45,000 lb) cask was attached to the 5000 kg

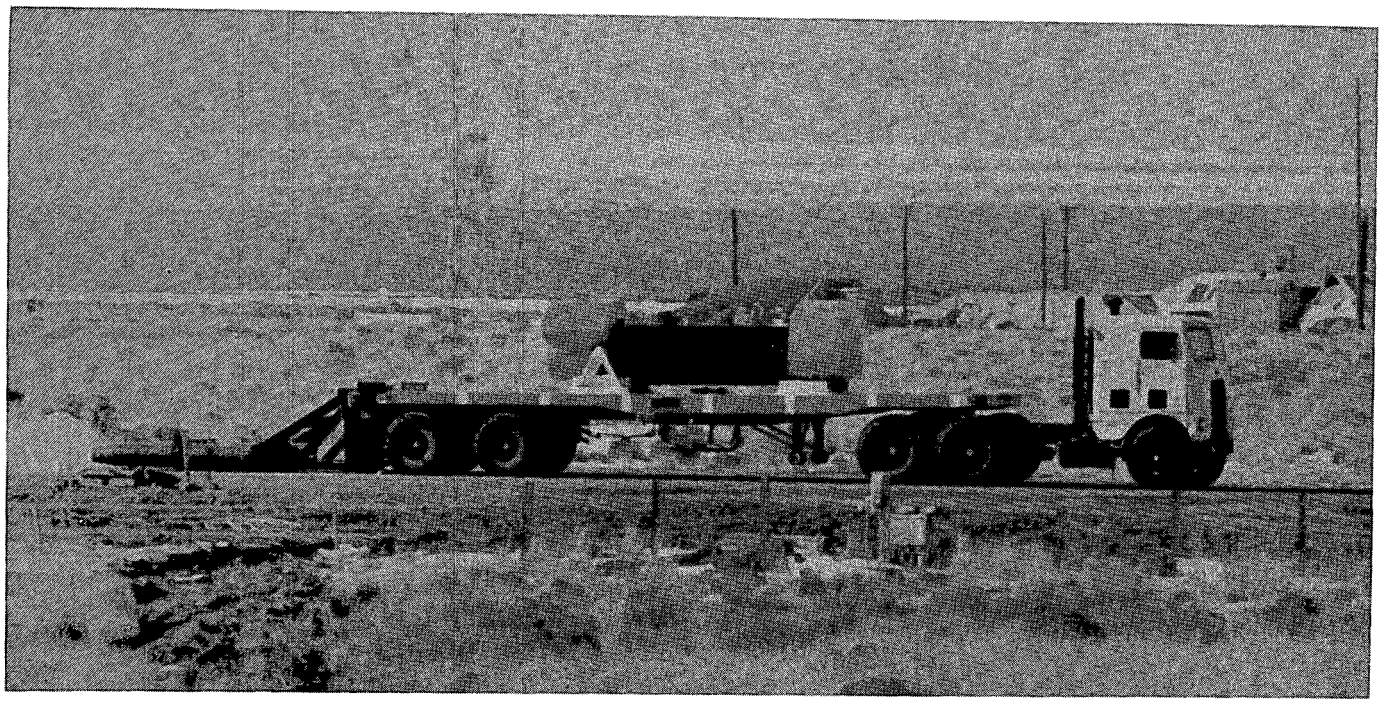

Figure 4.1 Full-scale system in the first test.

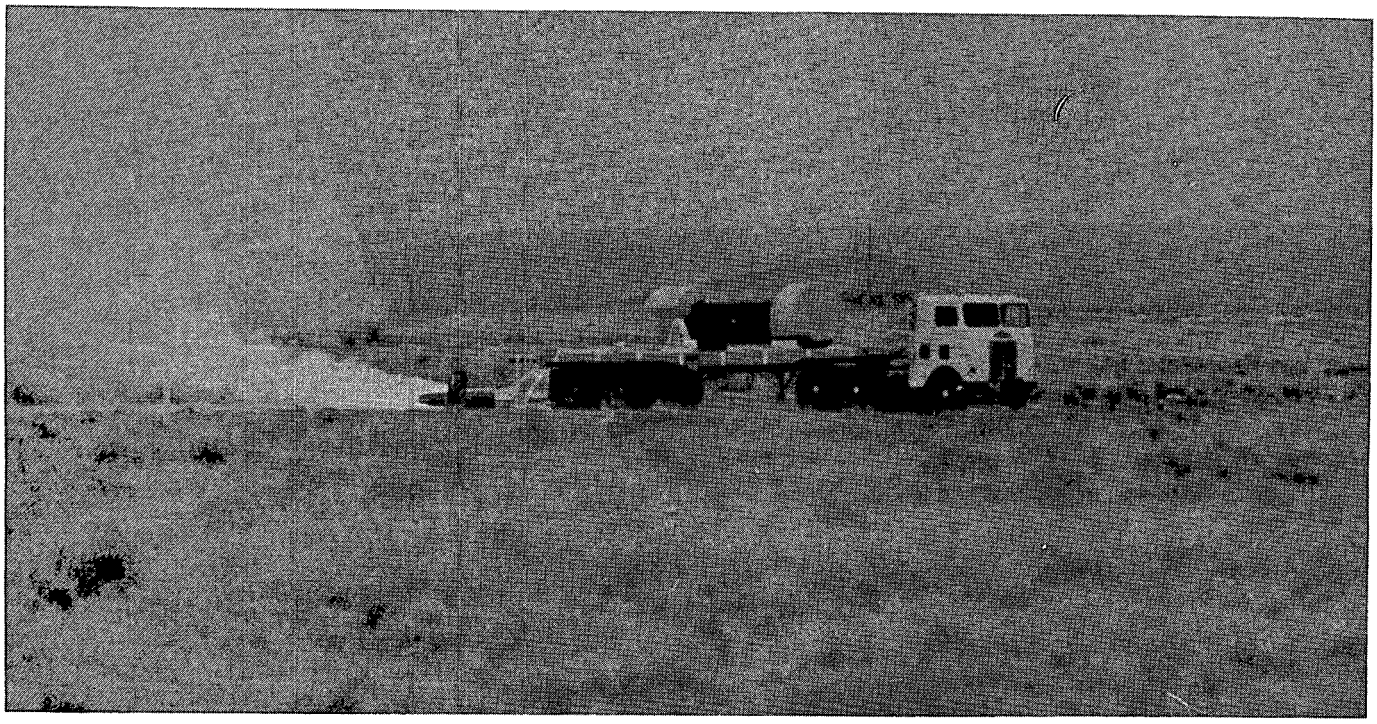

Figure 4.2 Full-scale system in the second test.

(11,000 lb) trailer using the standard tiedowns that were used while it was in service. The tractor was a used commercial unit weighing 5900 kg (13,000 lbs.).

The vehicular system used in the second, higher velocity, test was almost identical. There was, however, a slight difference in fifth wheel connection locations which in the second test moved the cask and trailer forward about 30 cm (12 in.). Figure 4.2 illustrates the transport system used in the second test as it is being accelerated down the track. (This system is most easily distinguished from the first by the fact that it had a light colored exhaust stack whereas the first had a black stack). The trailers and tiedown systems were identical. The tractor was very similar and structurally equivalent.

In each test, the system was accelerated up to speed by a very similar system of rocket motors. The different impact velocities were achieved by varying the number of rockets and the accelerating distance. Figure 4.3 illustrates the rocket motors and pusher sled used in the second test. A total of five large and three small rockets were fired in three stages. The sled was connected to the rails with track shoes and pushed against the back of the trailer, as can be seen in this figure. The sled was disengaged from the trailer by a sand brake built into the trench between the rails. The same technique and a very similar pusher sled were used in the first test.

In order to accelerate the system in a straight line into the target, the tractor was guided by the rails and connected to them by a system of track shoes. Figure 4.4 illustrates the guide system installed under the rear axle

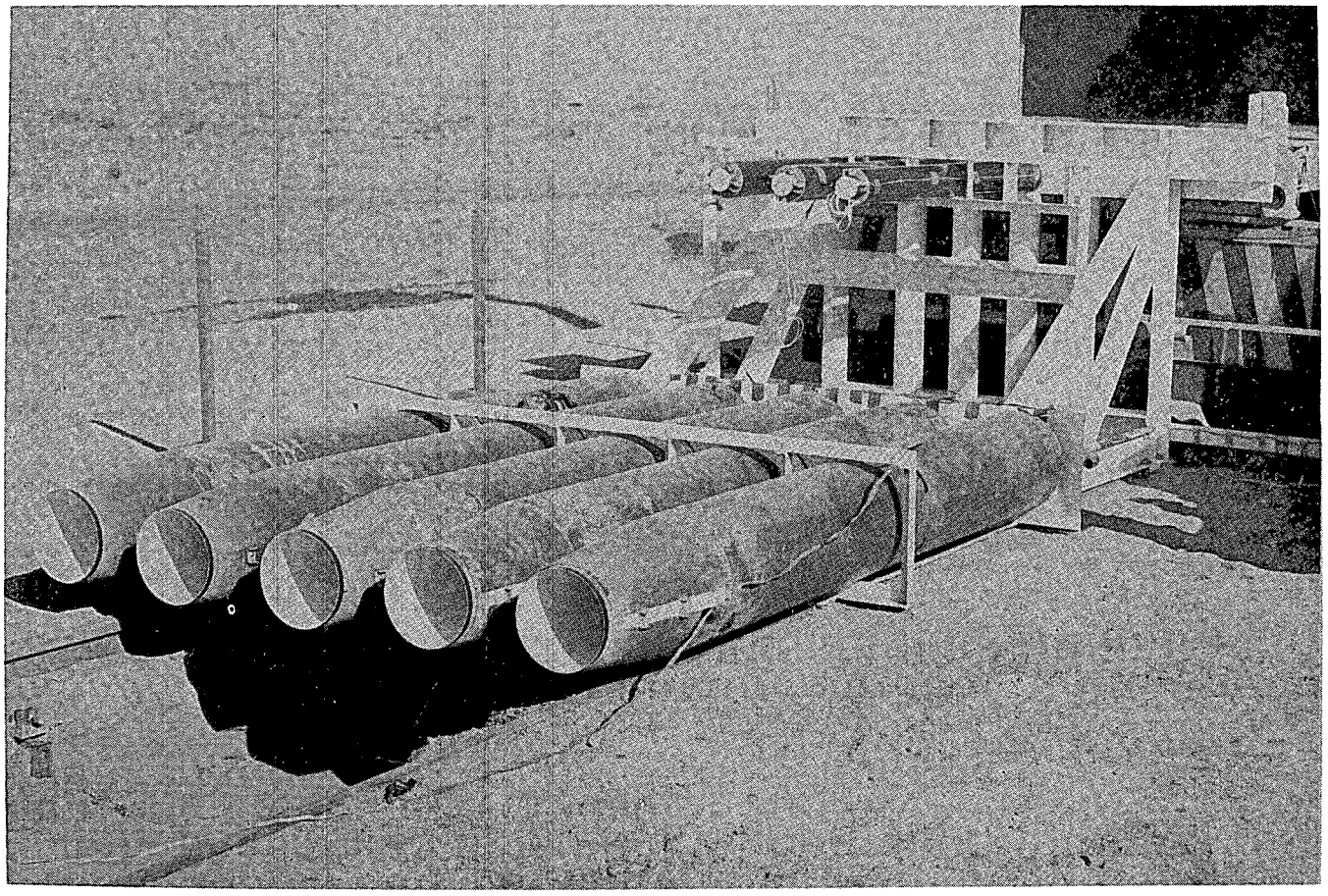

Figure 4.3 Propulsion system used in the second test.

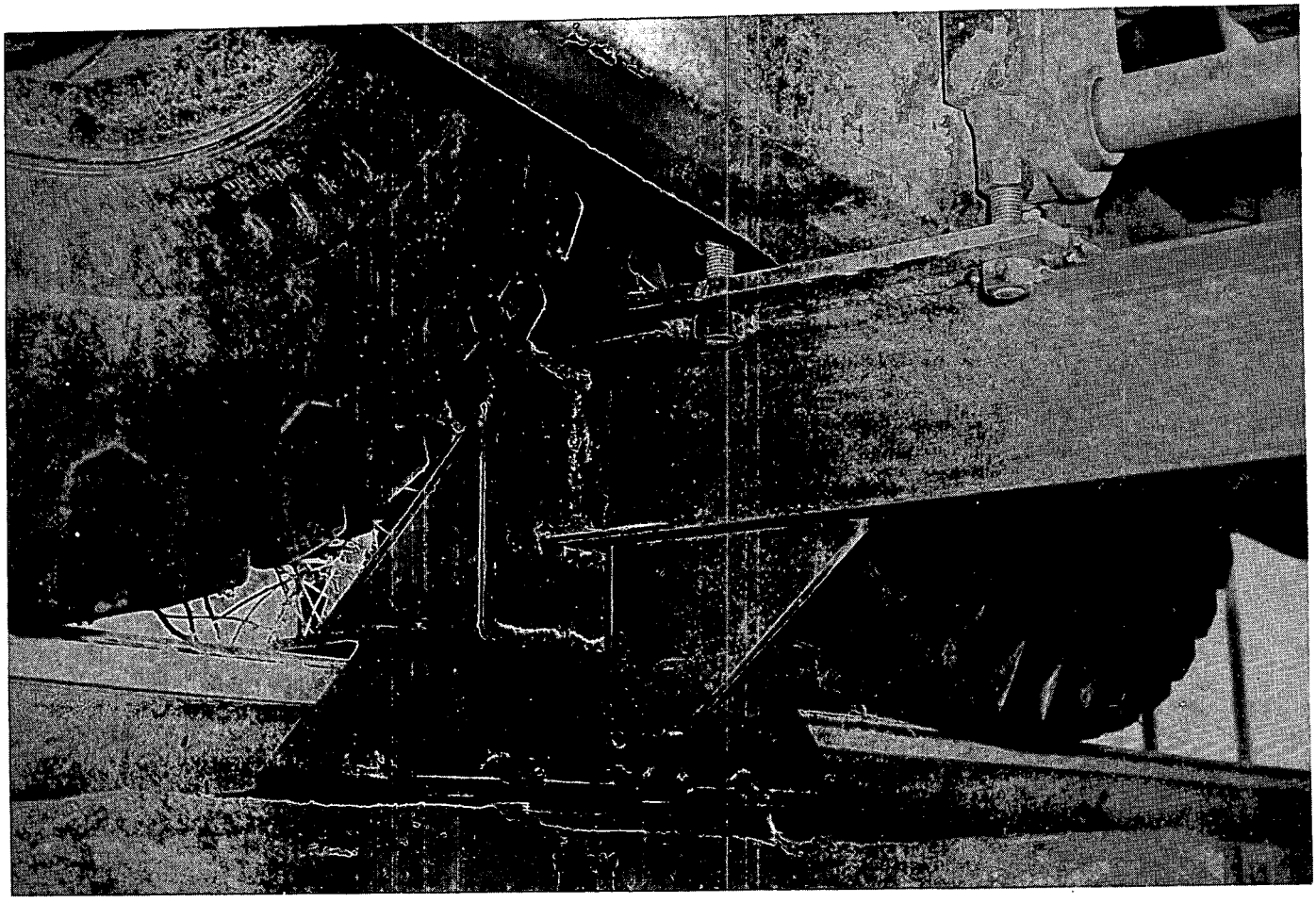

Figure 4.4 Illustration of the rail guide system.

assembly of the tractors. A similar system was used under the front axles. To allow the system to be free to move vertically at impact, the rail flanges were removed from a section of track directly in front of the target. Thus, the system was unrestrained by the rails in the vicinity of the target.

Figure 4.5 illustrates a closeup view of the target which was designed to be extremely rigid and specially constructed for the full-scale test series. The heavily reinforced concrete portion and its foundation had a mass of 627 kg (690 tons). This is backed with 1545 kg (1700 tons) of earth. The face of the target is 3.05m (10 ft) thick, 16.56m (20 ft) wide, and 6.56m (20 ft) high. The pipe casings to the sides and back of the target are earth filled and placed there to better retain the earth backing behind the concrete. The target was instrumented with accelerometers to record motion.

Figure 4.6 illustrates the target as seen by looking down the track. Here the trench between the rails and the sand which catches the pusher sled are clearly visible. As can be seen, the road bed was constructed to the top of the rails. The overhead cameras suspended between two poles can also be seen in the figure.

Extensive high speed photocoverage and instrumentation were provided for the tests. Numerous cameras were placed at the site to film the event from various angles. The cask was instrumented with five active piezoresistive accelerometers and two triaxial strain gage rosettes. The middle strain gage in each rosette was aligned with the circumferential direction of the cask. Two accelerometers were placed near

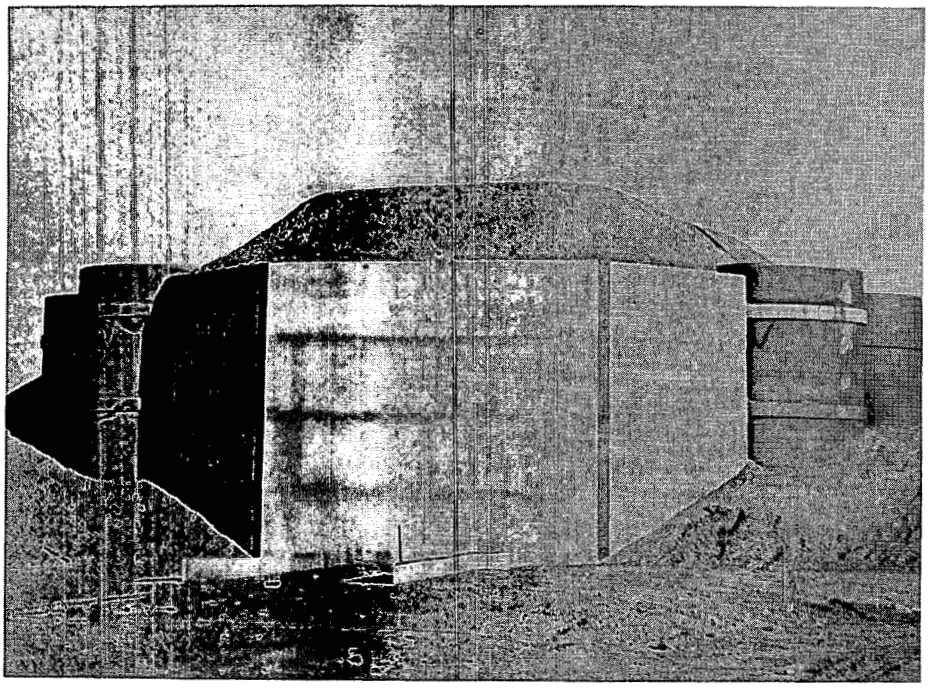

Figure 4.5 Close up view of the target.

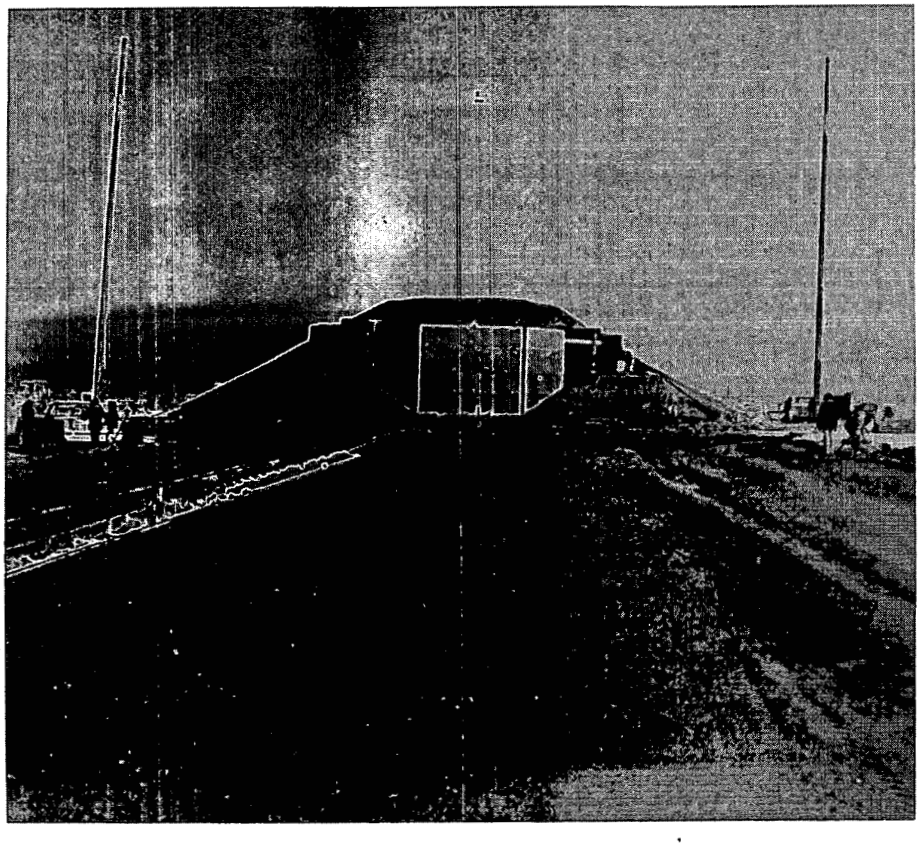

Figure 4.6 Illustration of the guide rails and target.

the front, two near the rear, and one at the cask center on one side. The rosette strain gages were installed on the cask outer shell very close to the impact end. Figure 4.7 illustrates a portion of the front end of cask. Here one of the rosettes and an accelerometer are clearly visible and marked by arrows. All the active cask instrumentation operated through a telemetry package, illustrated in Figure 4.8, which was bolted to the back end of the cask and fitted into a cavity in the rear impact limiter. The wires were routed through light stainless steel conduits which were tack welded to the sides of the cask. Signals from the instrumentation and telemetry package, which has a frequency capability of 2000 Hz, were remotely recorded on magnetic tape for later playback. The trailer structure was instrumented with two active accelerometers located underneath the cask and operated through a small telemetry pack. In addition to the active instrumentation, some crush disk and ball type passive accelerometers were placed at various locations throughout the structure and the cask. Passive water pressure sensors were placed inside the cask to record peak water pressure at impact. Appendix F, which is a reprint of a memorandum prepared prior to conducting the tests, describes the instrumentation plan in detail. This plan was closely adhered to in both tests.

4.3 Test Results

4.3.1 First Test

In the first test, the system impacted at 98 kph (61 mph). The photometrics and instrumentation functioned well. Figures 4.9 through 4.12 include a series of photographs illustrating the sequence of events in the first test. These

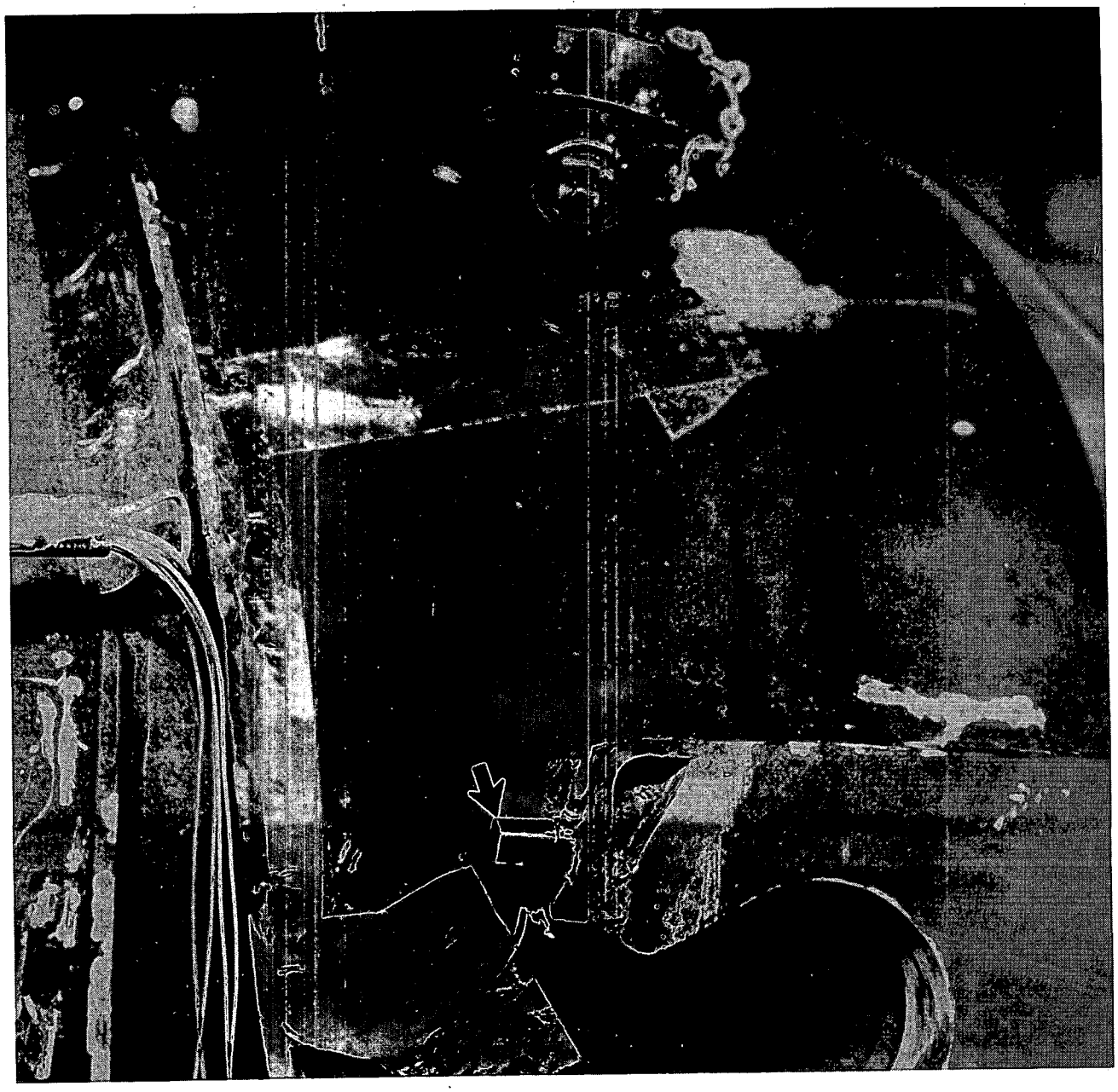

Figure 4.7 Close up view of cask instrumentation.

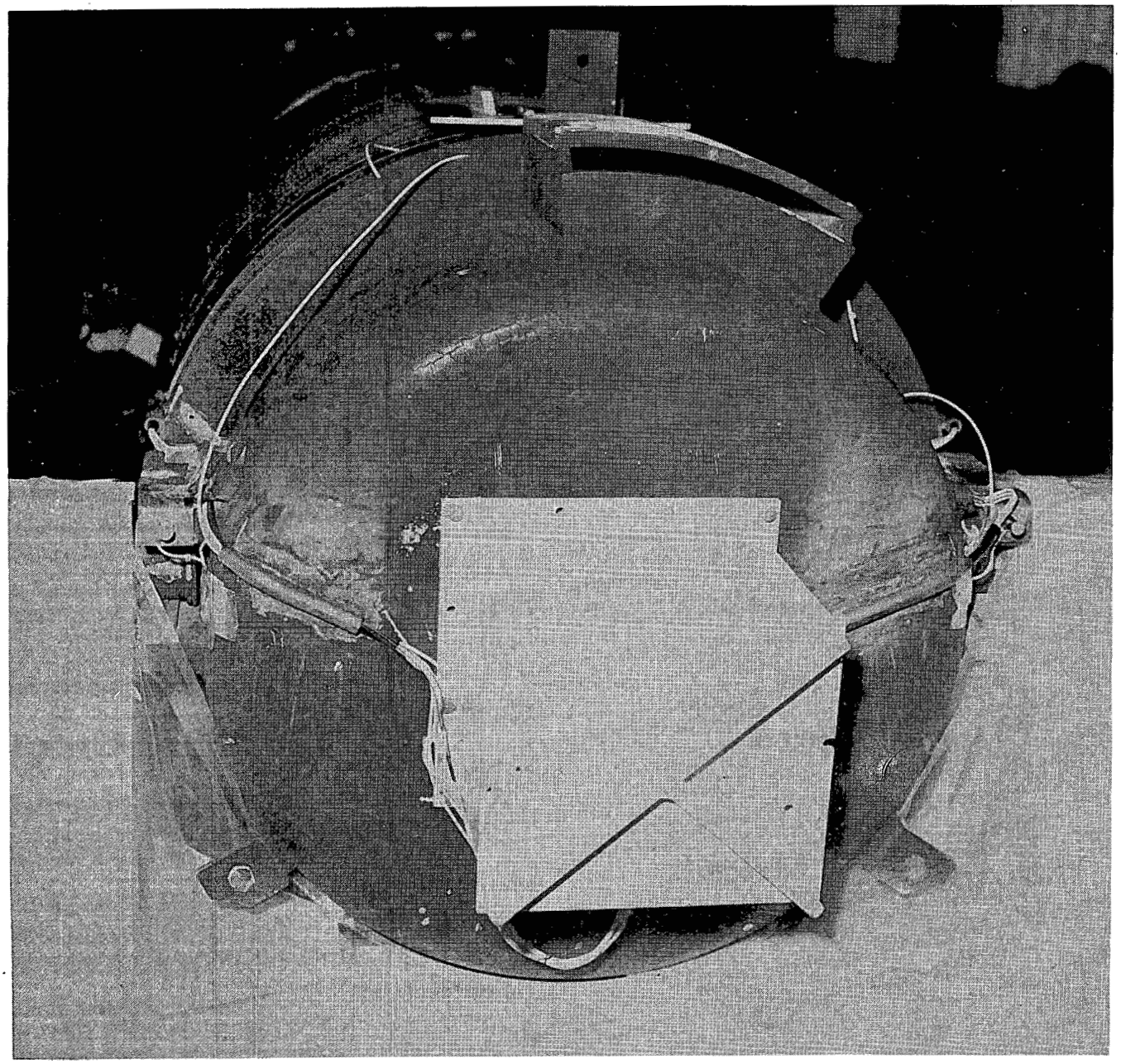

Figure 4.8 Illustration of the telemetry package on the cask.

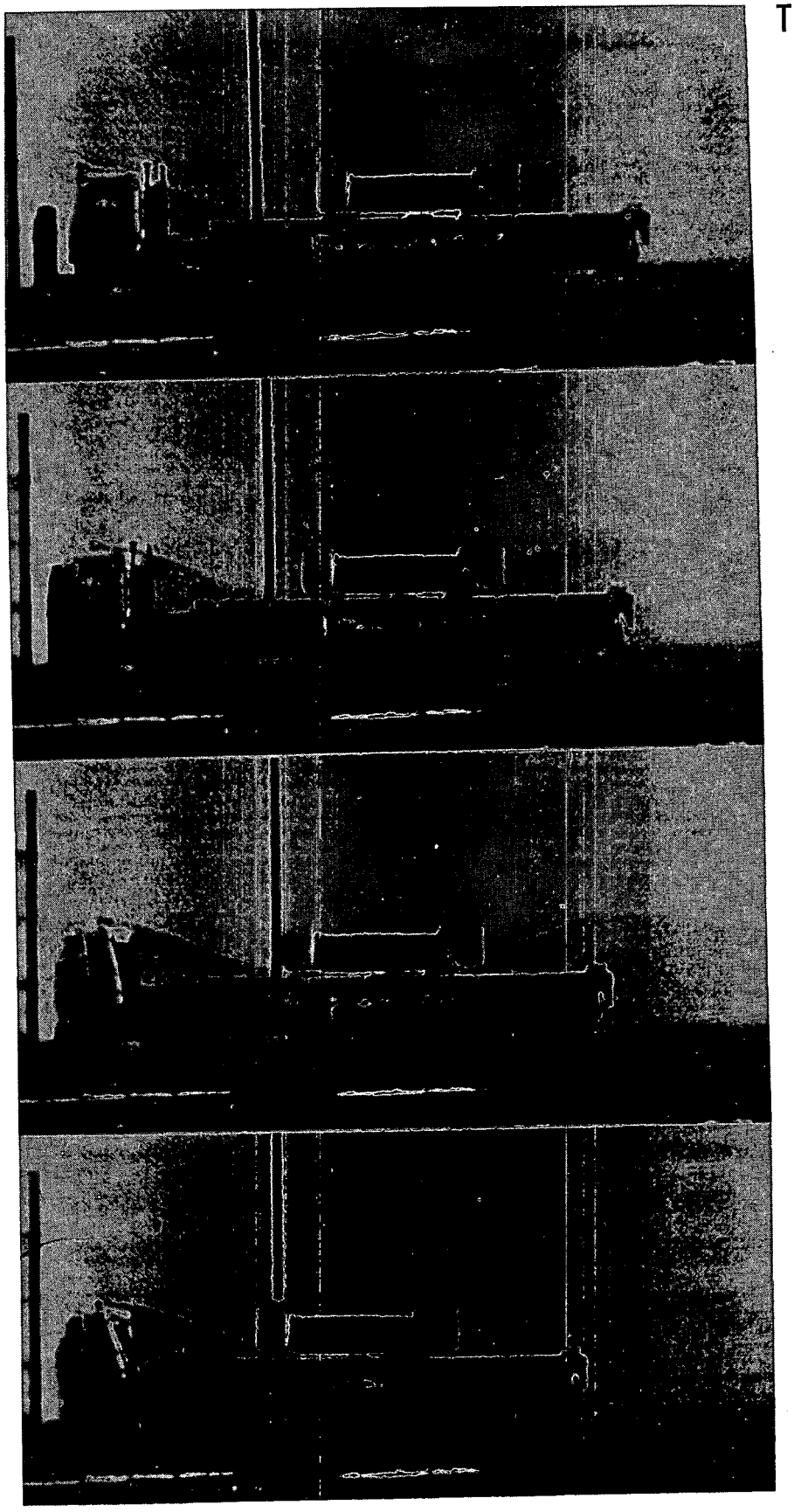

Figure 4.9 First test event sequence to 0.050 second.

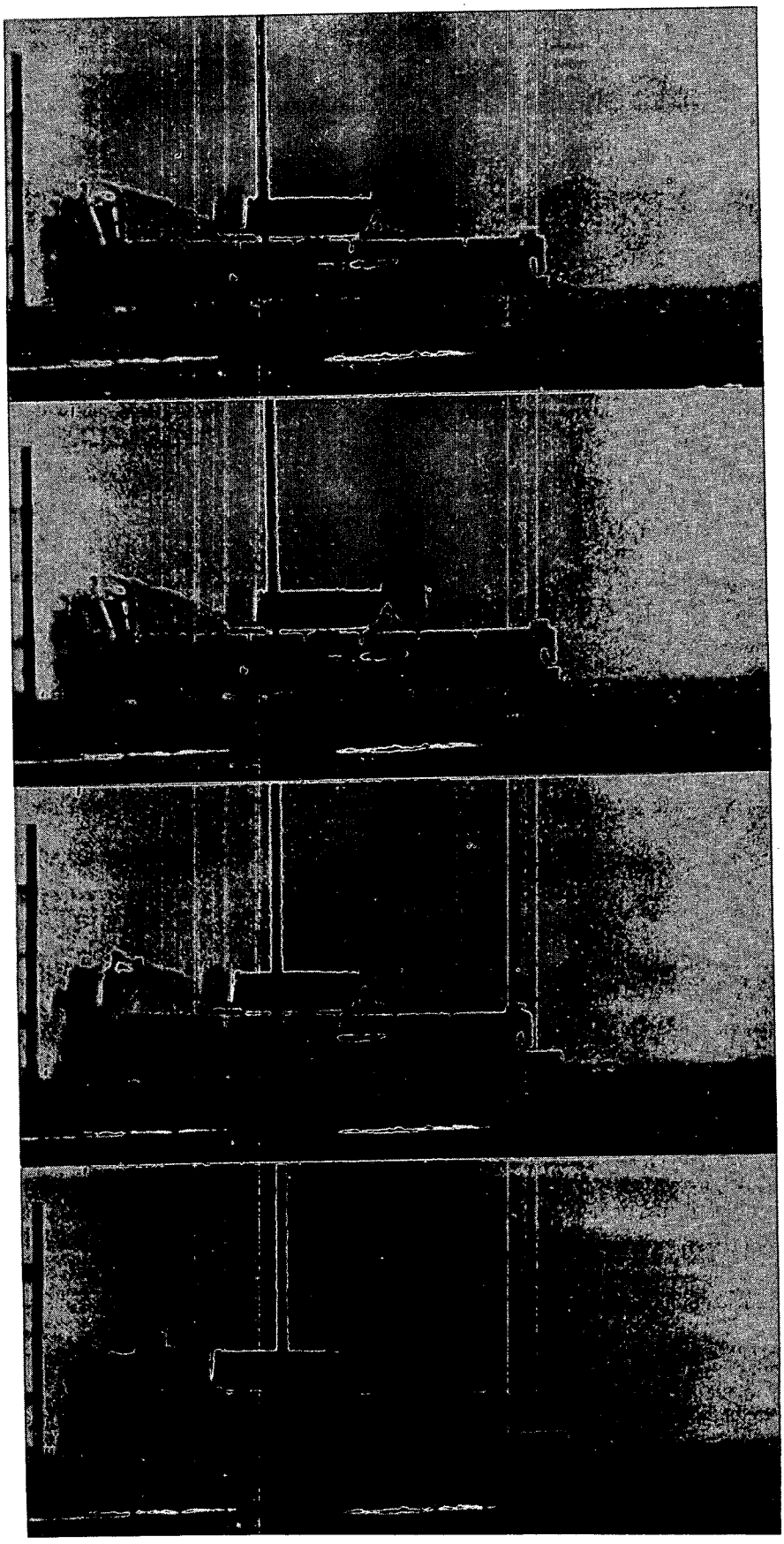

Figure 4.10 First test event sequence from 0.075 to 0.150 second.

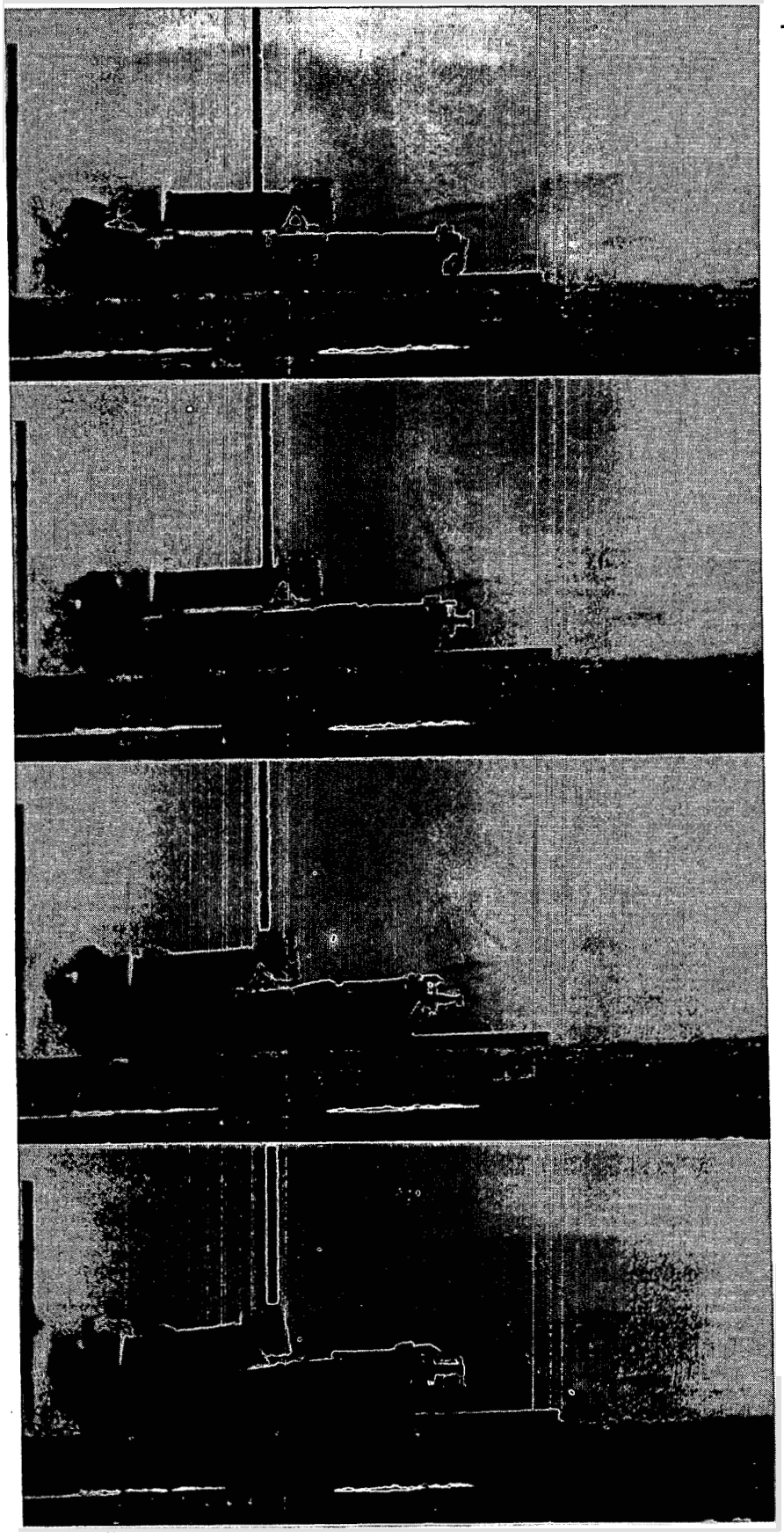

Figure 4.11 First test event sequence from 0.175 to 0.250 second.

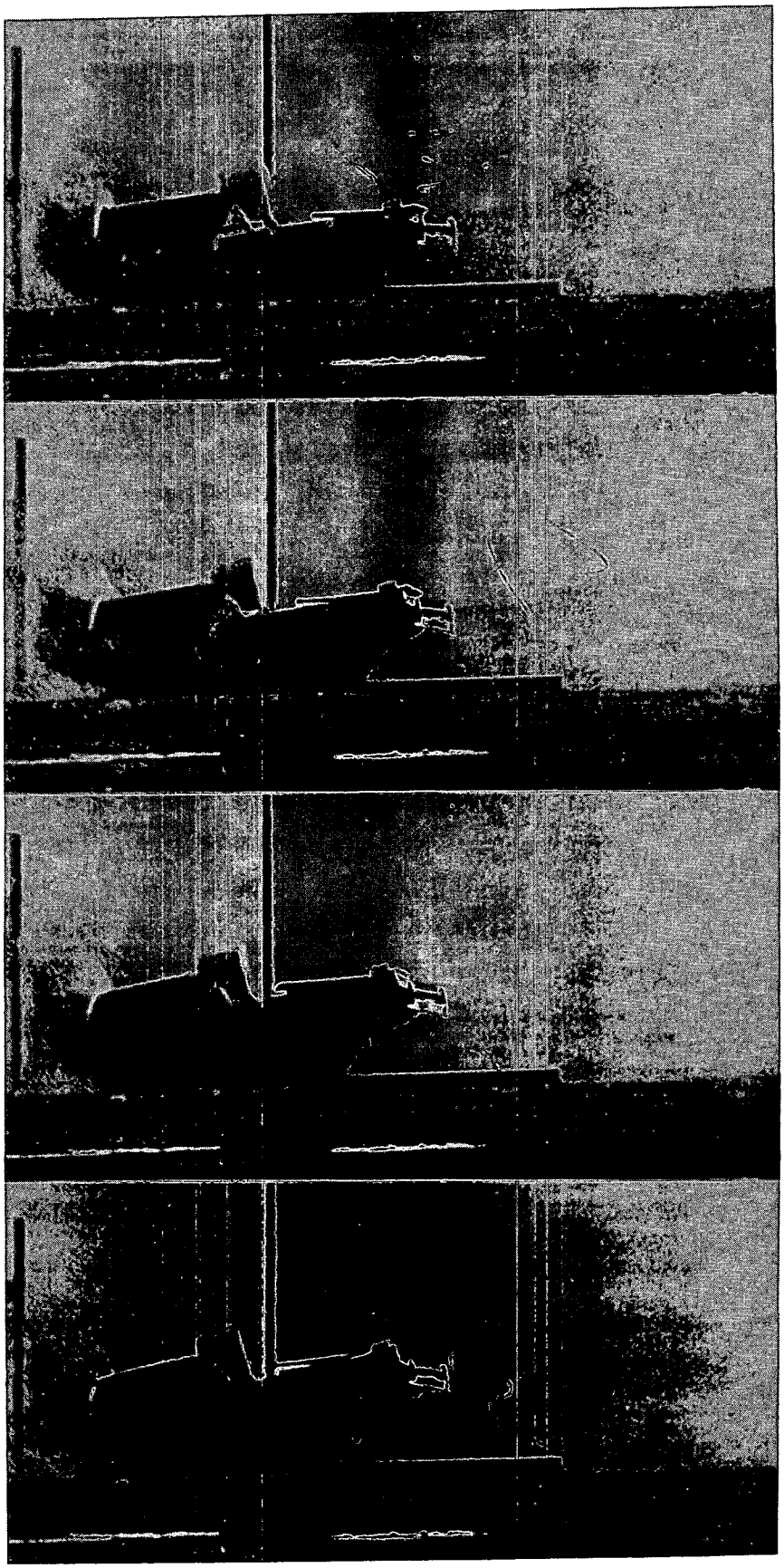

Figure 4.12 First test event sequence from 0.275 to 0.350 second.

were obtained from a side camera film by photographing every tenth frame. Time zero was designated as the instant when the front end of the tractor touched the wall. The events following contact and spanning 0.35 second can clearly be seen in these photographs.

As these illustrations reveal, the truck tractor was completely destroyed (quite early). The trailer moved forward through the cab and solidly impacted the target. The front end of the trailer then crushed and buckled up along the face of the target. The cask remained attached to the trailer and essentially horizontal during crush up of the vehicular structure. By the time that the cab had been crushed solid, the velocity of the cask was down to about 43 kph (27 mph). At this point in time, the impact limiter began to crush but was not completely compacted before the cask came to a horizontal stop. Following the target impact, the cask and trailer rotated through a maximum angle of approximately 30° with the horizontal and dropped back down to the road in front of the target.

The timing for the occurrence of the principal events in this test was as follows:

TIME (SECONDS)	EVENT
0.0	Tractor contacts face of target
0.030	Fifth wheel connection breaks
0.040	Tandem axle assembly shears off tractor
0.075	Trailer contacts back end of cab

TIME (SECONDS)	EVENT
0.103	Trailer encounters solid target
0.138	Buckling is initiated in trailer frame
0.181	Front end of impact limiter contacts cab
0.222	Cask moves slightly relative to tiedown structure
0.242	Cab is completely crushed
0.277	Trailer axles shear off
0.303	Cask comes to a horizontal stop

Figure 4.13 illustrates the condition of the system, including the cask, immediately after the test. Here the manner in which the tractor was completely crushed and the upward buckling of the trailer frame can be clearly seen. The cab and trailer structures came between the cask and the target, cushioning the impact somewhat. The cask moved slightly in relation to the tiedown system, completely failing the front connection. The rear tiedown was extensively damaged but did not fail completely. Note in this figure that the rear tiedown partially tore loose from the trailer structure and that the cask moved slightly relative to the tiedown. The impact limiter rotated somewhat over the front end of the cask, as can be seen, but remained attached to the cask.

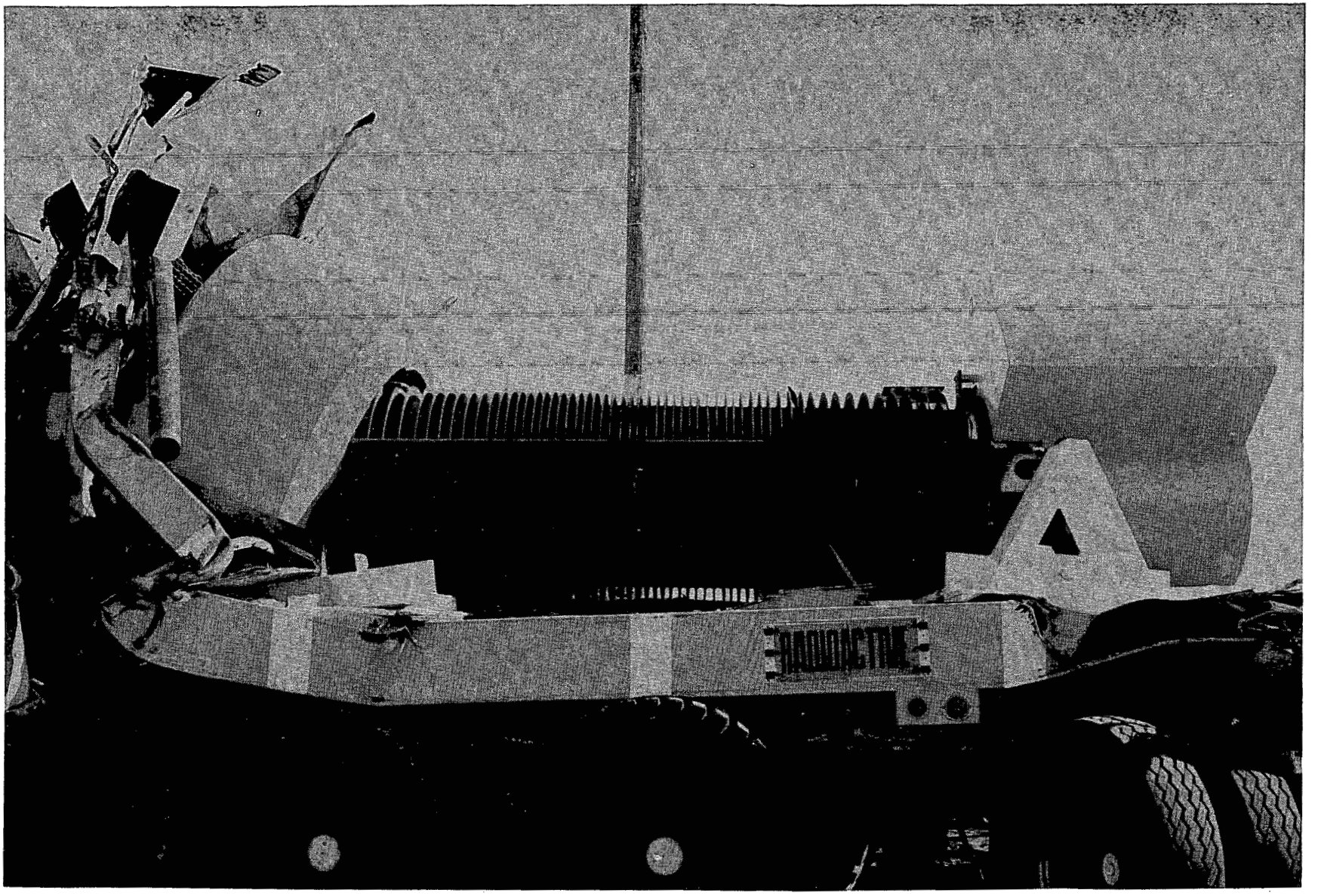

Figure 4.13 Illustration of the full-scale system after the first test.

The cask itself remained intact with only minor damage to external features. Some external piping near the front end as well as some of the cooling fins were damaged. The basic body of the cask was undeformed and there was no leakage. The head bolt tightness was found to have been lessened somewhat by the impact or the relaxation of the head gasket. The cover was removed without difficulty and the fuel elements were found to be intact and undamaged.

The shock which the cask underwent in this test was limited by the crush strength of the mitigating structures. These structures were not completely crushed in this test; therefore, the cask did not encounter the rigidity of the concrete target. Figure 4.14 is a deceleration-time plot obtained from the high speed photography data by following a spot at the center of the cask on one side. As can be seen, a peak g level of about 18 g's was calcualted from the film data. Figure 4.15 is a plot of cask deceleration as a function of displacement. This plot indicates relatively low levels in the early stages of the impact which climb rapidly in the final 1.5 m (60 in) of travel.

Appendix G includes pertinent data from this test. The displacement-time and velocity-time curves included in that appendix were obtained from the films by following the central spot on the cask. The displacement-time curve indicates that the cask came to a horizontal stop 0.31 second after the front end of the tractor made contact. The velocity-time curve indicates a smooth decrease in velocity without any abrupt changes in slope, indicating a smooth deceleration.

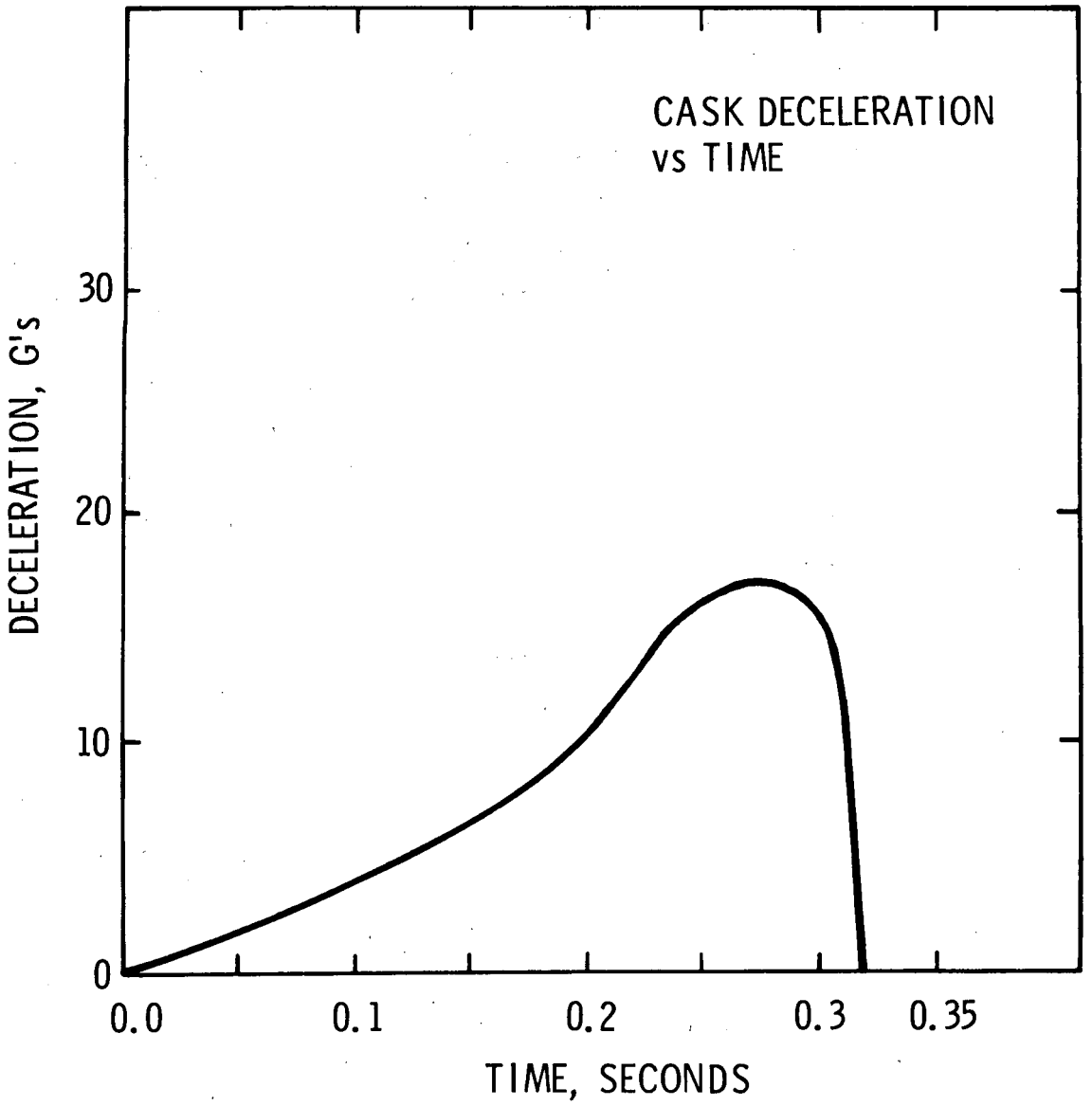

Figure 4.14 Cask deceleration as a function of time for the first test (from film data).

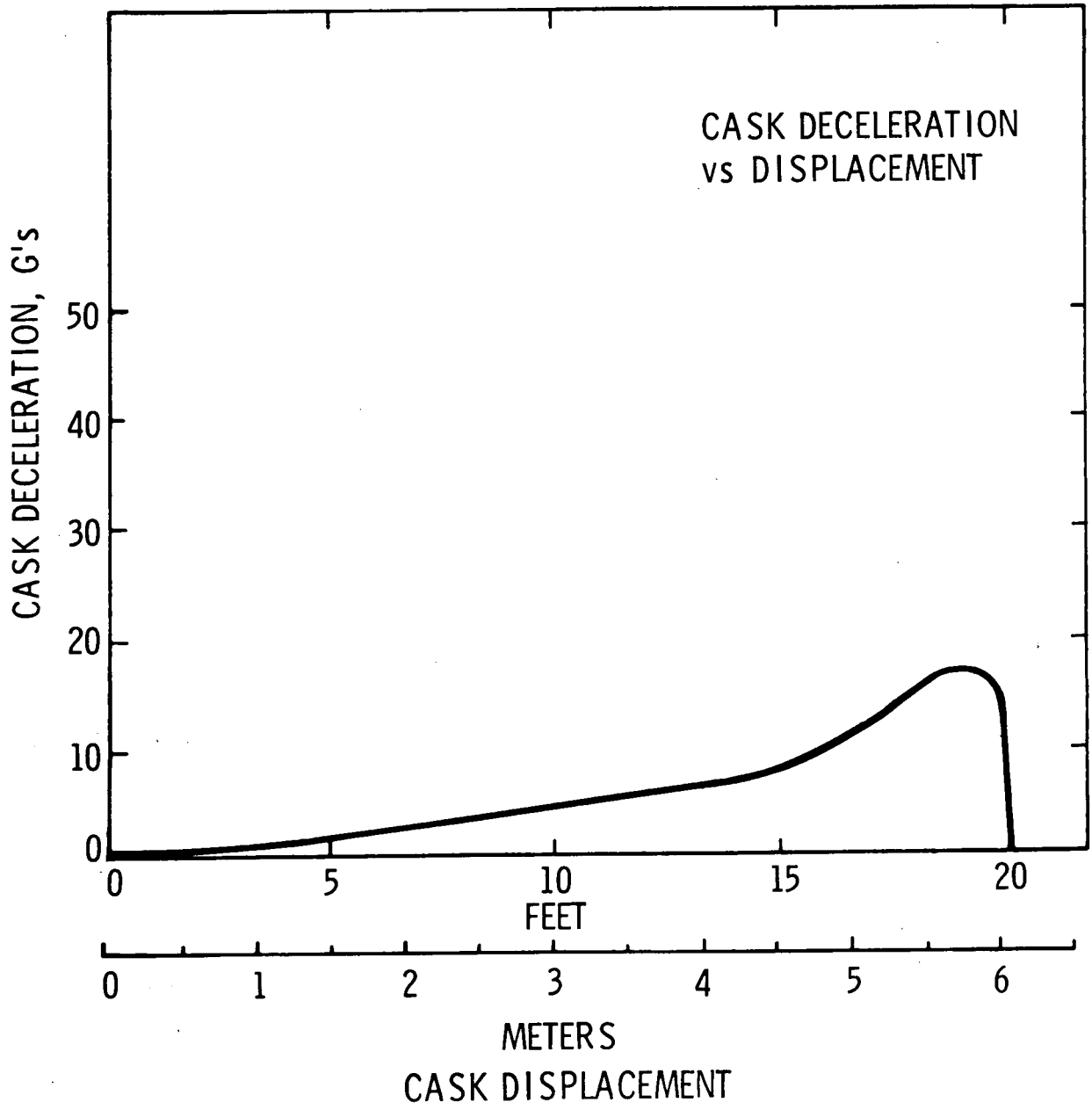

Figure 4.15 Cask deceleration as a function of displacement for the first test (from film data).

The film data were also used to plot the attitude of the cask through the impact. These data, also included in Appendix G, indicate that the cask bottomed out against the target with its center line making an angle of approximately 16° with respect to the horizontal.

Cask accelerometer data were obtained up to 0.25 second after the front end of the system made contact with the target. At this point, some wires were severed and the signals were lost. Four deceleration traces were obtained from accelerometers on the cask and are included in Appendix G. These data have been filtered to 50 Hz. The results are in agreement with the film data indicating peaks of about 20 g's.

The active accelerometers mounted on the trailer structure indicated peak deceleration levels of about 20 g's, which are in good agreement with the signals obtained from the cask. These trailer units, however, were lost earlier in time due to damage sustained by the antenna. The passive type accelerometers throughout the trailer structure indicated peak g levels which are believed to be unrealistically high, with readings as high as 1008 g's. The passive accelerometers on the cask also indicated unrealistically high readings as high as 1600 g's.

The active water pressure transducer inside the cask did not function correctly. The passive units could not be read indicating a pressure below the threshold at which a permanent indentation would be made on the device. The signals from the accelerometers on the target structure, when integrated, indicated essentially zero displacement for the target face.

4.3.2 Second Test

The impact velocity in the second test was 135 kph (84 mph), which represents twice the kinetic energy in the first test. Again, the photometrics and instrumentation functioned well. Figures 4.16 - 4.19 illustrate the sequence of events which occurred in this higher velocity impact. The duration was only two-thirds as long as in the first test. In terms of damage, the response of the vehicle in this test was approximately the same as in the first test. The tractor was completely destroyed and the front end of the trailer crushed and buckled up in approximately the same manner as in the first test. The cask remained with the trailer structure, with only the front tiedown failing. The rear tiedown exhibited less damage than in the first test.

As in the first test, the cask and trailer completely crushed the cab. The cab and buckled-up portion of the trailer again came between the cask and the target. In this test, the impact limiter did not remain in place but crushed partially and was ejected upward out of place, as can be clearly be seen in Figures 4.18 and 4.19. The cask encountered a hard target with a velocity of approximately 100 kph (62 mph). The cask attitude was much closer to horizontal than in the first test, producing very close to a perfect end-on impact.

The sequence of events and times for this test are as follows:

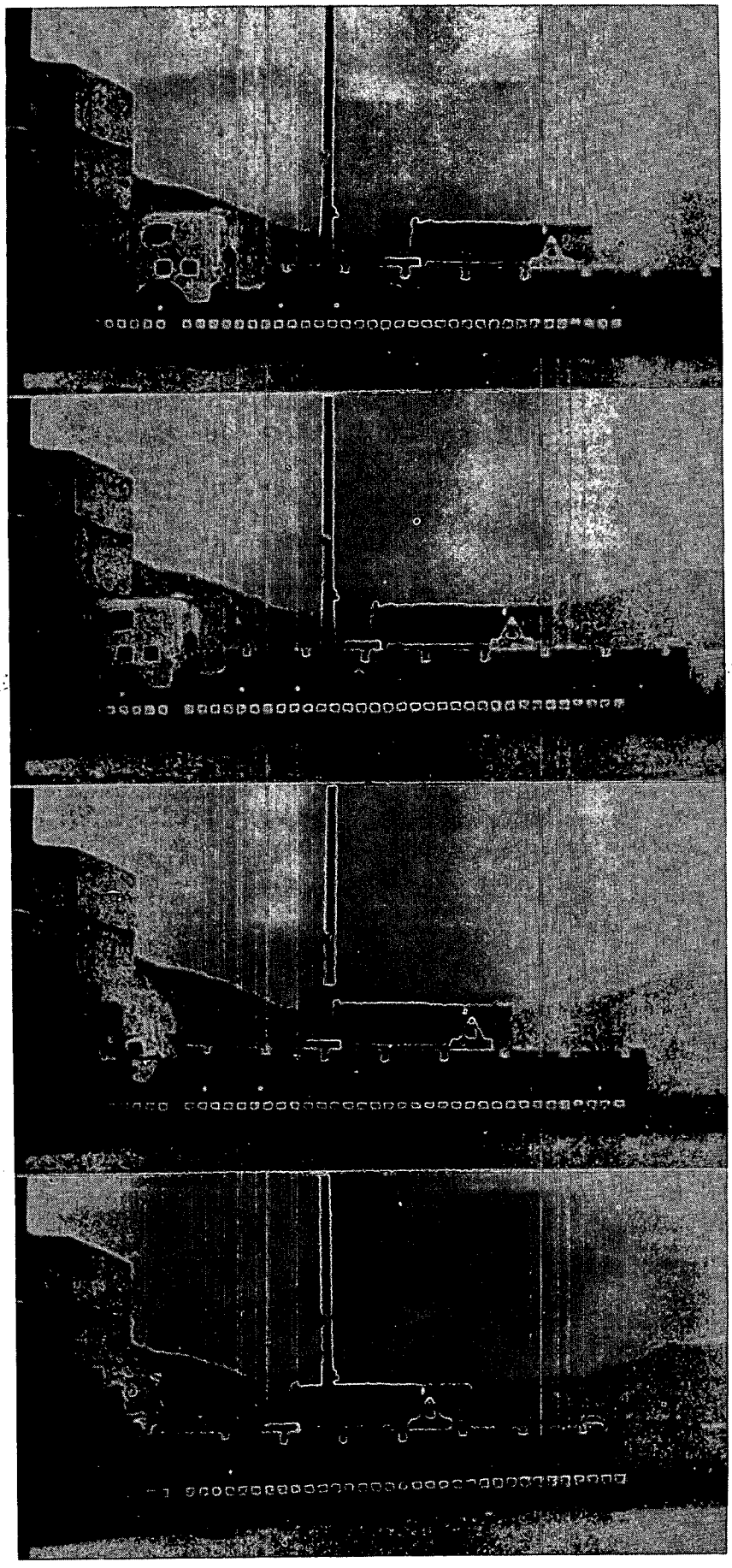

Figure 4.16 Second test event sequence to 0.050 second.

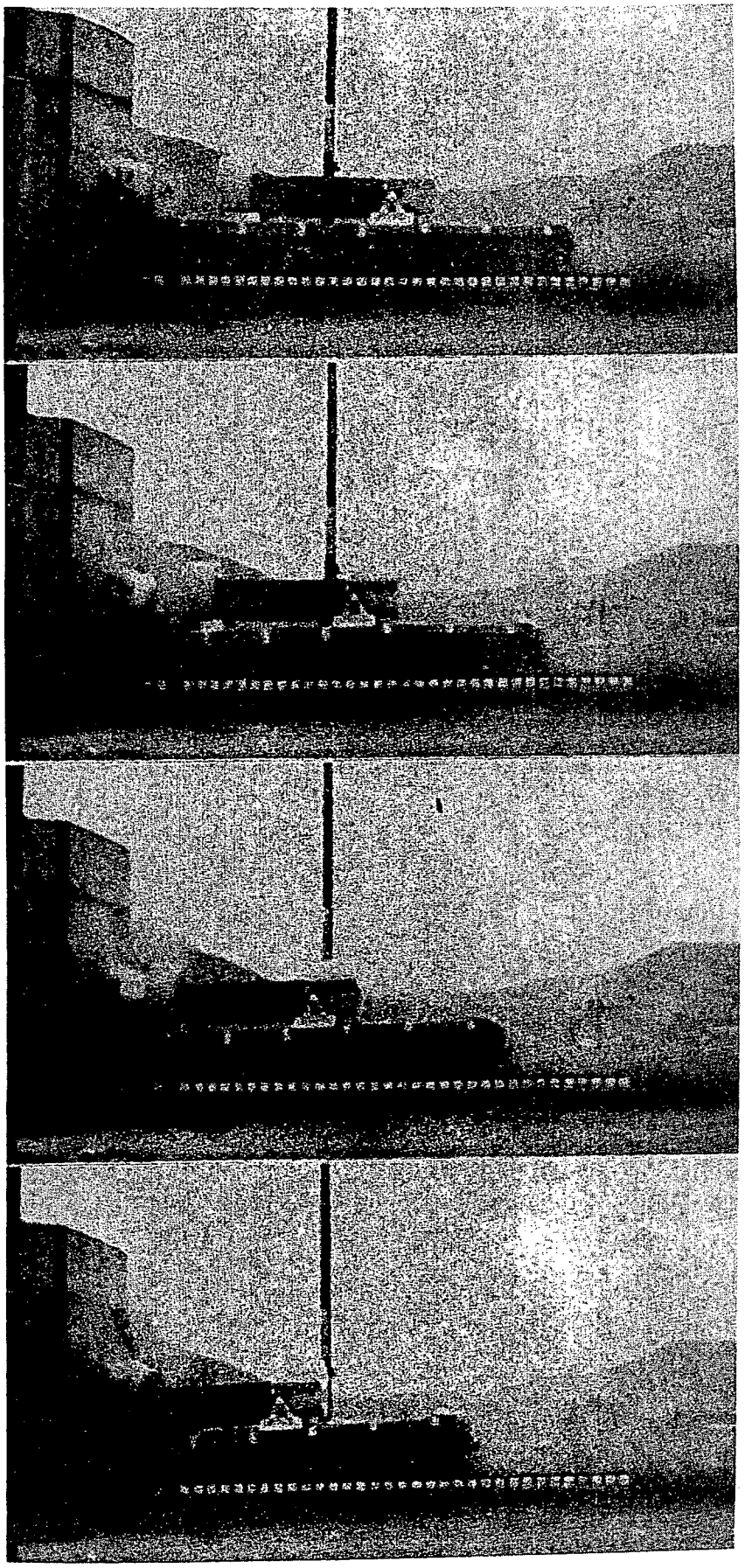

Figure 4.17 Second test event sequence from 0.075 to 0.150 second.

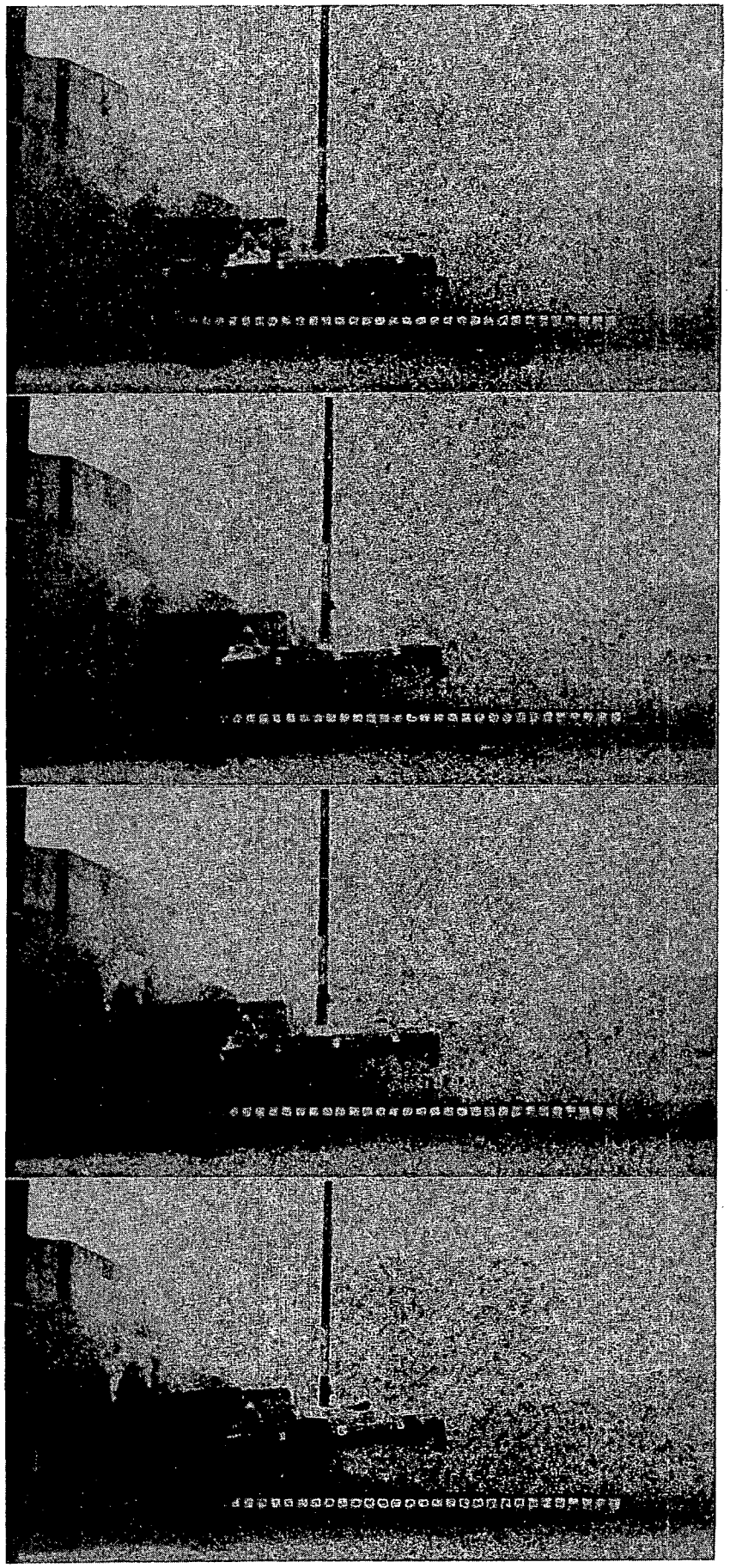

Figure 4.18 Second test event sequence from 0.175 to 0.250 second.

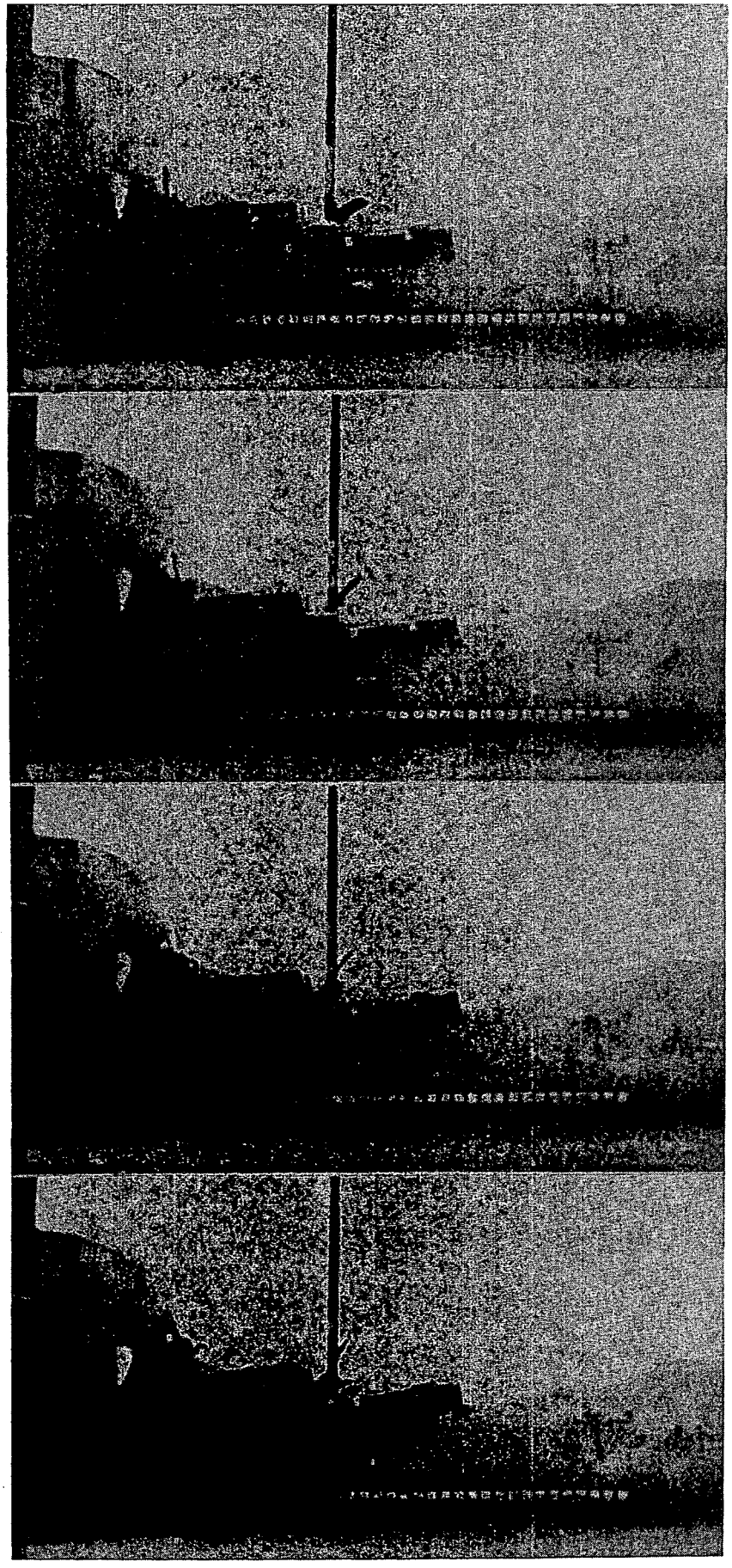

Figure 4.19 Second test event sequence from 0.275 to 0.350 second

TIME (SECONDS)	EVENT
0.00	Tractor contacts face of target.
0.034	Fifth wheel connection breaks.
0.036	Tandem axle assembly shears off.
0.044	Trailer contacts back end of cab.
0.078	Trailer encounters hard target
0.091	Buckling is initiated in trailer frame
0.127	Front end of impact limiter contacts cab
0.154	Cab is completely crushed.
0.190	Cask comes to a horizontal stop.

In this test, the cask encountered a hardened target at about 100 kph (62 mph). This severe impact caused relatively little damage to the cask, while totally demolishing the vehicle. Figure 4.20 is an overall view of the area after the test. In this figure, it can be seen that the cask remained attached to and upright with the trailer. The front impact limiter, which can be seen in Figure 4.20, came to rest some distance away from the cask after being ejected upwards.

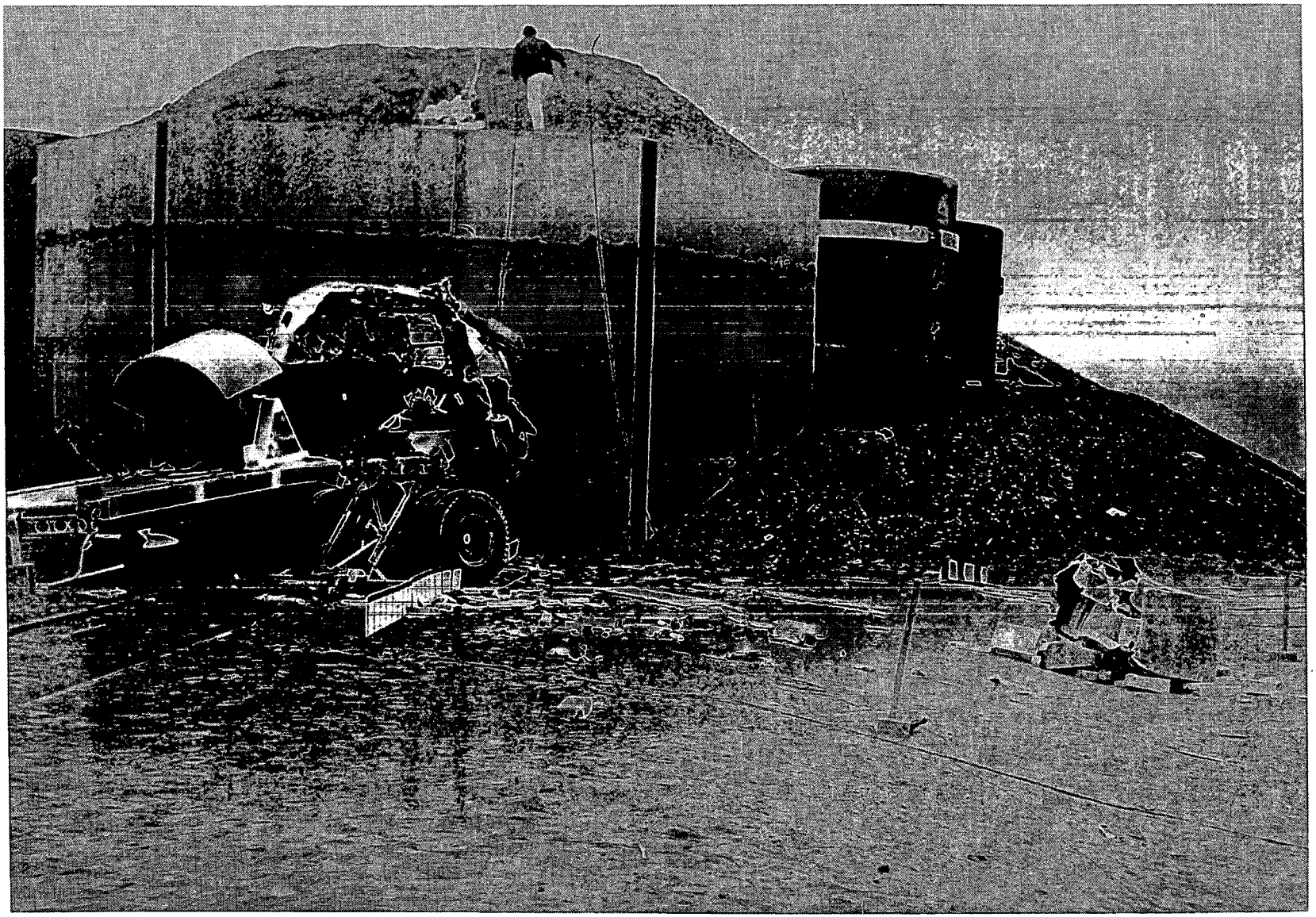

Figure 4.20 Overall view of the transport system and target area after the second test.

Figure 4.21 illustrates the system from the side. As in the first test, the truck cab was severely crushed, but this time to a slightly greater degree. The structures which came between the cask and the target were compressed to a thickness of about 13 cm (5 in.). The front end of the trailer structure crushed and buckled upward but did not travel up the target as far as in the first test. The kingpin, which connects the trailer to the tractor, was caught between the cask head and the target, leaving an indentation in the cask head. In a fashion similar to the first test, all the axle assemblies broke free from the frames

Figure 4.22 is a closeup view of the cask and trailer after the test. There was some very slight bulging on the front end of the cask and radial cracking of some of the cooling fins near the front. The fuel containment ability of the cask, however, was not threatened. There was minor seepage of water which first became noticable after the cask was being lifted out of the wreckage. It was estimated that about 100 cc of coolant leaked. No moisture could be detected on the trailer structure; hence, the seepage was initiated in the process of removing the cask from the wreckage.

Figure 4.23 illustrates the front end of the cask after the impact. As can be seen, the cover is firmly in place. The most readily apparent damage is the indentation in the head caused by the kingpin. Figure 4.24 and 4.25 illustrate both sides of the front end of the cask after the impact. Some slight bulging and radial cracks of the cooling fins are noticeable in these photographs. Also, it can be seen that

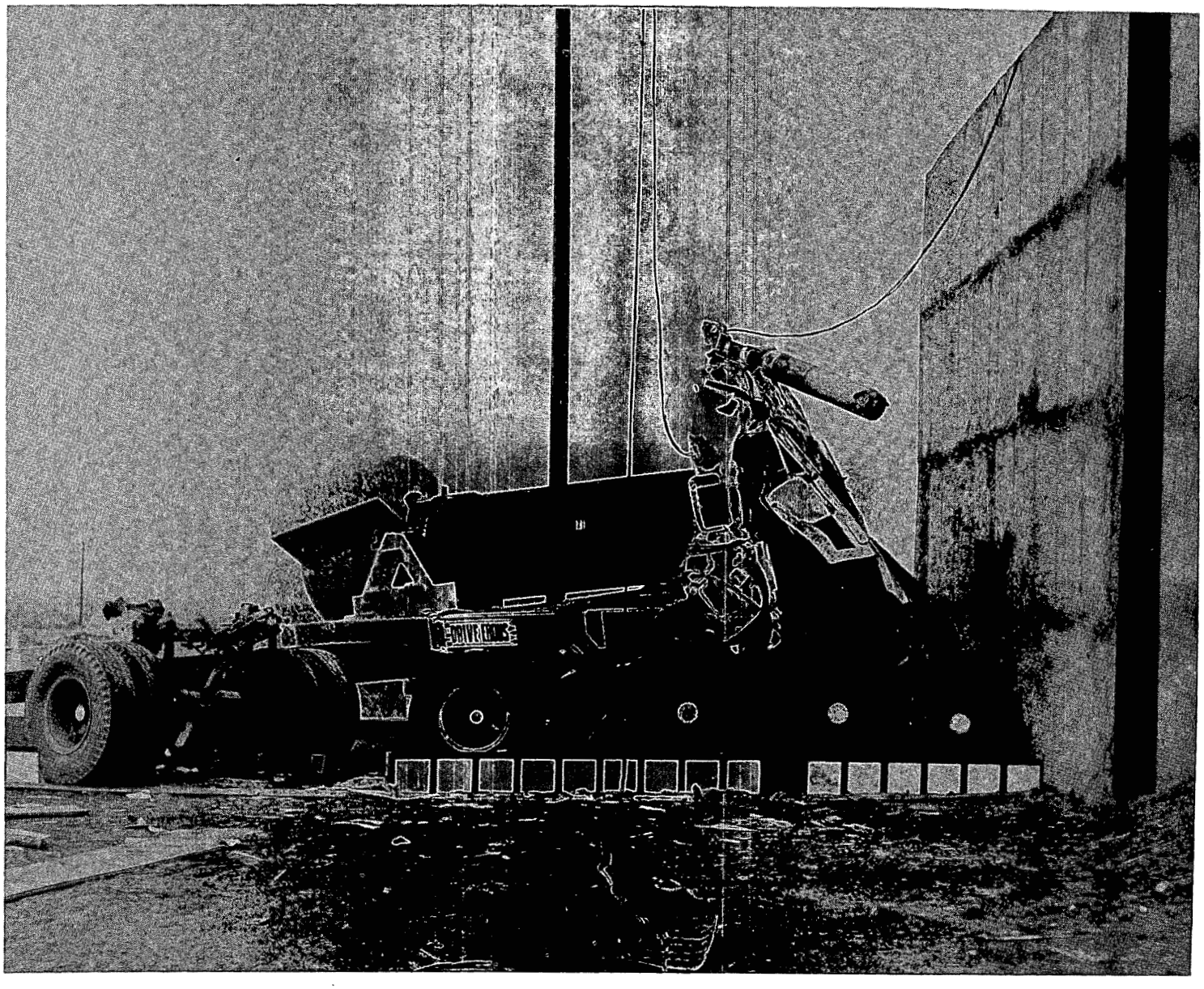

Figure 4.21 Side view of the transport system after the second test.

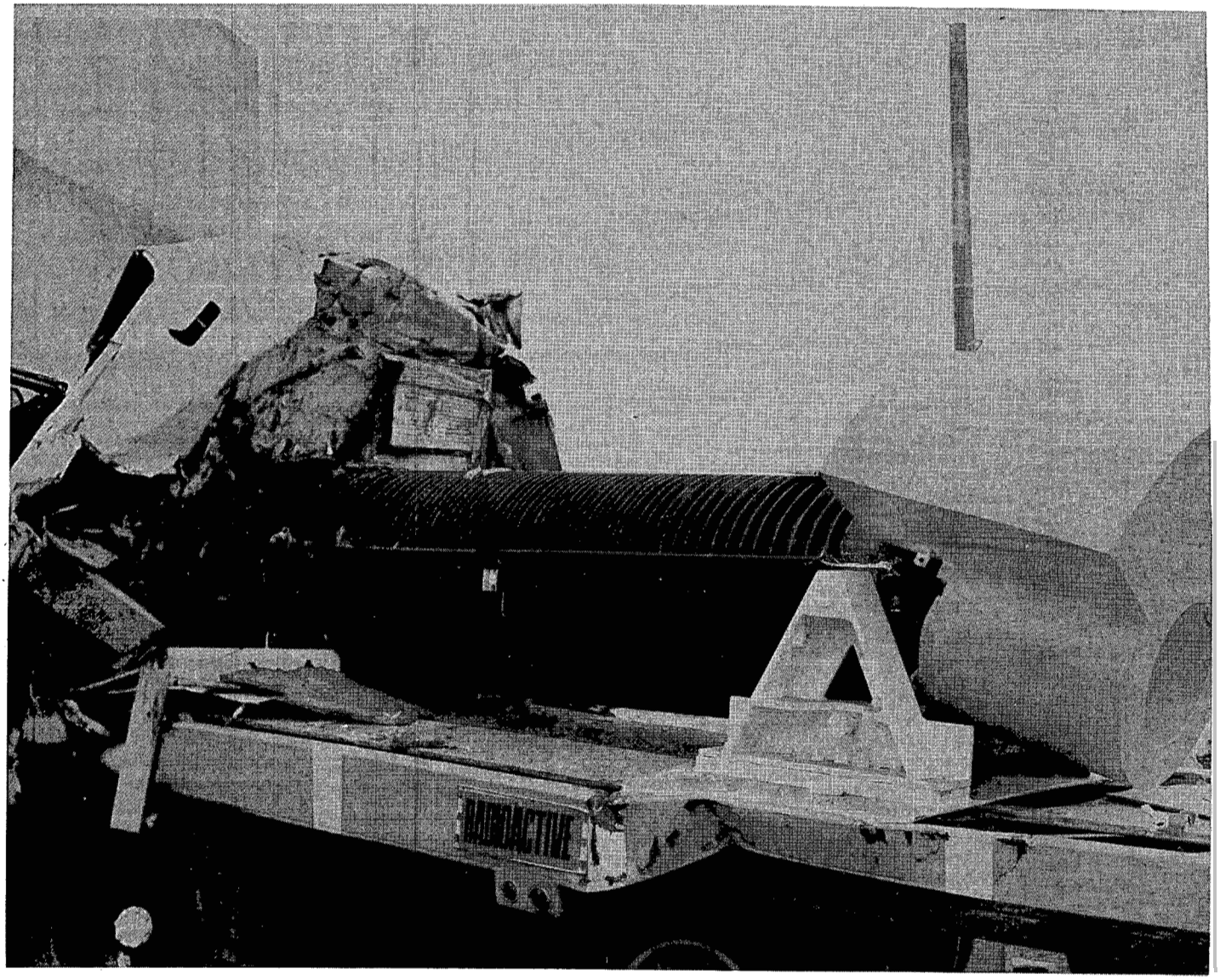

Figure 4.22 Close up side view of the cask and vehicle after the second test.

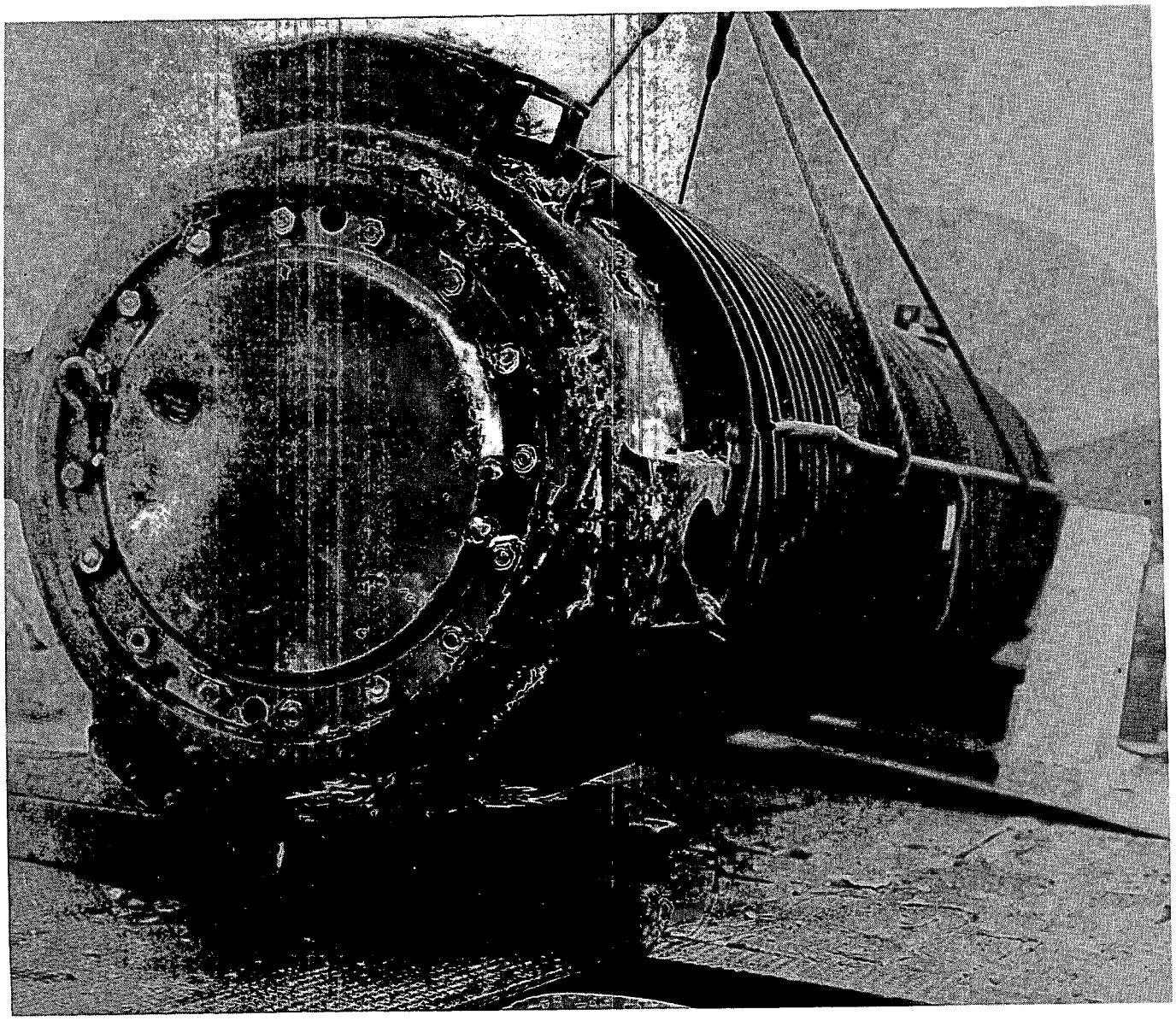

Figure 4.23 End view of the impact end of the cask after the second test.

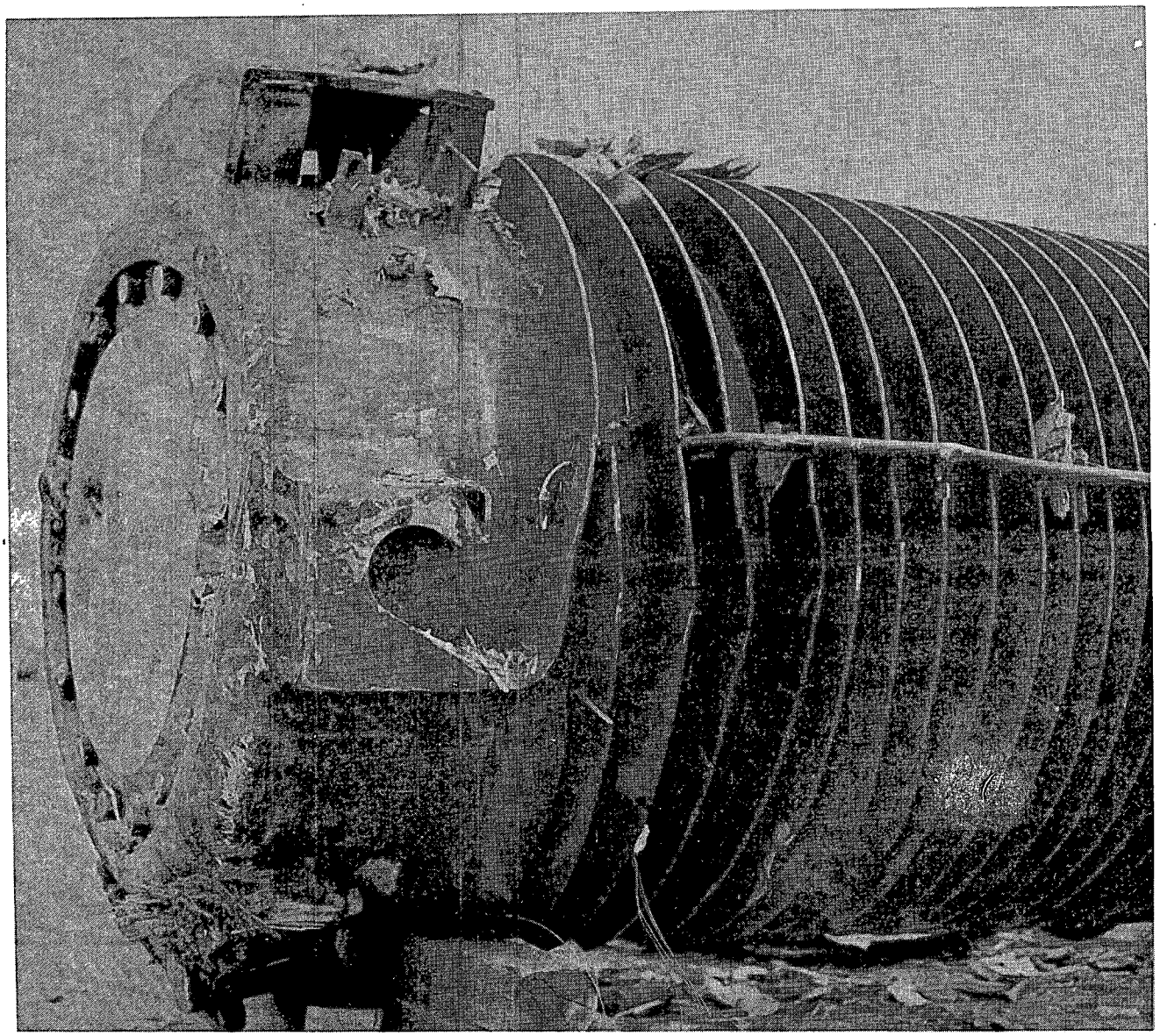

Figure 4.24 Left side view of the impact end of the cask after the second test.

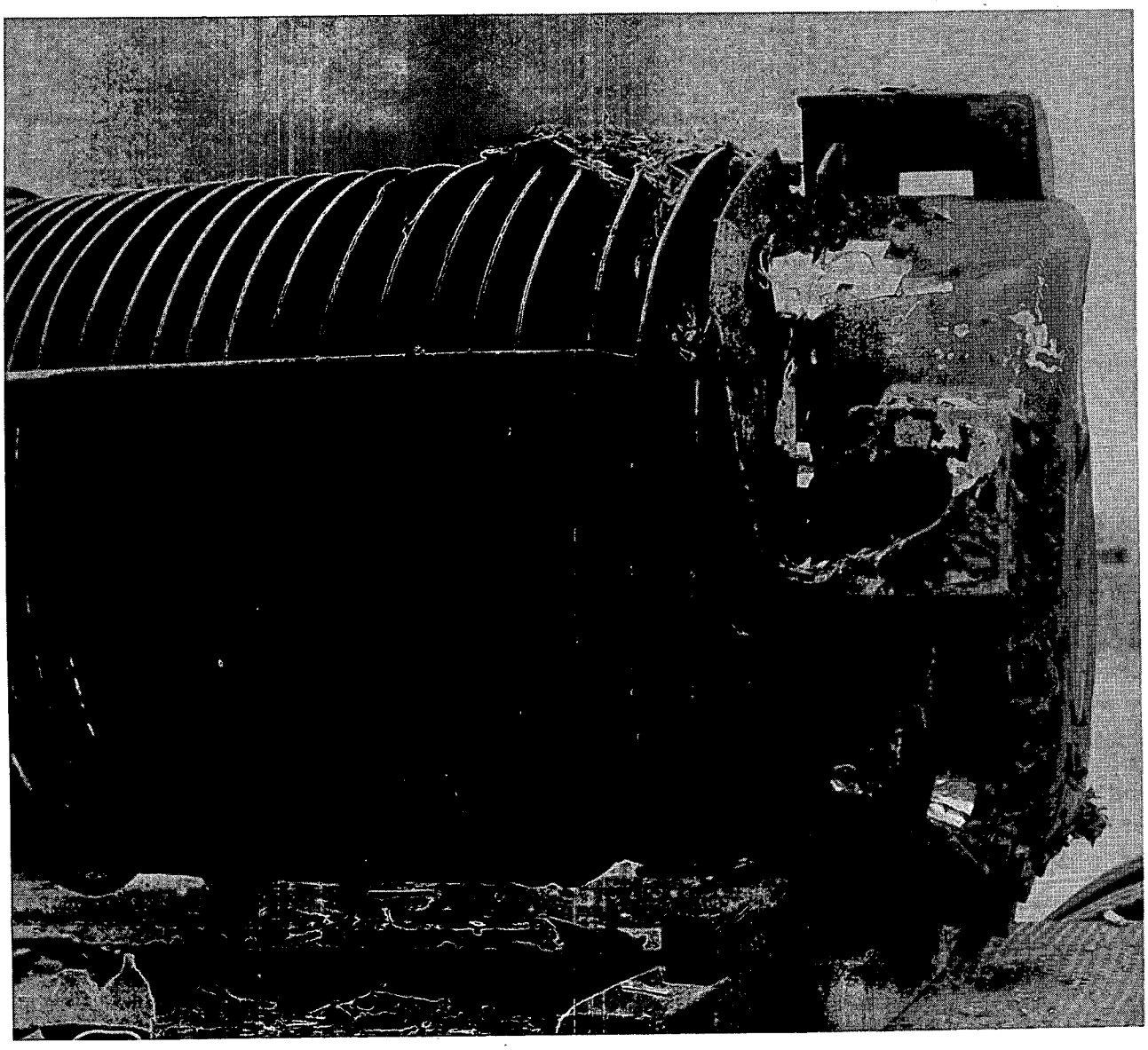

Figure 4.25 Right side view of the impact end of the cask after the second test.

the front attachment plate on the cask was bent backwards somewhat.

Figure 4.26 illustrates, in an exaggerated fashion, the average cask deformation profile obtained from post-test measurements of the cask. The maximum hoop strain was 3%. The deformation was largely confined to the front 1.5 m (60 in) of the cask. A length measurement on the cask indicated that it shortened by 6 cm (2.36 in) or 1.6%. On the back end of the cask, there was a .95 cm (.375 in) gap between the lead shielding and the outer shell.

The instrumentation and data reduction for the second test were similar to that of the first. Again, data were obtained from motion picture films and from onboard instrumentation. Pertinent data for this test are included in Appendix H.

For purposes of comparison with the first test, a deceleration plot was calculated from the film velocity-time data as in the first test. Figure 4.27 illustrates the results. As can be seen, it was calculated that the cask sustained a deceleration of 70 g's, which is approximately four times higher than in the lower velocity test. Figure 4.28, also obtained from film data, is a plot of cask deceleration as a function of cask displacement.

The displacement-time curve for the cask, included in Appendix H, is more linear than the corresponding curve for the firest test and indicates that the cask traveled to its maximum horizontal displacement in 0.19 second. The velocity-time curve for the cask obtained from this test is not as smooth as that from the first test indicating a

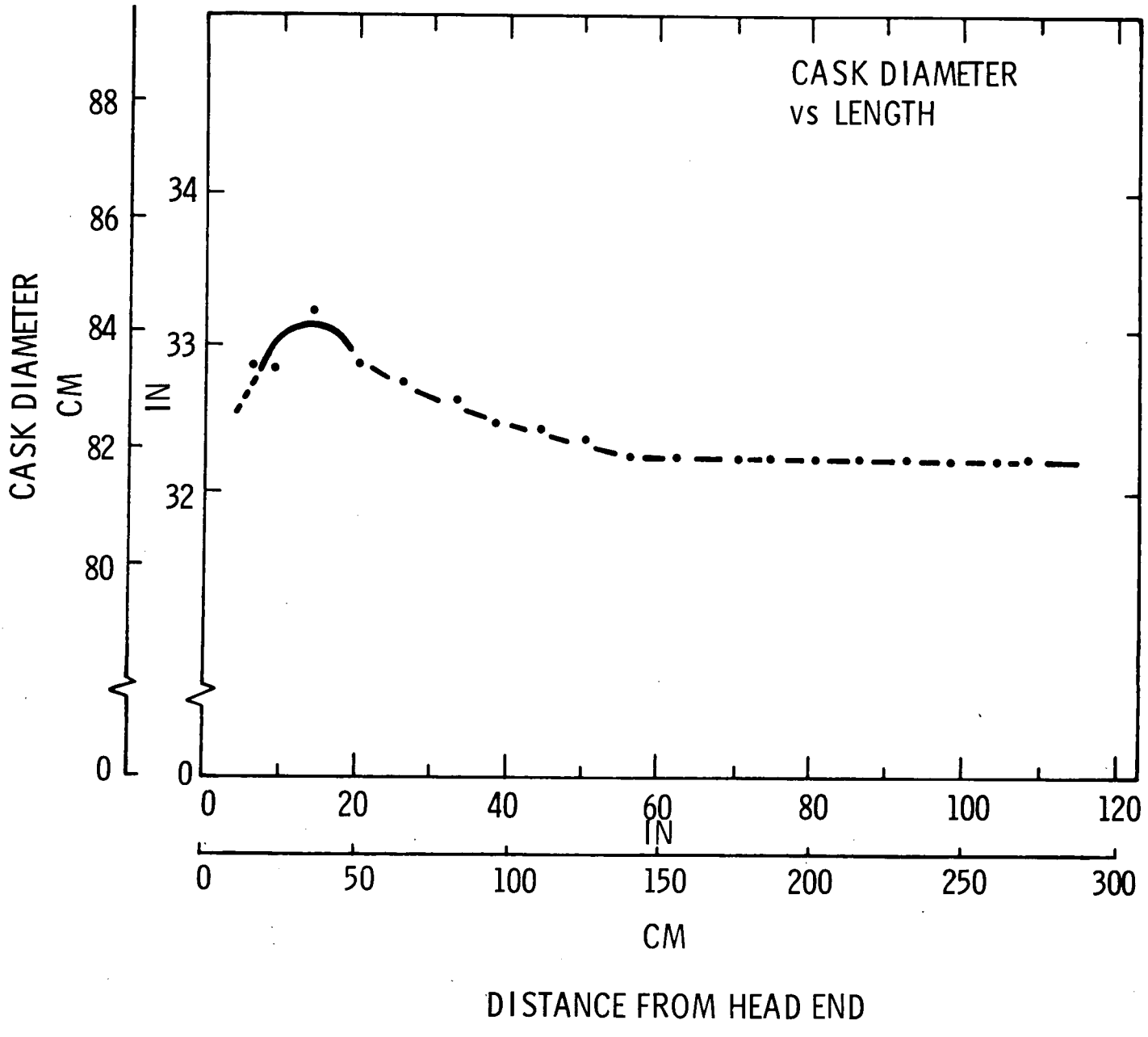

Figure 4.26 Deformation pattern for the full-scale cask after the second test.

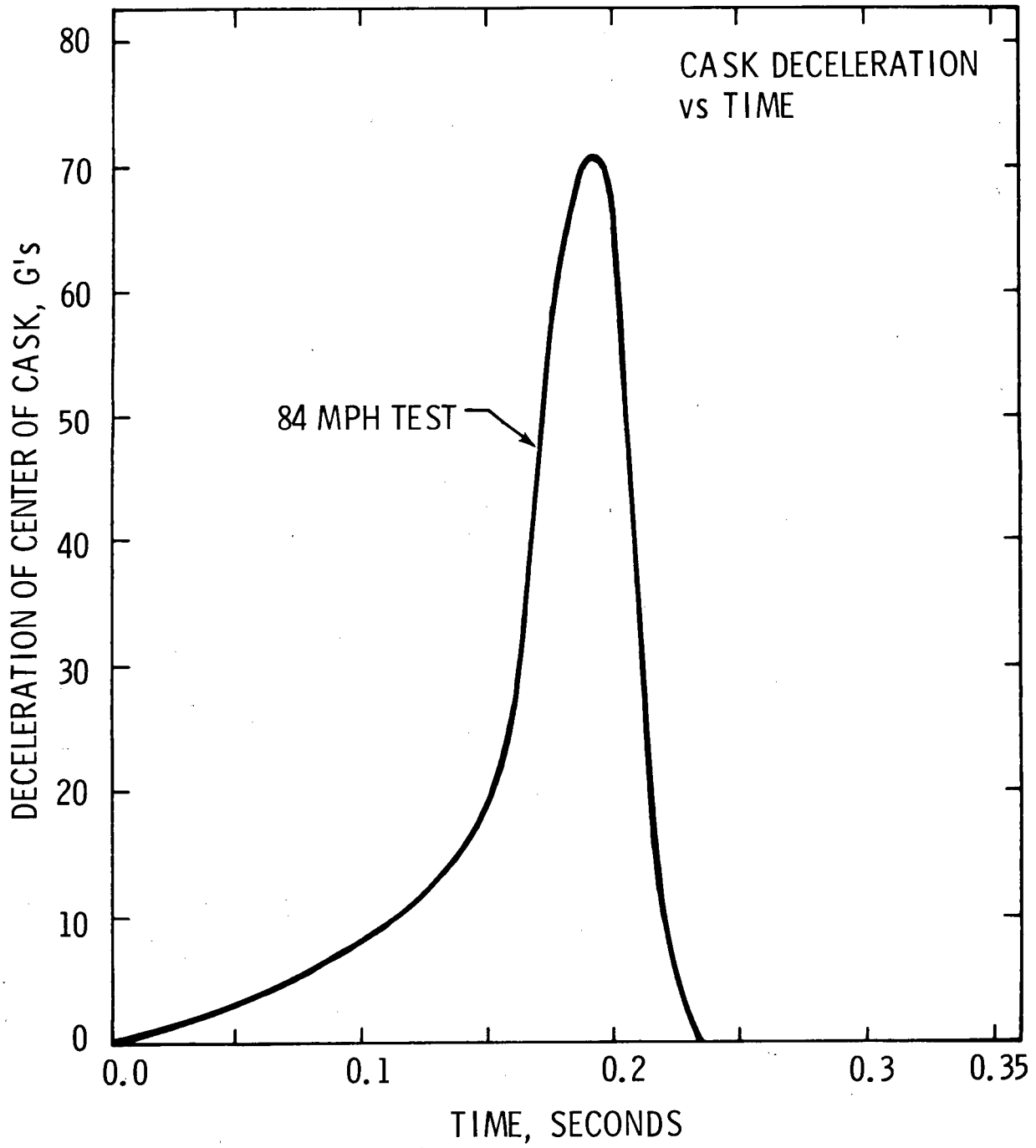

Figure 4.27 Cask deceleration as a function of time for the second test (from film data).

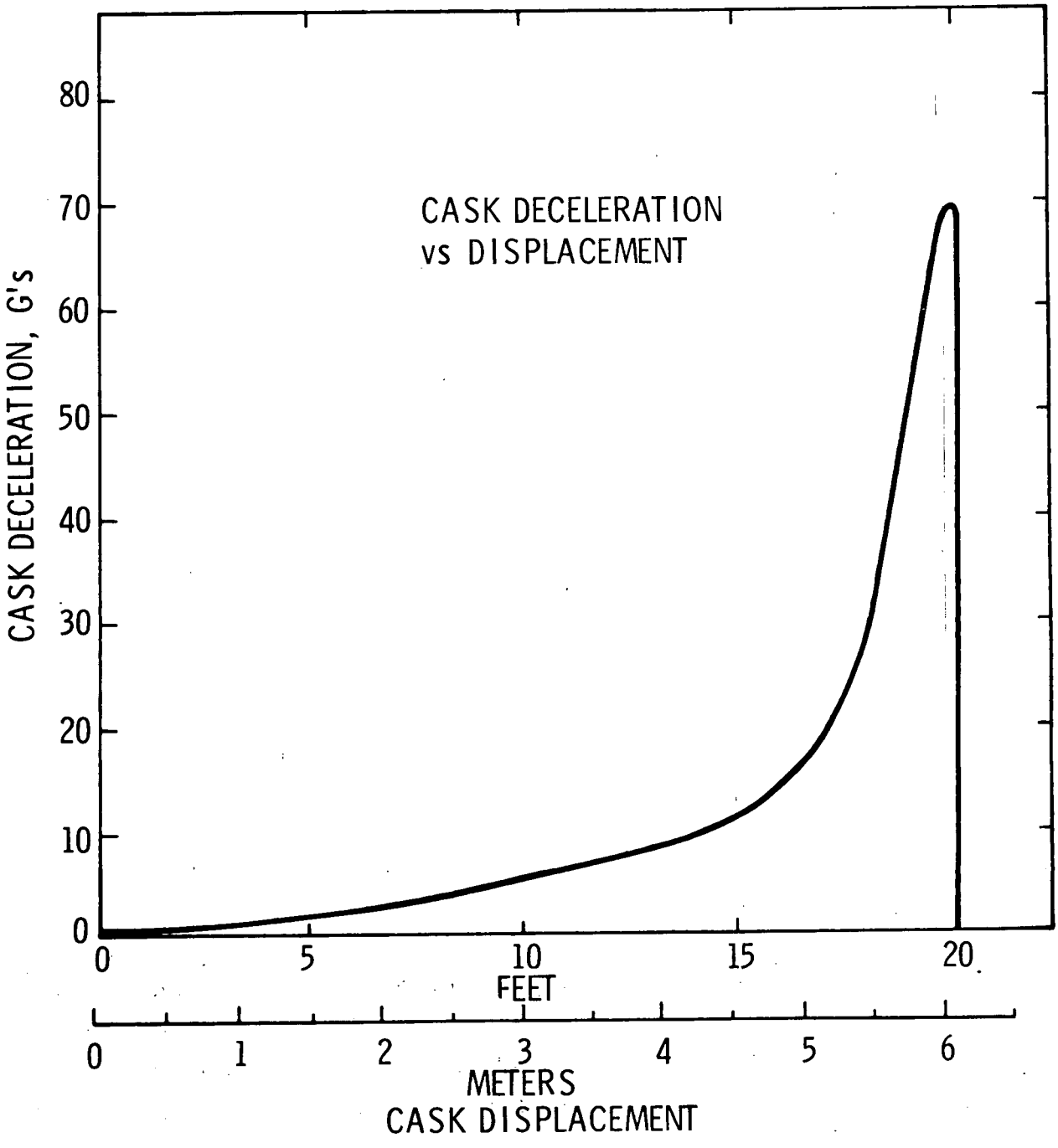

Figure 4.28 Cask deceleration as a function of displacement for the second test (from film data).

definite change in slope at 100 kph (62 mph), corresponding to an elapsed time of 0.155 second. At this point in time, the vehicular structures between the cask and the target were completely crushed and resistance to cask motion stiffened. The final slope of the curve indicates an average cask and trailer deceleration of approximately 70 g's.

The cask attitude throughout the impact in the second test remained much more horizontal than in the first test as indicated by the plot in Appendix H. The cask angle at the time that it bottomed out against the target was 2° from horizontal.

Five accelerometer traces from different locations on the cask were obtained from this test. Peak accelerations recorded varied from 125 to 185 g's. The active accelerometers on the trailer structure were lost partially through the impact. They recorded a maximum of 50 g's prior to failing. Again, all accelerometer signals were filtered to 50 Hz.

The passive accelerometers again indicated unrealistically high levels which were not very different from those recorded in the first test. Levels as high as 1000 g's on the trailer structure and 800 g's on the cask were observed.

The water pressure transducers inside the cask were destroyed in the impact. The recording system for the target accelerometers also malfunctioned. However, close examination of the films did not reveal any detectable target motion.

The cask active accelerometer signals were integrated to calculate displacement-time and velocity-time curves for the cask. The five accelerometers gave very similar results. Curves corresponding to the back left accelerometer have been included in Appendix H. These accelerometer results are again in good agreement with the film data in terms of pulse shape and times. The peaks, however, are somewhat higher than those indicated by the film data. The integrated accelerometer velocity and displacement data are also in good agreement with the film data.

The strain gages on both sides of the cask gave very similar readings. They indicated low strains up to about 0.18 second. At this time, the signals took a large step jump to the maximum value of the calibration range, well beyond the yield point of the material. Thus, the strain gages indicated that the cask did not sustain permanent deformations until very late in the impact. The results from the right side rosette have been included in Appendix H.

The impact firmly wedged the head in place and it was removed only with considerable difficulty by jacking it out with screws. After the head was removed, a large force had to be applied to pull out the fuel elements. This was due to the formation of a slight bulge on the inner diameter at the impact end. Figure 4.29 illustrates the elements being pulled out. As can be seen, some of the individual fuel rods buckled in the impact, but the bundle retained its basic configuration. Figure 4.30 illustrates the overall condition of the fuel bundle. Also, the ballast attached to the back end can be seen in this figure.

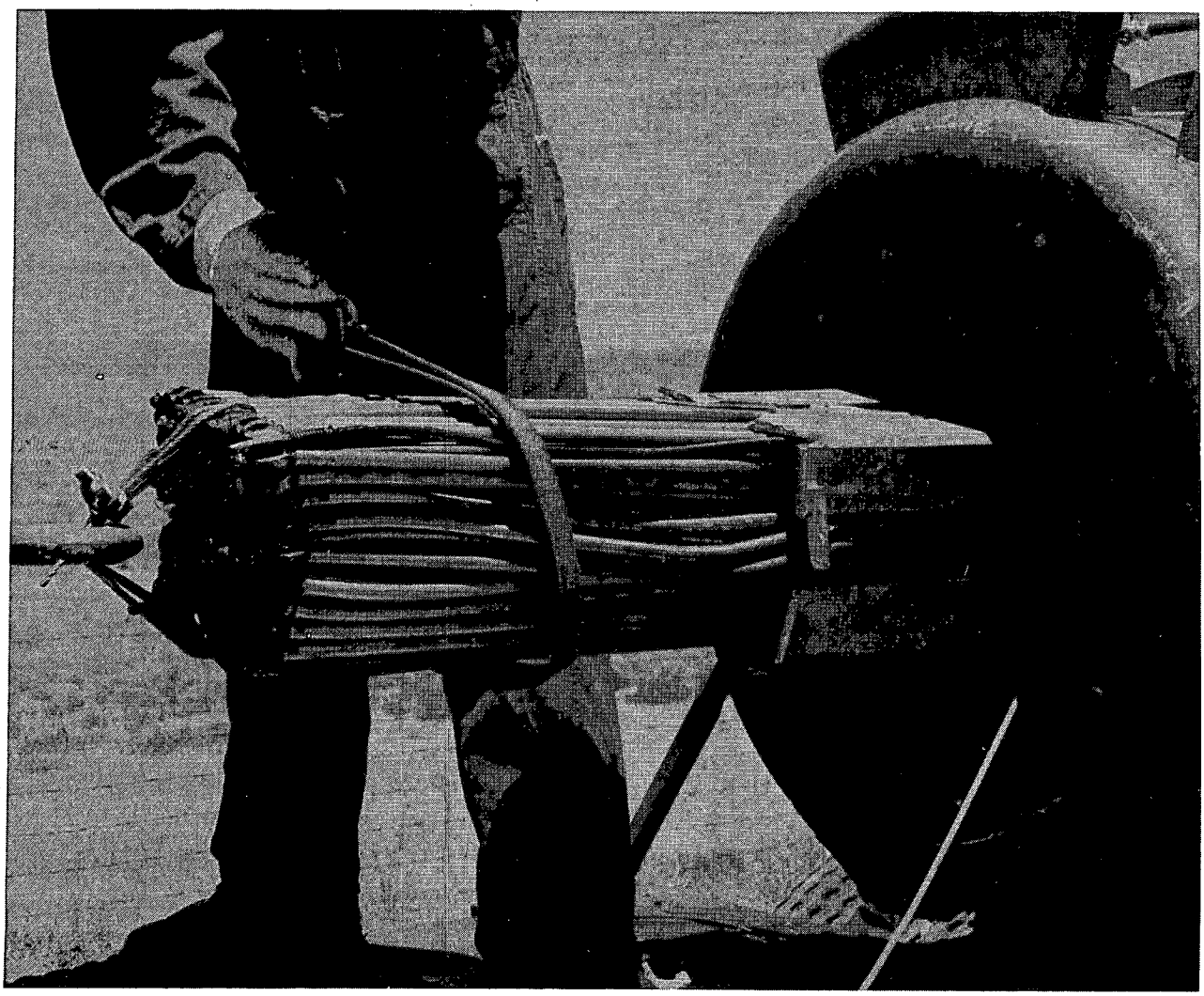

Figure 4.29 Fuel bundle being pulled out of the cask after the second test.

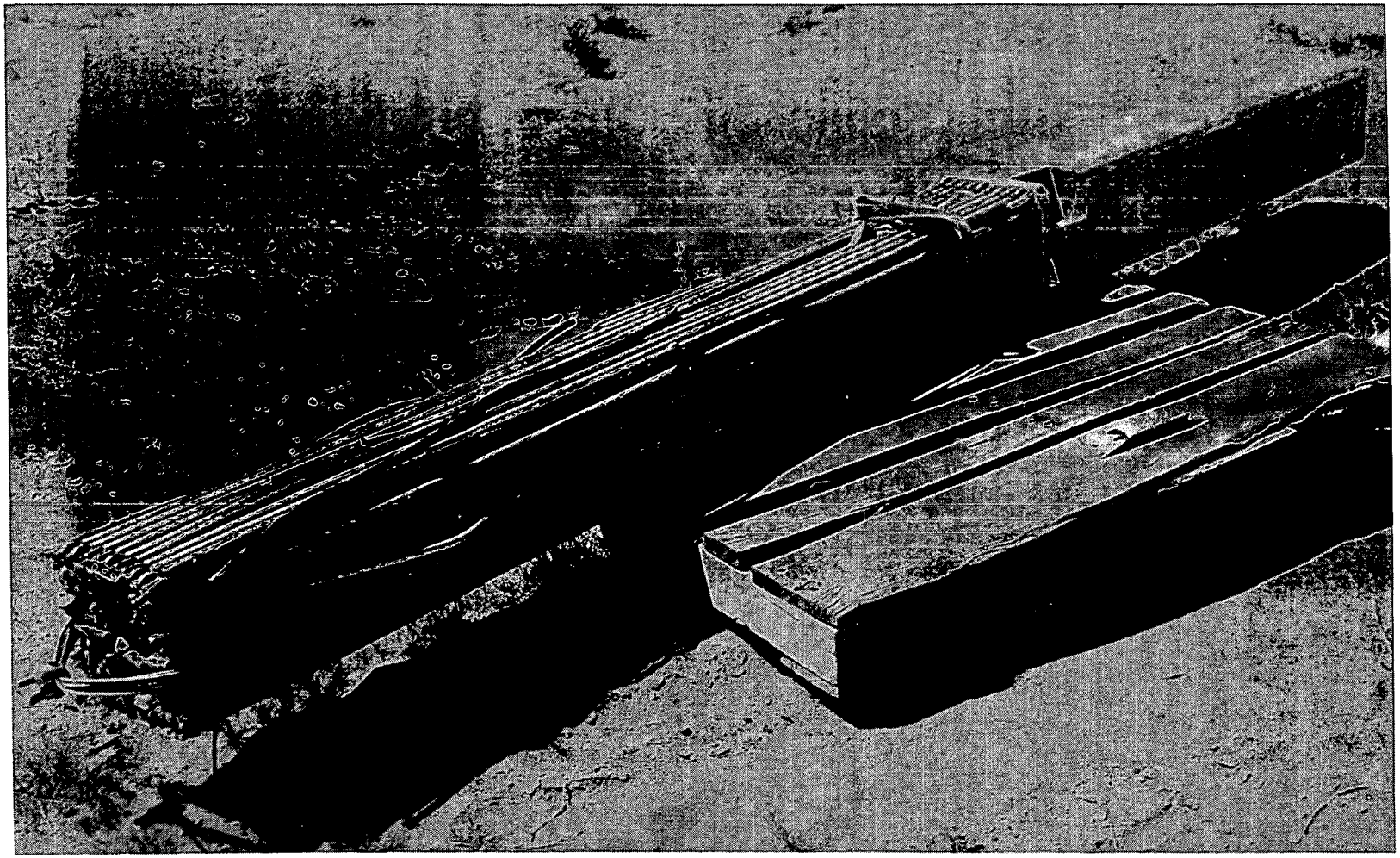

Figure 4.30 Fuel bundle and ballast after the second test.

4.4 Discussion

In the first test at 98 kph (61 mph) the main cask body was not permanently deformed. This was due to the energy shock attenuation of the vehicle and impact limiter and to the fact that the tiedown system held the cask to the trailer structure. The second test, at 135 kph (84 mph) representing twice as much kinetic energy in the system, resulted in very minimal damage to the cask and did not pose a serious threat to its fuel containment ability. In this second test the vehicle structure did not have sufficient energy absorption capability to prevent the cask from encountering a hard target at a relatively high velocity. The front impact limiter did not remain in place and its effect was very minimal. The resultant damage to the cask would not have been greatly different if it had not been dislodged. This is due to the fact that, at impact, the cask had several times more energy than the limiter could be expected to absorb.

The deceleration levels encountered by the cask at various displacements and down to a point near to the face of the target were almost identical in the two tests. This can be verified by superimposing the deceleration-displacement curves from the two tests and shifting the curve from the second test to the right 30 cm (1 ft) to account for the slight difference in fifth-wheel locations. When this is done, the curves can be seen to be in very good agreement to a point about 1 m (3.3 ft) from the maximum displacement. At this point the curves diverge with the peak from the second test being much higher. The excellent agreement throughout the majority of the crush-up phase indicates that structurally the two vehicular systems responded almost identically in terms of crush force and energy absorption.

An estimate of the buckling strength of the front portion of the trailer structures can be obtained by noticing the times at which buckling occurred in the series of photographs from the tests and by finding the corresponding g level in the deceleration-time plots. It will be found that in both cases the deceleration level at that point in time was about 8 g's. Assuming that a mean of 25,000 kg (55,000 lb) is being decelerated, the crush or buckling strength of the trailer was approximately 440,000 lb, which is very close to the number estimated in the lumped parameter model (Appendix A, Figure A-4).

Regarding the behavior of the tiedowns, it should be noted that they were designed to withstand an axial, lateral, 10-g loading. This is approximately what the cask sustained during crush up of the front end of the trailer. Had the trailer structure been slightly stronger, it is possible that the tiedowns would have failed. The tiedown system was just strong enough to take advantage of the energy absorption capability of the trailer. In this respect, the transport system tested was apparently a well-balance design.

In the first test, the deceleration levels calculated from the film data agreed well with the accelerometer results. In the second test, the accelerometer signals exhibited peaks which were somewhat higher than the film data indicated. It must be deduced that the discrete film data are not sufficiently fine to capture some of the high frequency peaks. They do, however, give a pulse shape which is representative of a rigid body deceleration for the cask. This was verified by integrating the film deceleration-time plots (Figures 4.14 and 4.27). In each case, this procedure

indicated the correct velocity change which the cask underwent.

The strain gage data from the second test indicated that the strain went beyond the elastic range at 0.18 second. This corresponds to approximately the last 15 cm (6 in) of travel. Thus, the cask thoroughly compressed the cab and buckled-up portion of the trailer structure before it began to deform. Consequently, the deformations which the cask body sustained occurred only during the last 10 milliseconds of the impact.

The passive accelerometer data which was recorded indicated unrealistically high deceleration levels. It must be deduced that the response of the structure was such that it caused the small ball inside the units to impact the crush dish repeatedly, producing a cumulative effect. In other words, the accelerometers "rattled" and gave erroneous readings. Any future use of these devices on full-scale tests should be carefully evaluated.

5.0 Comparison of Analysis and Scale Model Tests to Full-Scale Test Results

5.1 First Test

The mathematical analysis and scale model tests closely predicted the results of the first full-scale test.

In comparing the full-scale test results with the lumped parameter model predictions, the response of the full-scale system closely paralleled the calculated favorable results. These results, as described previously in Section 2.2, indicated that the cask would decelerate gradually while crushing the vehicle structures. It was calculated that the tractor would be completely demolished and that the front portion of the trailer would be extensively damaged. The results also indicated that the kinetic energy of the cask would be expended before the impact limiter was completely crushed. Thus, calculations indicated that under these conditions the cask would not see a hard target and would not undergo any permanent deformations to its basic body structure. This predicted behavior was observed in the full-scale test.

The full-scale test results also agreed well with the observed behavior in the scale model test. As the scale model predicted, the tractor was completely demolished and the king pin connection broken. The front portion of the full-scale trailer structure plowed through the cab, hit the target, and buckled upward, coming between the cask and the target. The cask hit the target in close to an end-on

attitude but did not completely crush the limiter nor did it sustain any deformation to its basic structure. All of this predicted behavior was observed in the scale model test. Comparisons of model-to-prototype behavior can be made by examining Figures 3.2 - 3.3 and 4.9 - 4.13.

For purposes of a more quantitative comparison, Figure 5.1 compares the displacement-time results from the numerical analysis and the scale model test with results from the full-scale test. As can be seen, both analysis techniques (numerical and scale modeling) agreed well with the full scale tests results. Figure 5.2 illustrates a comparison of the velocity-time results. As can be seen, both the numerical lumped-parameter model and the scale-model results closely paralleled the velocity-time history for the full-scale cask. The damage which the cask sustained was also well predicted. The mathematical model predicted that the impact limiter would not be completely crushed. This precluded any deformation to the basic cask structure. In the scale model test, it was observed that indeed the impact limiter was not fully compressed. The model cask did not sustain any measurable deformation. In the full-scale test, the basic cask-body structure likewise was completely underformed, verifying the predictions.

5.2 Second Test

The response of the full-scale system in the second test also agreed well with pretest predictions based on mathematical analysis and scale modeling.

The numerical analysis for the second test indicated that the vehicle system would be destroyed in much the same

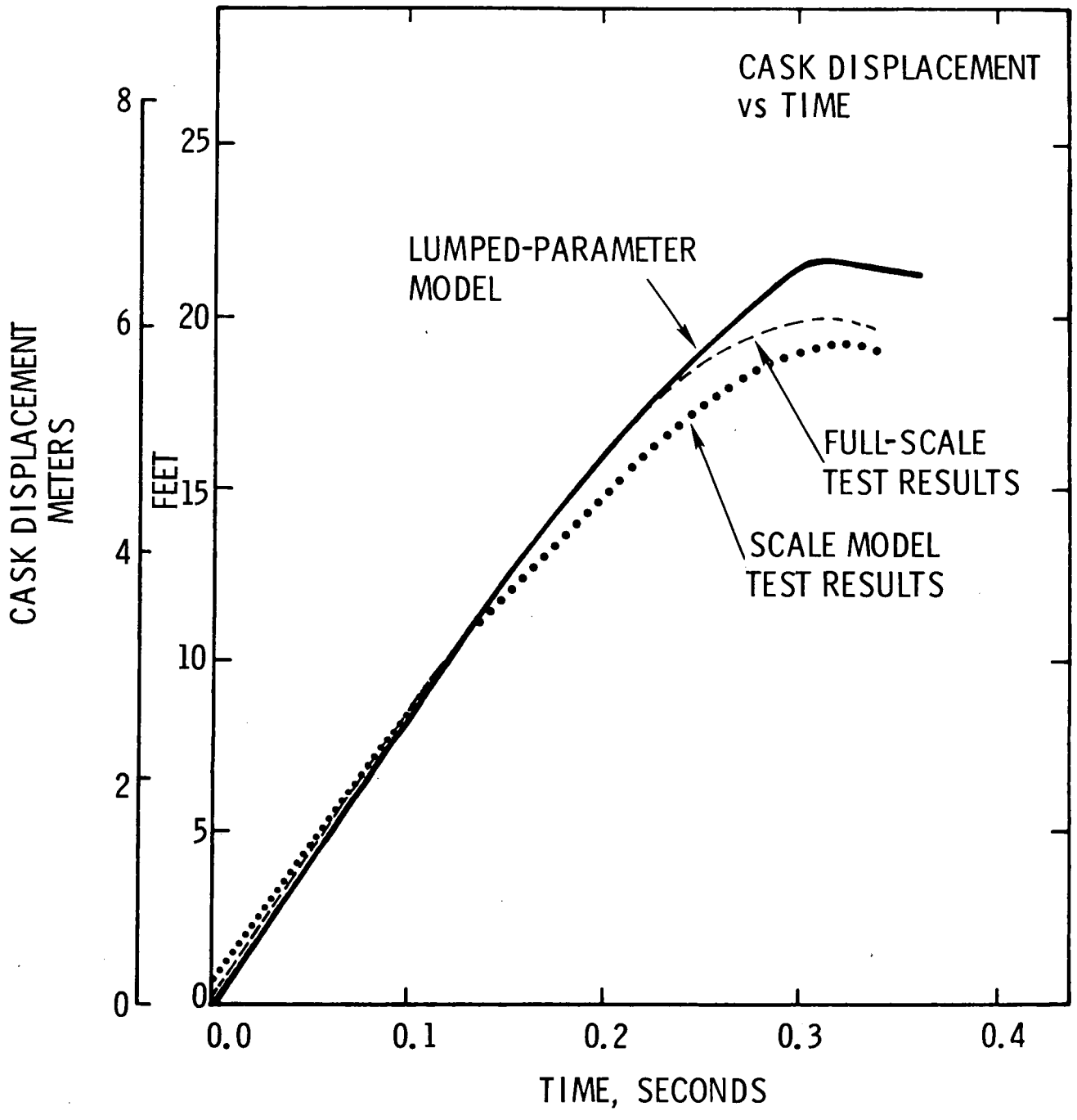

Figure 5.1 Cask displacement as a function of time for the first test from analysis, scale model, and full-scale.

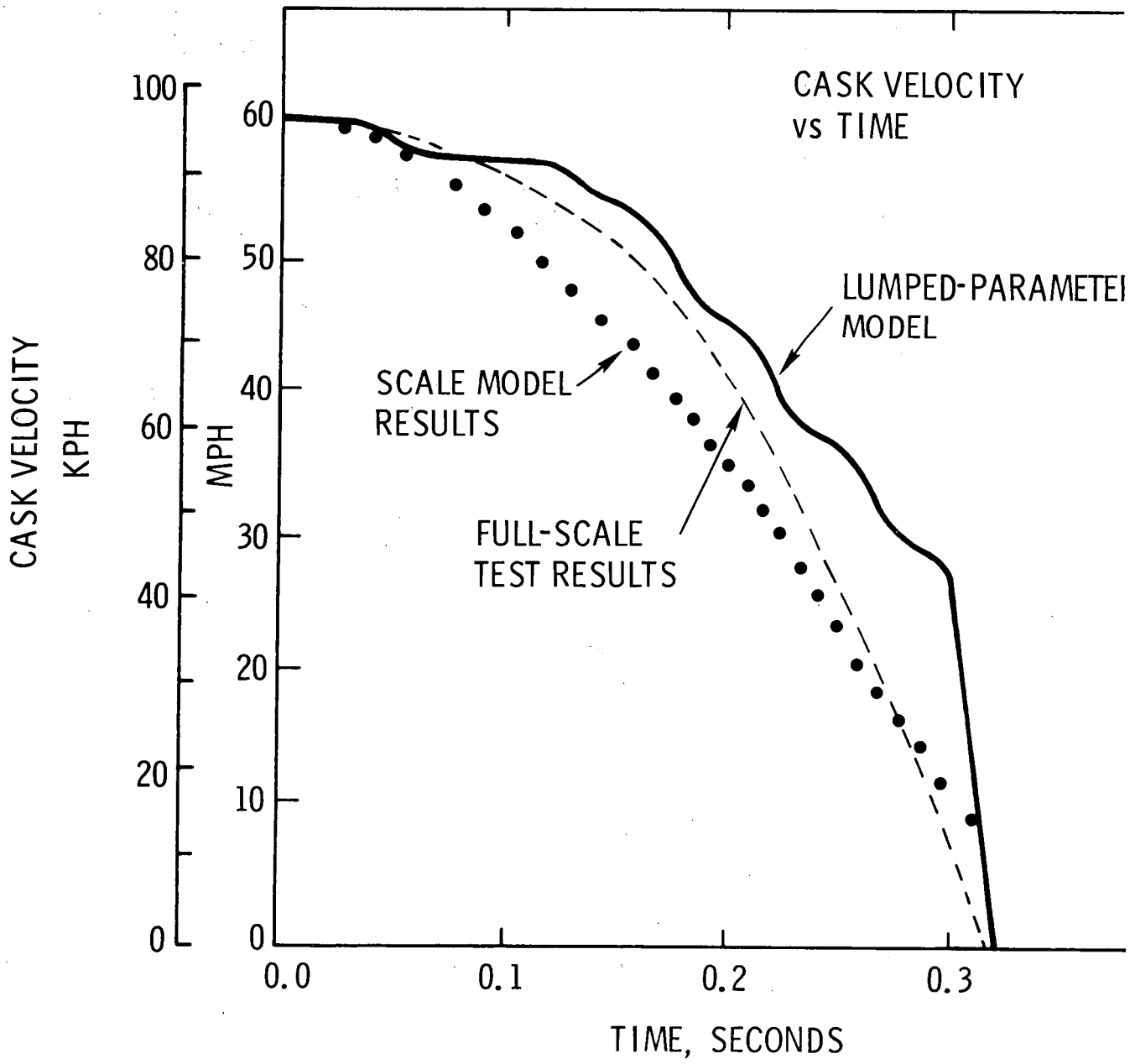

Figure 5.2 Cask velocity as a function of time for the first test from analysis, scale model, and full-scale.

manner as in the first test but more quickly with the duration of the event being 0.2 second. It predicted that the cask would impact the target at a relatively high velocity, completely crushing the impact limiter. Thus, the analytical model predicted that the cask would undergo some permanent deformation.

Figure 5.3 illustrates the displacement-time results from the second full-scale test superimposed on the favorable lumped-parameter model analysis of Section 2. As can be seen, the displacement-time behavior of the full-scale system closely paralleled the behavior predicted by the analysis. Figure 5.4 illustrates a comparison of the velocity-time results, which also show good agreement. The deceleration of the cask in the full-scale test proved to be smoother than the model had predicted. Close examination of the films indicated that the cask encountered a hard target (after completely crushing the vehicle structures) at 100 kph (62 mph). This compares with a value of 105 kph (65 mph) predicted by the lumped-parameter model. The final deceleration of the cask in the full-scale test was milder than the model predicted. The time duration of the impact and the general shape of the velocity-time curves were in excellent agreement.

The dynamic finite-element model results described in Section 2.3 proved to be on the conservative side, as expected, but still gave excellent indications of how the cask would deform in the final impact into the target. An examination of the deformed finite-element mesh (Figure 2.7) and the measured deformation contour of the cask (Figure 4.26) indicate excellent qualitative agreement, although the peak deformation predicted was over estimated. The model

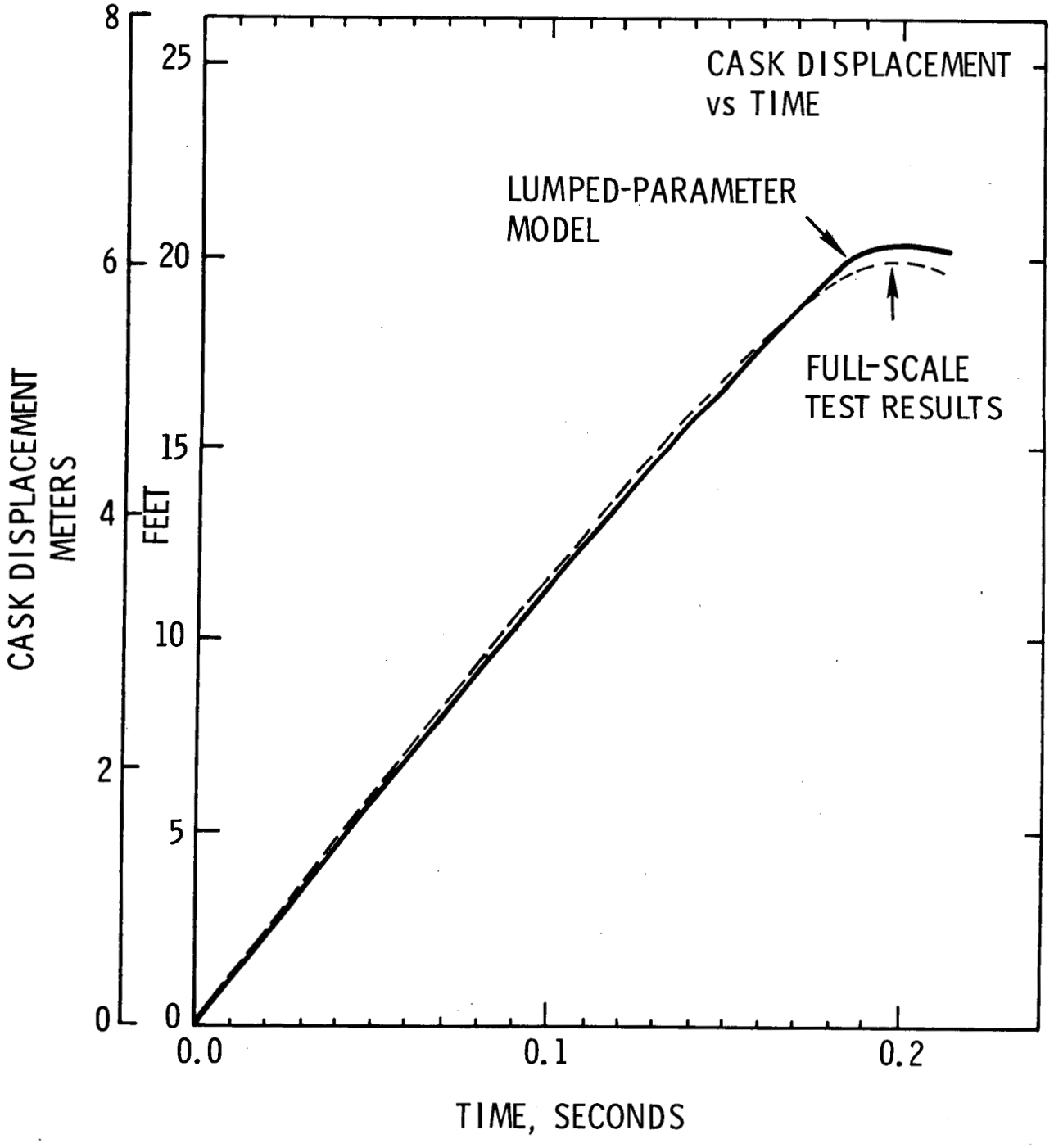

Figure 5.3 Cask displacement as a function of time for the secon test from analysis and full-scale.

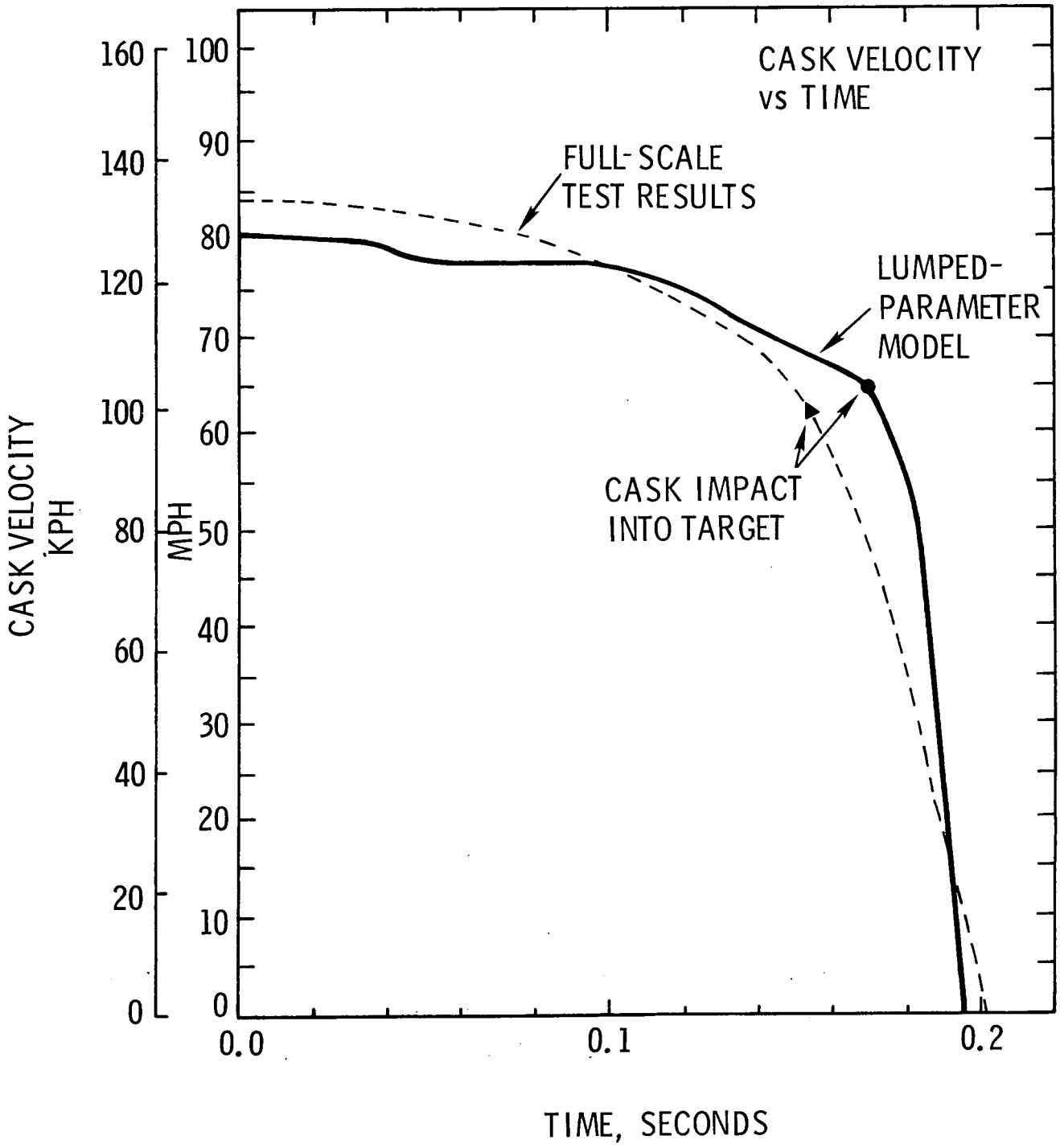

Figure 5.4 Cask velocity as a function of time for the second test from analysis and full-scale.

indicated a maximum hoop strain of 9%; whereas measurements on the full-scale cask after the impact indicated a 3% strain. The finite-element model indicated that the cask would shorten by 2%; actual measurements on the cask indicated a 1.6% compaction. The larger deformations indicated by the finite element model are partly due to the slightly higher impact velocity used in the model and to conservative assumptions made in the model's construction.

The second scale model test discussed in Section 3.4 did not correspond exactly, in terms of impact velocity, to the second full-scale test, being somewhat lower (122 vs. 135 kph). However, since the tiedowns were artifically weakened in the scale model test, the model cask tore loose of the trailer early in the impact and hit the target at a velocity comparable to that in the second full-scale test, where the system impacted at a higher velocity but the tiedowns held allowing considerable slowing of the cask. Therefore, it is reasonable to compare the resultant damage to the casks.

The deformations of the model cask (Figure 3.5) are in excellent agreement with those sustained by the full-scale unit. In each case, the maximum hoop strain was 3%. Figure 5.5 compares this magnified deformation profile in the two tests with the model dimensions being multiplied by the scale factor. As can be seen, the deformations are very similar. Most of the difference is due to the fact that, because stock tubing was used in the model, it was slightly off scale (about 2%). If the model deformation curve in Figure 5.5 is shifted upwards to account for this, the agreement improves significantly.

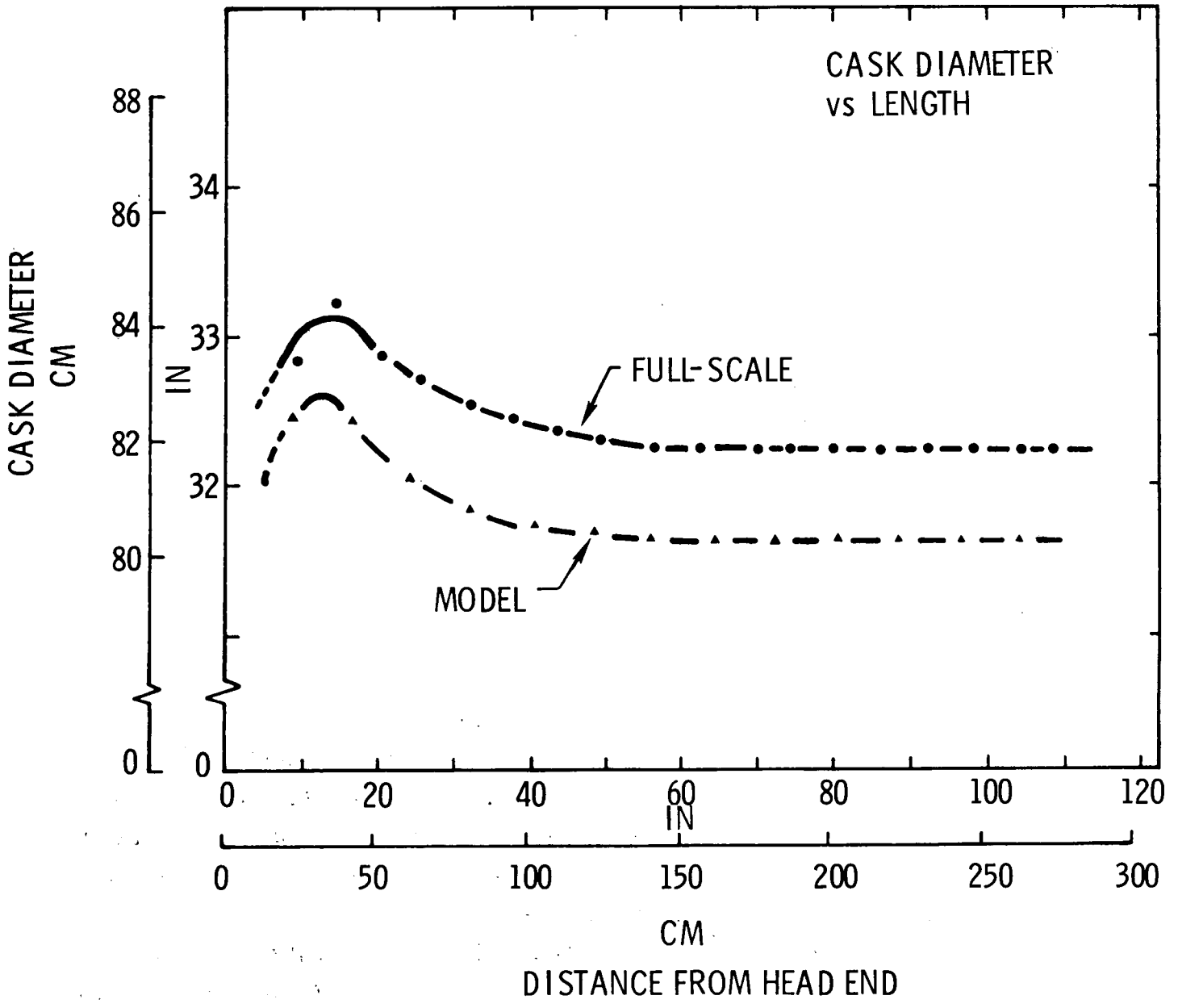

Figure 5.5 Magnified deformation pattern for the scale model and full-scale cask after the second test.

5.3 Discussion

Both the analytical and scale-modeling techniques yielded results which accurately predicted the behavior of the full-scale system. The response of the full-scale system was entirely predicted in terms of the rigid body dynamics of the cask through the impact and the resultant damage to the cask occurring during the final cask-target impact. The response of the vehicular system and the time frame for the impact were also in good agreement with the pretest analysis and scale modeling.

Analytically, the displacement for the cask in the first test was somewhat overestimated (Figure 5.1) due to the fact that a shorter tractor was substituted for the test. A slight modification was made to the model between tests to more accurately reflect the hardware, and the agreement between analysis and the actual test improved (Figure 5.3). The numerically calculated velocity time histories for the cask accurately and conservatively predicted what was seen in the real test.

Preliminary calculations indicated that the cask would impact the target in close to an end-on configuration. The second step in the analysis, the dynamic finite element model, predicted that the deformations which the cask would sustain in the final impact (even in the worst possible case) would not violate the cask's integrity or cause loss of contents. (This analysis was carried to velocities of 129 kph (80 mph) although it was felt that the highest probable impact velocity would be 105 kph (65 mph).) Thus, these two analytical techniques used together predicted the response of

the vehicle and cask in a very violent accident with a very reasonable degree of accuracy.

The scale models also simulated the behavior of the prototype quite well. A more detailed comparison was possible in the first test, where the impact velocities were equal. In this case, the scale model test yielded results which closely paralleled the prototype response, indicating that practical and adequate scale models can be constructed to simulate the behavior of this type of full-scale hardware in a very severe accident. In the second test, where the final impact of the cask was very comparable to what the full-scale cask sustained, the deformations exhibited by the model cask were in excellent agreement with those exhibited by the prototype.

Thus, the results of both the analytical work and the scale modeling agreed well with the full-scale test results. The models were always constructed with some degree of conservatism, and this was reflected in comparisons with the response of the full-scale system.

6.0 Conclusions and Recommendations

A primary purpose of the tests was to assess the utility and validity of mathematical and scale modeling techniques in predicting the response of shipping casks in two extremely severe and unlikely transportation accident conditions. These two tests have shown that, despite complications introduced by the uncertainties of used equipment, these analysis techniques can give very good indications of the response of full-scale shipping casks and transport systems. The pretest analyses, including both numerical work and scale modeling, accurately predicted the rigid body dynamics of the cask and its final condition after the impact. The influence of the vehicle structure was also well predicted. These same techniques applied to new designs, which are more accurately defined in terms of construction details and material properties, will produce better results.

Scale modeling is a very practical way of predicting damage to shipping casks in extremely severe impacts at skewed angles or onto irregular surfaces. Construction and testing of scale models is relatively inexpensive and straightforward. Mathematically, these problems are extremely difficult to handle. A three-dimensional finite-element model, which would be necessary under such conditions, is not yet practical. Somewhat simplified (adequate) scale models used in impact tests will accurately predict the response of the new design.

For the analysis of an end impact, the finite-element technique described and demonstrated in this report gives very reasonable results. It is felt that the sliding interface feature is very necessary when analyzing a lead shielding container. A possible refinement to this model would be to include friction in the interface. Also, the effect of the fins might be compensated for by increasing the model thickness of the outer shell, uniformly smearing the fin area onto the outer surface. It is felt that this technique with a small amount of refinements will yield excellent results.

The lumped-parameter model of the system represented a first effort at applying this technique to analyze an entire transport system. As a first effort, it was kept simple. The accuracy of the model could be increased by better force-displacement information for the couplings, and a finer discretization of the structure. Better force-displacement information can be obtained from static crush tests of scale model components of the system. It is believed that strain-rate effects for structures such as these can be neglected. This was, to some extent, confirmed by observing that the vehicular crush resistance in both full-scale tests, at the two impact velocities, was about equal. A finer discretization of the structure should have provisions for the shearing off of wheel and axle assemblies, on both the tractor and trailer models. This recommendation is based on film analysis for both tests. Such improvements to the lumped-parameter model will result in more refined and better predictions.

Analysis and testing have shown that a lead shielded container of the type described in this report is extremely

rugged and can undergo a very severe, realistic, end-impact into a very rigid surface with relatively minor deformations resulting. The containment ability of the cask was not severely threatened.

This investigation revealed that the cask tiedown system is a sensitive parameter in the system impact response. In order to take advantage of the significant energy absorption capability of the trailer, the tiedowns must be sufficiently strong to hold the cask as the trailer structure crushes. Thus, it is believed that the trailer and tiedowns should be an integral and balanced design.

The good correlation between analysis and scale modeling and the results of the full-scale tests has demonstrated that given an accident situation or impact environment, the response of a full-scale system can be predicted with a reasonable degree of accuracy.

REFERENCES

1. Yoshimura, H. R. and Huerta, M., "Full Scale Tests of Spent-Nuclear Fuel Shipping Systems," International Atomic Energy Administration Paper No. IAEA-SR-10/17, July, 1976, also Sandia Laboratories Report No. SAND 76-5707, July 1976.

2. Huerta, M. "Full Scale Truck Test," Memorandum to H. R. Yoshimura, Sandia Laboratories, Albuquerque, New Mexico, January 13, 1977.

3. Huerta, M., "80 MPH Truck Crash Test," Memorandum to H. R. Yoshimura, Sandia Laboratories, Albuquerque, New Mexico, March 11, 1977.

4. Gabrielson, V. K., Reese, R. T., "SHOCK Code Users Manual, A Computer Code to Solve the Dynamic Response of Lumped-Mass Systems," Report No. SCL-DR-69-98, Sandia Laboratories, Livermore, California, November 1969.

5. Key, S. W., "HONDO, a Finite Element Computer Program for the Large Deformation Dynamic Response of Axisymmetric Solids," Report No. SLA-74-0039, Sandia Laboratories, Albuquerque, New Mexico, April 1974.

6. Jones, R. E., "QMESH: A Self-Organizing Mesh Generation Program," Report No. SLA 73-1088, Sandia Laboratories, Albuquerque, New Mexico, June 1974.

7. McGovern, D. E., and Thunborg, S., "On the Use of Modeling in a Structural Response Problem, "Report NO. SC-RR-70-888, Sandia Laboratories, Albuquerque, New Mexico, March 1971.

8. Duffey, T. A., "Scaling Laws for Fuel Capsules Subjected to Blast, Impact, and Thermal Loading," Report No. SC-RR-70-134, Sandia Laboratories, Albuquerque, New Mexico, May 1970.

9. Baker, W. E., et al., Similarity Methods in Engineering Dynamics, Hayden Book Co., Inc., Rochelle Park, New Jersey, 1971.

10. Murphy, G., Similitude in Engineering, Ronald Press Co., New York, 1950.

11. Langhaar, H. L., Dimensional Analysis and Theory of Models, John Wiley and Sons, Inc., 1951.

12. Clark, H. G., "Impact Resistance of Casks," Chemical Engineering Progress Symposium Series, Vol. 61, No. 56, 1965, American Institute of Chemical Engineers, New York.

APPENDIX A

Details of the Lumped-Parameter Model

APPENDIX A

Details of the Lumped-Parameter Model

This appendix includes some details of the lumped-parameter model illustrated in Figure 2.1 of the text. This model formulation waas used with the SHOCK computer program. Basically, SHOCK numerically solves the second-order differential equations of motion associated with a spring mass model given some initial conditions. Spring (coupling) definitions may be non-linear and can load and unload along different paths, simulating a hysteresis effect. In the model of this study, extensive use was made of the HYSTER option to simulate crush-up of structures. The HYSTER type 1 coupling can be used to simulate only a compressive or tensile load using numerous line segments. The HYSTER type 2 option can simulate both a compressive and tensile load but is limited to fewer line segments.

The coupling definitions used in this model are illustrated in Figures A-1 through A-9. Damping was not used in the model.

The weight values, in pounds, of the masses were as follows:

M2 = 6,000
M3 = 7,000
M4 = 1,300
M5 = 2,600
M6 = 45,000
M7 = 2,600
M8 = 4,600

Mass 1 was held fixed while the others were given initial velocity conditions equal to the expected system impact velocity. This model was used to analyze both a 60 and an 80 mph impact. For the analysis of the second test, the free travel of coupling 1-6 (Figure A-9) was shortened by 30 inches to more accurately reflect the full-scale hardware.

The coupling definitions were structural analysis estimates based on measurements made of the hardware and expected yield strength values of the materials. In modeling slender elements subject to buckling, some judgment must be made regarding their crush force. For example, the trailer structure was assumed to crush at a load equal to one-half the yield force based on its cross-sectional area.

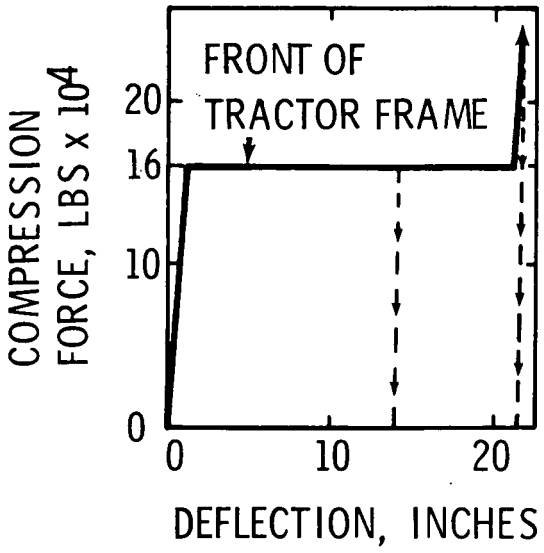

FIGURE A-1. COUPLING 1-2, HYSTER TYPE 1

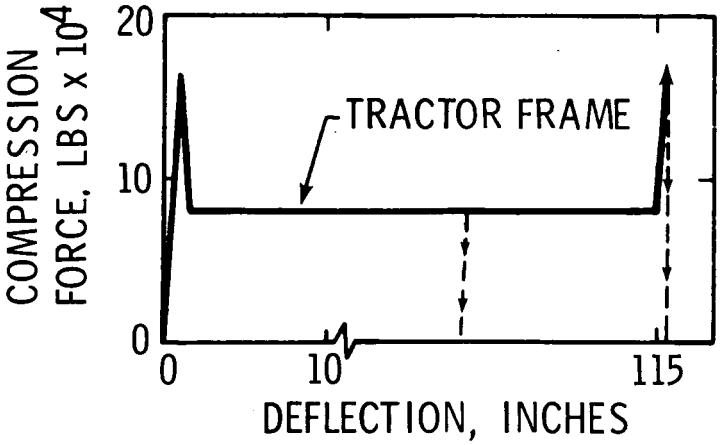

FIGURE A-2. COUPLING 2-3, HYSTER TYPE 1

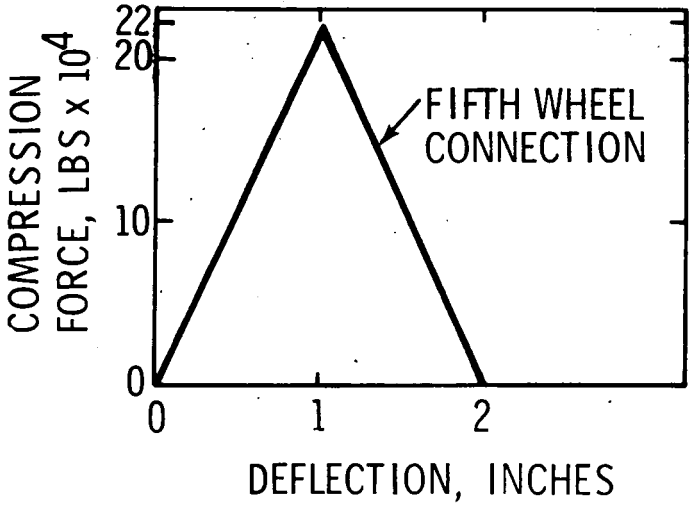

FIGURE A-3. COUPLING 3-4, HYSTER TYPE 1

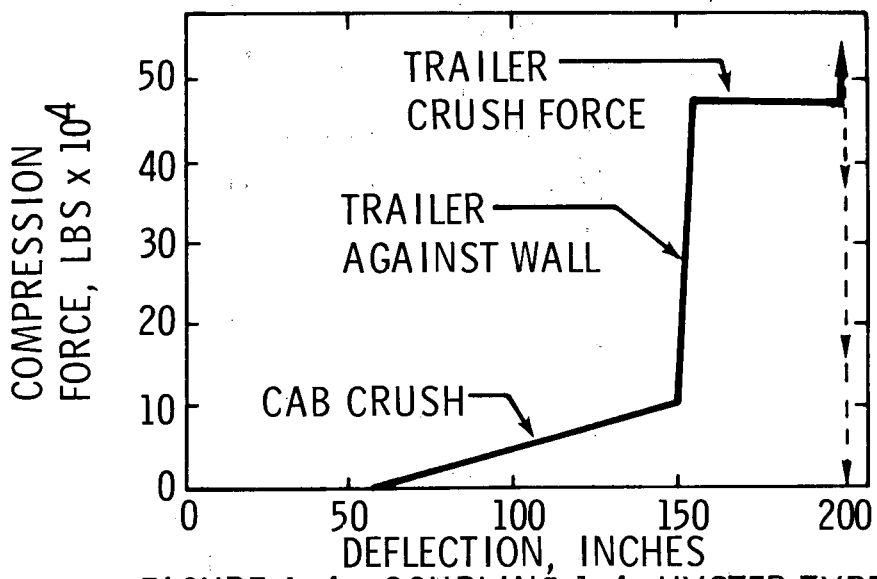

FIGURE A-4. COUPLING 1-4, HYSTER TYPE 1

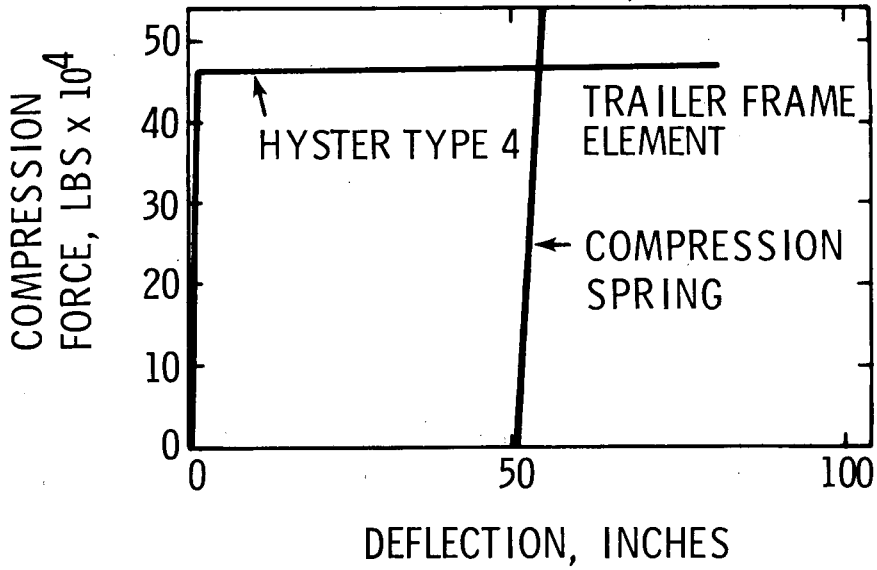

FIGURE A-5. COUPLING 4-5, HYSTER TYPE 4 AND LINEAR SPRING

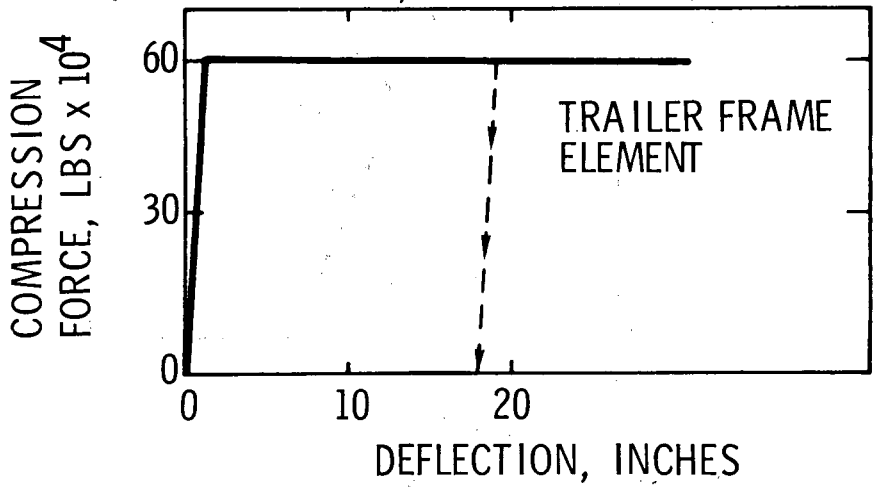

FIGURE A-6. COUPLING 5-7. HYSTER TYPE 4

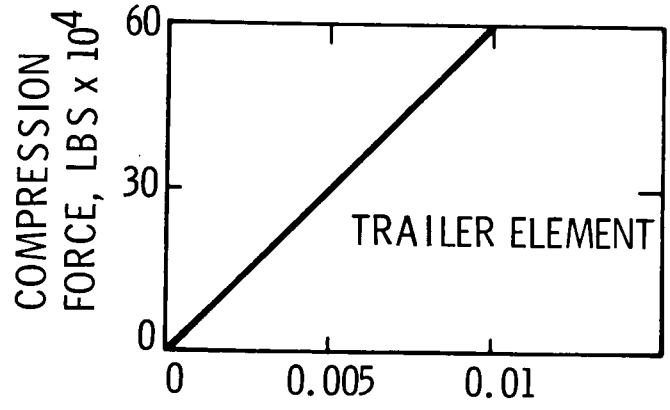

FIGURE A-7. COUPLING 7-8, LINEAR SPRING

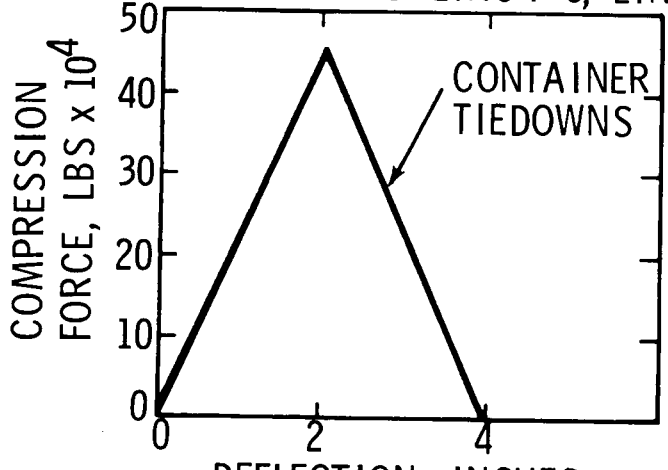

FIGURE A-8. COUPLING 5-6 AND 6-7, HYSTER TYPE 1

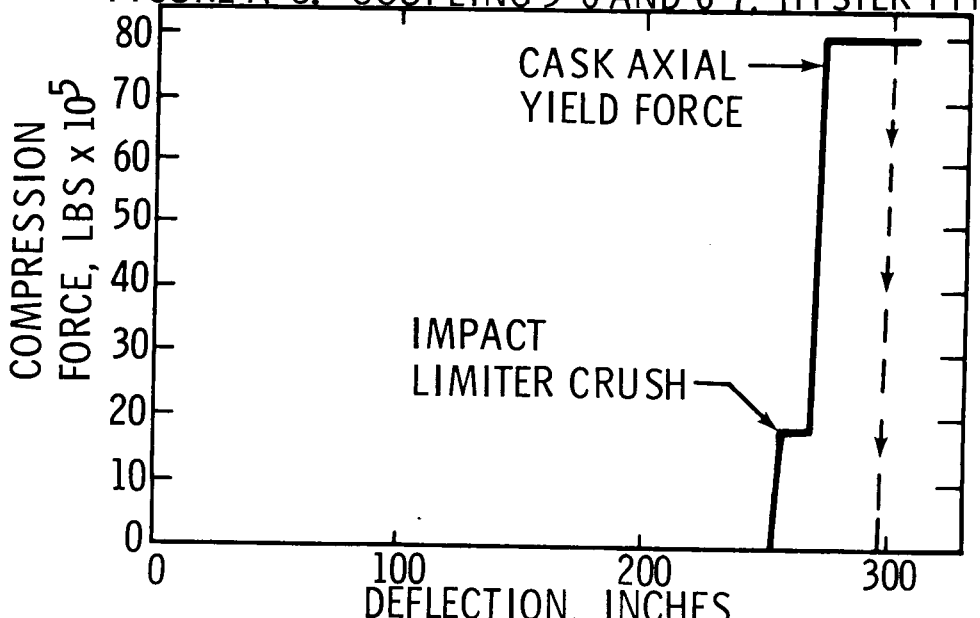

FIGURE A-9. COUPLING 1-6, HYSTER TYPE 1

APPENDIX B

Input to the HONDO Program

APPENDIX B

Input to the HONDO Program

The mesh for the dynamic finite-element cask model used with the HONDO program was generated using QMESH [6], a separate program. The cask model actually contains two separate finite-element bodies, one corresponding to the lead shielding material and the other to the steel shells. The separate materials are free to interact and slide relative to one another. Node motion of one into the other is restricted by restoring forces which act when a node crosses the boundary. The materials are allowed to slide relative to each other with or without friction. The entire body is given an initial velocity in the axial direction into a simulation of an unyielding surface. This is accomplished in the HONDO model by preventing node motion past a z-coordinate value (see Figure 2.6) with a very stiff spring boundary condition. The computational results of this model then indicate the deformations that a cask would sustain in an end impact into a rigid target.

A bilinear elastic-plastic stress-strain curve is used to describe the deformation behavior of the materials. This then means that an elastic modulus and a plastic modulus must be input to the program. Other material properties which must be input include yield strength, Poisson's ratio, and density. The table below includes the values used in this analysis.

APPENDIX B (cont'd)

	STEEL	LEAD
Elastic modulus, Psi	29.0×10^6	27.75×10^3
Plastic modulus, Psi	3.0×10^5	24.75×20^2
Yield Strength, Psi	35.0×10^3	4.3×10^3
Poissons' ratio	.42	.30
Density, lbs/in^3	.282	.409

APPENDIX C

Analysis of the Cask Closure System

APPENDIX C

Analysis of the Cask Closure System

This appendix calculates stresses in the head bolts due to inertial loads of the contents, the cask head, and the impact limiter. The cask is equipped with 16 - 3/4 inch bolts which keep the head in place. The impact limiter is attached to four of the head bolts. The following data is used in the analysis

bolt root diameter:	0.620 in
bolt root area:	0.302 in^2
bolt ultimate stress:	110,000 psi
weight of cask internals:	1,900 lbs
weight of cask head:	1,120 lbs
weight of impact limiter:	1,600 lbs

It has been calculated that the cask will see a maximum of 20 g's during crush-up of the structure. (The final impact of the cask into the wall can produce much higher peak decelerations but these are not viewed as a threat to the bolting system.) The stress in the four bolts supporting the impact limiter is

$$\sigma = \frac{(1600)(20)}{(4)\ (0.302)} = 26{,}490 \text{ psi}$$

Assuming that the inertial load of the internals and the head is carried by the remaining 12 bolts, the stress in these bolts is:

$$\sigma = \frac{(20)(1120 + 1900)}{(12)(0.302)} = 16{,}666 \text{ psi}$$

The bolts supporting the limiter are then stressed to a higher value. This means that they will strain more and the assumption that the inertial loads of the internals and head will be carried by the remaining 12 bolts is valid.

Shear stress in the threaded system can be calculated as follows: The nuts are 0.75 in. high. The shear area is:

$$A = (\text{root diameter})(\pi)(0.75)$$
$$A = (0.620)(\pi)(0.75) = 1.46$$

The highest stressed bolts carry 8,000 lbs. The shear stress is then:

$$\tau = \frac{8000}{1.46} = 5479$$

The ultimate nominal strength of the bolting material is 110,000 psi and the ultimate shear strength can be conservatively expected to be half this value. The calculated stresses, therefore, are well within these limits.

In order to verify material properties, two of the bolts were statically tested in tension. They each took a minimum load of 35,000 lbs and exhibited a very large amount of ductility. These test results then indicate a material strength of 115,000 psi. It is calculated that the bolting system will not fail due to inertial loads during crush-up of the vehicle structure.

APPENDIX D

Working Drawings for the Scale Model

DESIGN AGENCY PART NO.	REVISIONS					
	LTR	ZONE	DESCRIPTION	DATE	CHKD	ENGR
T42481-000	A		VAN THEEMSCHE 9652 / YOSHIMURA 5432	5-11-76		
	B		M.HUERTA, 1292 PUHARA, 9652	11-2-76		

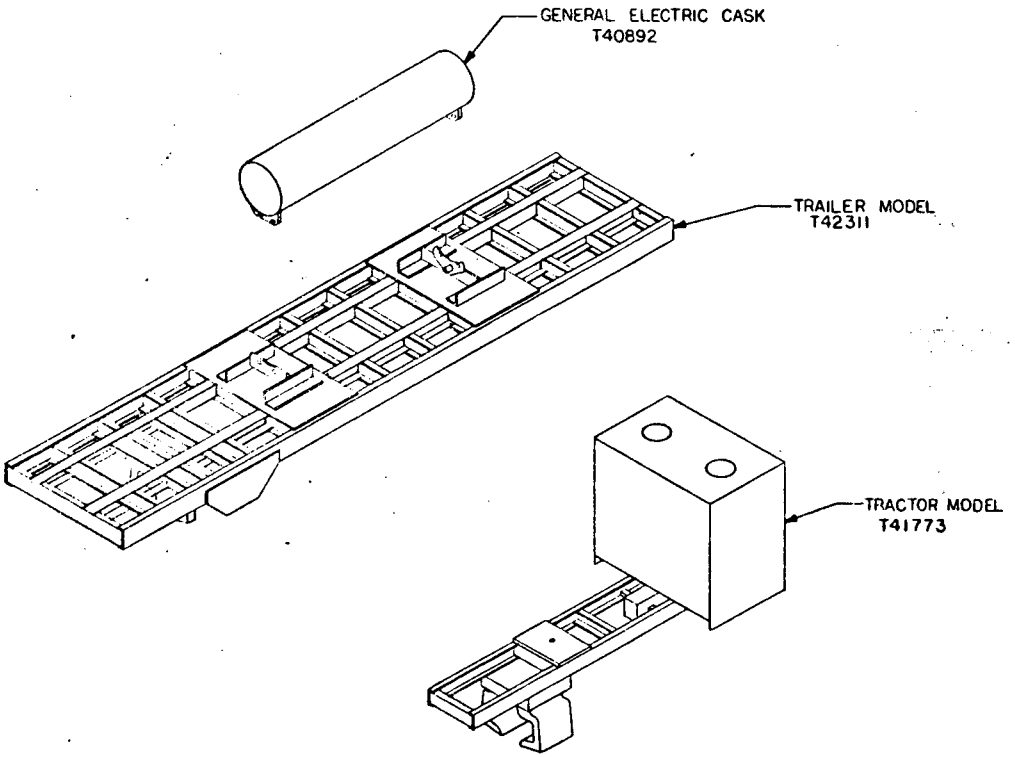

AGENCY APPROVALS			SHEET 1	TITLE
ORG	DATE	APPROVALS	ISSUE B	TRUCK CASK TRANSPORTER
5432			SHEET INDEX	
			PART CLASSIFICATION: UNCLASSIFIED	
			DWG CLASSIFICATION LEVEL: UNCLASSIFIED	SIZE D | CODE IDENT. NO. 14213 | DWG. NUMBER T42481
9652				SCALE 1/4 | SHEET 1 OF 1

T42481

NOTES:

1. ALL EXTERIOR WELDS TO BLEND AND BE GROUND SMOOTH.
2. MINIMUM WELD THICKNESS TO BE EQUAL TO THINNEST ITEM BEING JOINED.
3. ALL WELDS ARE SEAL WELDS.
4. MATERIAL: ALL PARTS THAT ARE STAINLESS STEEL TO BE OF TYPES 302, 304, 321, 347, OR 348.
5. PRIOR TO POURING OF THE LEAD ALL LEAD CONTAINING SURFACES SHALL BE CLEANED OF SCALE, RUST, DIRT, GREASE, OIL, ETC. LEAD SLAG AND SIMILAR IMPURITIES SHALL NOT BE ADMITTED.
6. PAINT PER ENGR INSTRUCTIONS.
7. TARGET WEIGHT OF CASK TO BE 78 LBS. LEAD (ITEM 15) TO PROVIDE THE VARYING FACTOR.

DESIGN AGENCY PART IDENTIFICATION NO.
T40892-000

REVISIONS					
ZONE	LTR	QTY	DESCRIPTION	DATE	APPD
	A		R.YOSHIMURA 5432; PUHARA, 9652		
	B		CHGD THICKNESS OF ITEMS 8 & 9 M.HUERTA, 1342 ; PUHARA, 9652		
	C		REDESIGNED ITEMS 8 & 9 M. HUERTA, 1342; PUHARA 9652		

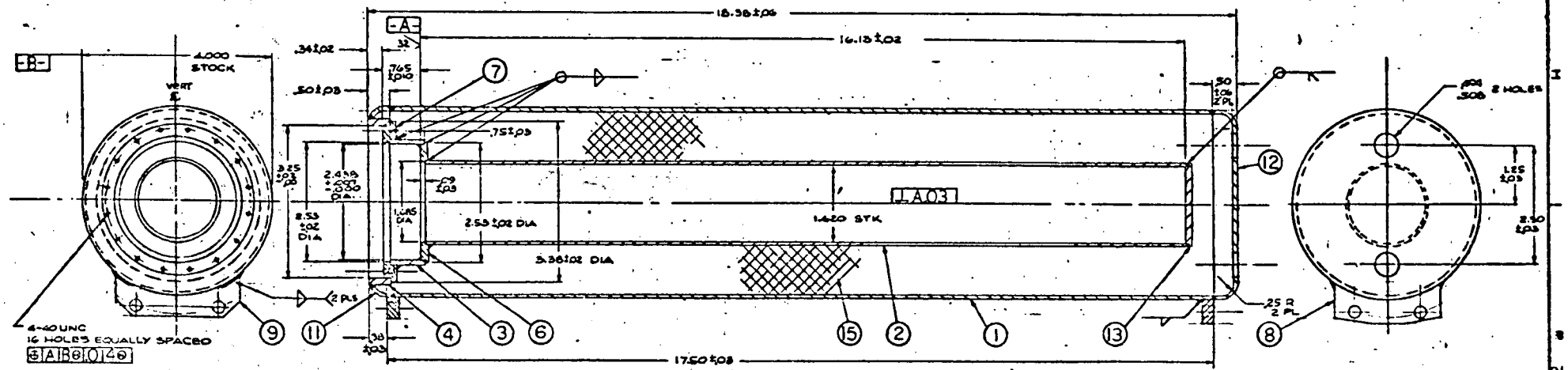

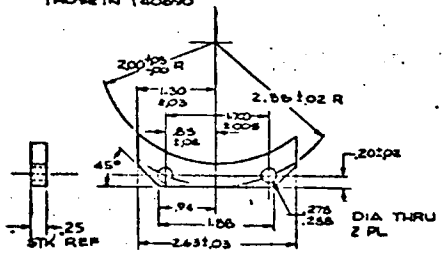

DETAIL ITEM 9

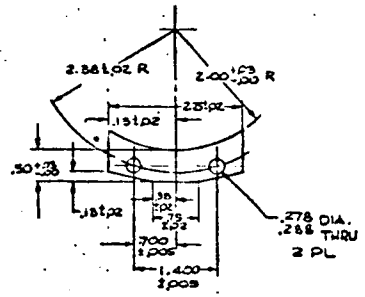

DETAIL ITEM 8

AR		LEAD CHEMICAL GRADE	15
			14
1		SHEET, STAINLESS STL .125 THICK	13
1		SHEET STAINLESS STL .156 (9 GA)	12
1		SHEET STAINLESS STL .156 (9 GA)	11

LIST OF MATERIAL

1		PLATE STAINLESS STL .250 THICK	10
1		PLATE STAINLESS STL .250 THICK	9
1		PLATE STAINLESS STL .25 THICK	8
1		PLATE STAINLESS STL .188 THICK	7
			6
1		TUBING STAINLESS STL 3.25 I.D. x .125 WALL	5
1		TUBING STAINLESS STL 2.5 2500 x .095 WALL	4
1		TUBING STAINLESS STL 1.75 00 x .065 WALL	3
1		TUBING STAINLESS STL 4.00 00 x .095 WALL	2
			1

DWG NO T40892

LIST OF MATERIAL

AGENCY APPROVALS			SHEET	1
ORG	DATE	APPROVED	ISSUE	

SHEET INDEX

PART CLASSIFICATION: UNCLASSIFIED

DWG CLASSIFICATION LEVEL: UNCLASSIFIED

TITLE

CASK

FOR MOD. IFIC08129 & IFI00137

SIZE	CODE IDENT. NO.	DWG NUMBER
D	14213	T40892

SCALE FULL SHEET 1 OF 1

NOTES:

1. MATERIAL: ALL PARTS MADE OF STAINLESS STEEL TO BE TYPE 321, 347, OR 348.

DESIGN AGENCY PART IDENTIFYING NO.	REVISIONS ISSUE	DESCRIPTION	PREPARED BY	DATE	CHKD	APPD
T40891-000	A	R YOSHIMURA 5432 J PUHARA, 9652				

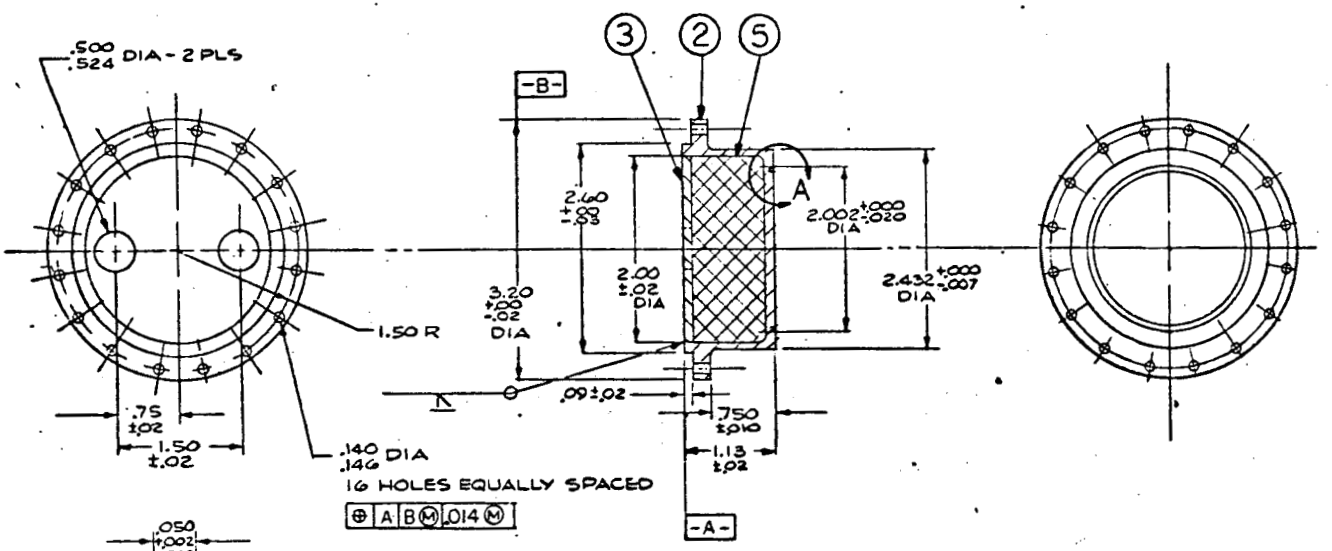

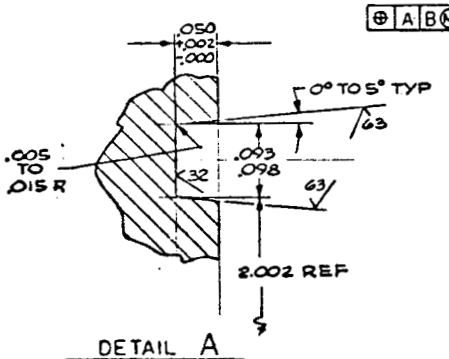

DETAIL A
NO SCALE

NO REQD	DESIGN AGENCY NUMBER	DESCRIPTION	NOTE	SHEET ZONE	ITEM
AR		LEAD, CHEMICAL GRADE			5
					4
1		SHEET, STAINLESS STEEL - .125 (11 GA)	1		3
1		ROUND, STAINLESS STEEL - 3.25 DIA	1		2
					1

LIST OF MATERIAL

AGENCY APPROVALS			SHEET	1					
ORG	DATE	INITIALS	ISSUE	A					
			SHEET INDEX						
			PART CLASSIFICATION: UNCLASSIFIED						
			DWG. CLASSIFICATION LEVEL: UNCLASSIFIED						

TITLE: CAP-WITHOUT EXTENTION

SIZE	CODE IDENT. NO.	DWG. NUMBER
C	14213	T40891
SCALE FULL		SHEET 1 OF 1

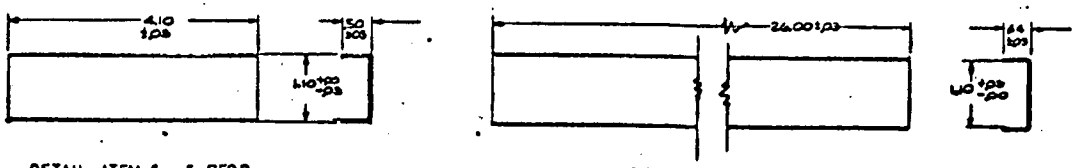

DETAIL ITEM 6 — 5 REQD
SCALE-FULL SIZE
MIN. BEND RADIUS=.06 MIN

DETAIL ITEM 5 — 2 REQD
SCALE-FULL SIZE
MIN. BEND RADIUS=.06 MIN

DESIGN AGENCY PART OR DRAWING NO.	REVISIONS					
	LTR	QTY CHG	DESCRIPTION	ENGINEER OR	DATE	CHKD
T41773-000	A		M.HUERTA,1342;J.PUMARA,9652			

NOTES:

1. TO BE FURNISHED BY ENG'G DIV. 9388.
2. PAINTING TO BE SUPERVISED BY ENG'G.
3. CAB TO BE LOCATED BY 3 SCREWS ONLY.
4. STRESS RELIEVE & STRAIGHTEN WELDED STRUCTURES AFTER WELDING.

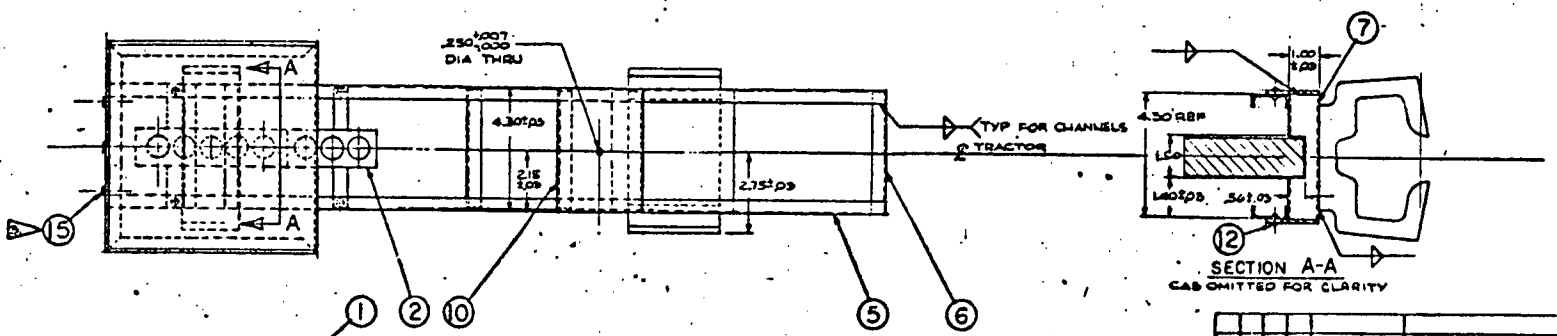

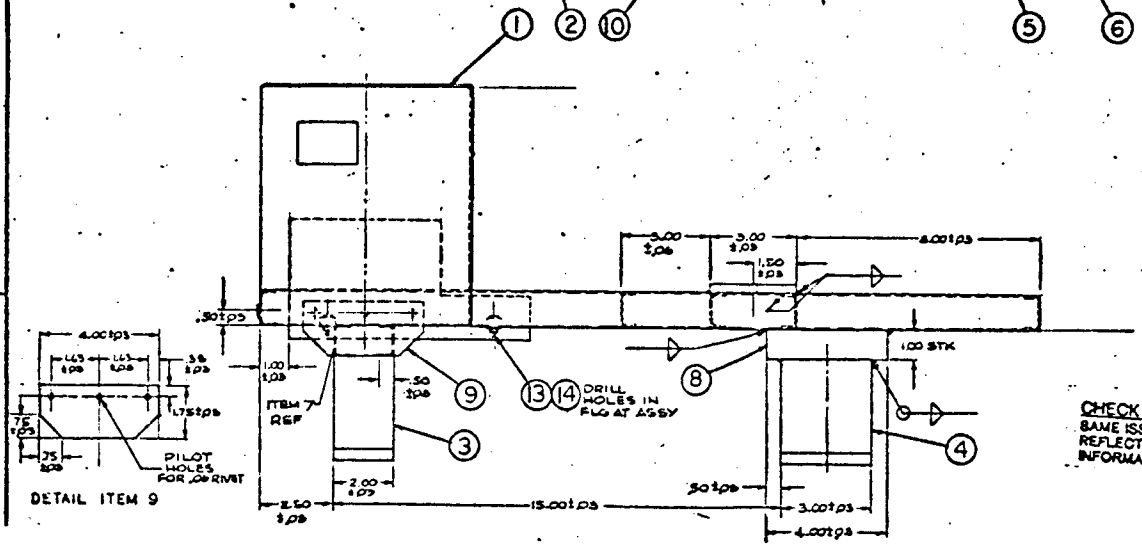

CHECK PRINT ONLY
SAME ISSUE PRINT MAY REFLECT DIFFERENT INFORMATION.

					18
					17
					16
3			SCREWS, SHEETMETAL		15
4			NUT, 4-48 UNF		14
4			BOLT, HEX HD - 4-48 UNF X .625 LG		13
6			RIVET, .06 DIA UNIV. HD		12
					11
1			PLATE-LOW CARBON STEEL, .25 THK		10
2			GUSSET-LOW CARBON STEEL, .125 THK		9
1			SOLID PLATE-LOW CARBON STEEL		8
2			FWD SHOE CHANNEL 1" x 1/2" x		7
5			CROSS CHANNEL 20 (.0359) GA (COLD ROLL		6
2			FRAME CHANNEL 20 (.0359) GA LOW CARBON		5
1			REAR SHOE	1	4
1			FWD SHOE	1	3
1	T41775-000		ENGINE & TRANSMISSION		2
1	T41774-000		TRACTOR CAB		1

QTY REQD	QTY PER ASSY	DESIGN AGENCY PART OR DRAWING NO.	DESCRIPTION	MATERIAL	SHEET NO.

LIST OF MATERIAL

AGENCY APPROVALS			SHEET	TITLE
ORG	DATE	APPROVALS	ISSUE A	TRACTOR MODEL 1/8 SCALE
			SHEET INDEX	
			PDT CLASSIFICATION: UNCLASSIFIED	
			DWG CLASSIFICATION LEVEL: UNCLASSIFIED	SIZE D; CODE IDENT. NO. 14213; DWG NUMBER T41773; SCALE 1/8 NOTED; SHEET 1 OF 1

DWG NO. T41773

T41773

135

NOTES:

1. RIVETS MAY BE USED IN PLACE OF SCREWS. LOCATE APPROX. AS SHOWN.
2. MINIMUM BEND RADIUS TO BE .06 R
3. FINISH : PAINT PER ENGINEERING INSTRUCTIONS
4. CALCULATED WEIGHT OF THIS ASSY IS APPROX .75#.

DESIGN AGENCY PART OR DRAWING NO.	REVISIONS				
	LEVEL	LETTER	DESCRIPTION	DATE	CHKD
T41774-000		A	M.HUERTA,13-2 J.PUMARA,9652		

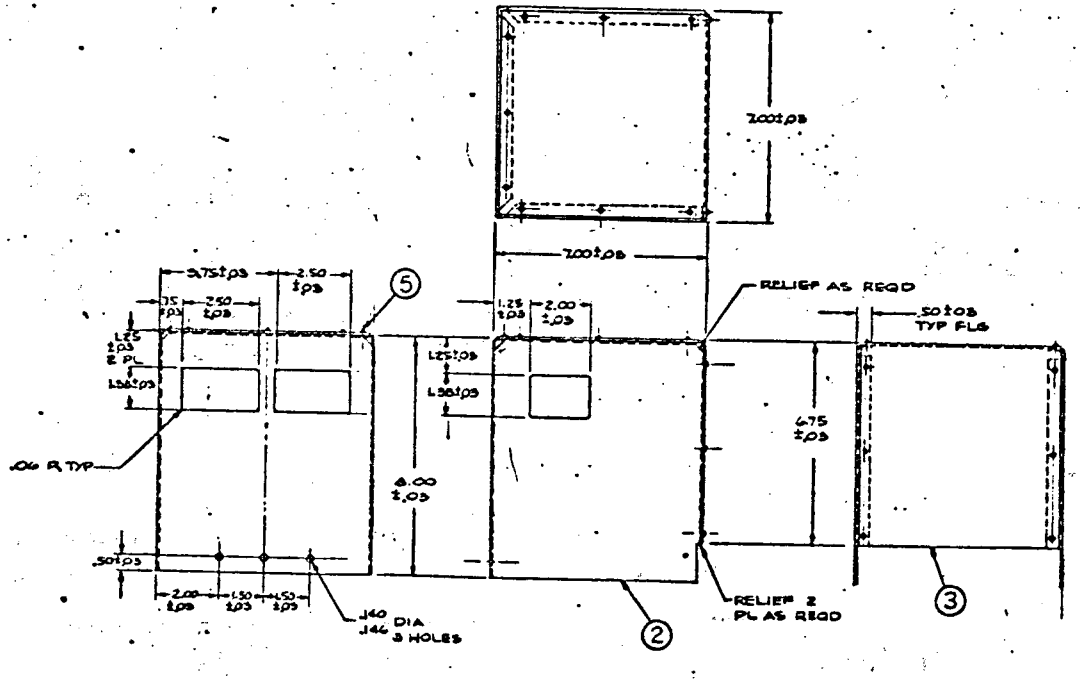

QTY		DESCRIPTION			
AR		SHEETMETAL SCREWS			5
1		SHEET, LOW CARBON 30(.012) GA			4
1		SHEET, LOW CARBON 30(.012) GA			3
					2
					1

LIST OF MATERIAL

AGENCY APPROVALS

ORG	DATE	APPROVALS

SHEET INDEX

SHEET 1
ISSUE A

PART CLASSIFICATION: UNCLASSIFIED

DWG CLASSIFICATION LEVEL: UNCLASSIFIED

TITLE: TRACTOR CAB

SIZE D | CODE IDENT. NO. 14213 | DWG NUMBER T41774

SCALE 1/2 | SHEET 1 OF 1

T41774

T41774 1

D132698

DESIGN AGENCY PART IDENTIFICATION	REVISIONS				
	ISSUE	DESCRIPTION	PREPARED BY	DATE	CHKD	ENGR
T41775-000	A	M. HUERTA,1342,PUHARA,9652		4-15-76		
	B	2.5 WAS 4.00-DELETED NOTE 2 M.HUERTA 1282/PUHARA,9652		11-1-76		

NOTES:

1. MATERIAL: MAKE FROM LOW CARBON STEEL.
2.
3. BOLTING OF ENGINE MOUNTS TO BE DETERMINDED AT ASSY. SEE DWG T41773.

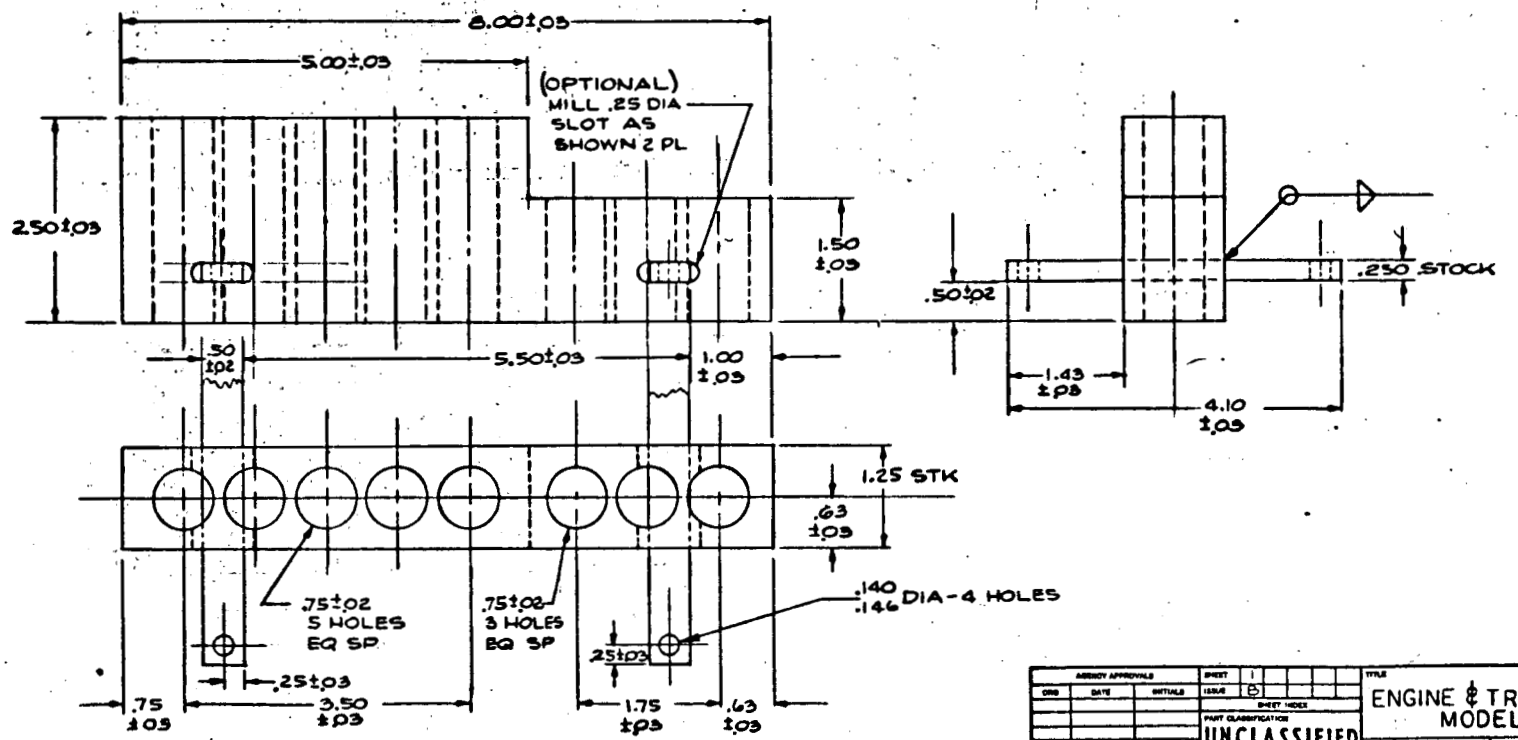

AGENCY APPROVALS			SHEET						TITLE
ORG	DATE	INITIALS	ISSUE	B					ENGINE & TRANSMISSION MODEL
			SHEET INDEX						
			PART CLASSIFICATION	UNCLASSIFIED					
			DWG. CLASSIFICATION LEVEL	UNCLASSIFIED					
			SIZE	C	CODE IDENT. NO.	14213	DWG. NUMBER	T41775	
			SCALE	FULL			SHEET 1 OF 1		

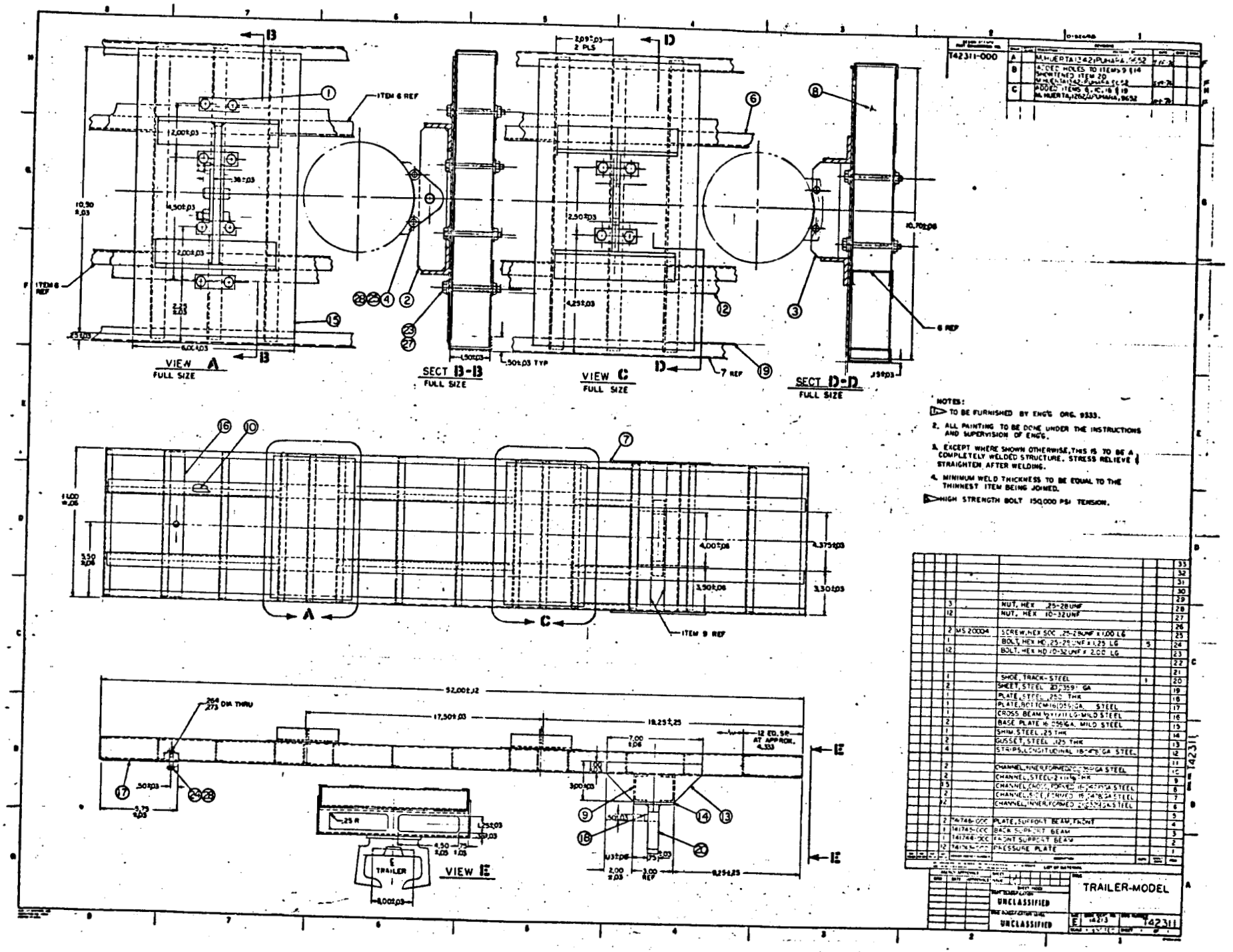
VIEW A
FULL SIZE
SECT B-B
FULL SIZE
VIEW C
FULL SIZE
SECT D-D
FULL SIZE
VIEW E
FULL SIZE
ITEM 6 REF
ITEM 9 REF
TRAILER
52.00±.12
17.50±.03
18.25±.25
12.00±.03
4.50±.03
2.00±.03
38±.03
2.50±.03
4.25±.03
6.00±.03
1.50±.03
.50±.03 TYP
4.00±.06
3.50±.06
3.375±.03
3.30±.03
8.00±.03
NOTES:
1. TO BE FURNISHED BY ENG'G ORG. 9333.
2. ALL PAINTING TO BE DONE UNDER THE INSTRUCTIONS AND SUPERVISION OF ENG'G.
3. EXCEPT WHERE SHOWN OTHERWISE, THIS IS TO BE A COMPLETELY WELDED STRUCTURE. STRESS RELIEVE & STRAIGHTEN AFTER WELDING.
4. MINIMUM WELD THICKNESS TO BE EQUAL TO THE THINNEST ITEM BEING JOINED.
HIGH STRENGTH BOLT 150,000 PSI TENSION.
T42311-000
TRAILER-MODEL
UNCLASSIFIED
T42311

DRAWING AGENCY PART OR IDENTIFYING NO.	REVISIONS				
	ISSUE	DESCRIPTION	PREPARED BY	DATE	CHKD	APPD
T41744-000	A	VAN THEEMSCHE 9652/HUERTA 1342				

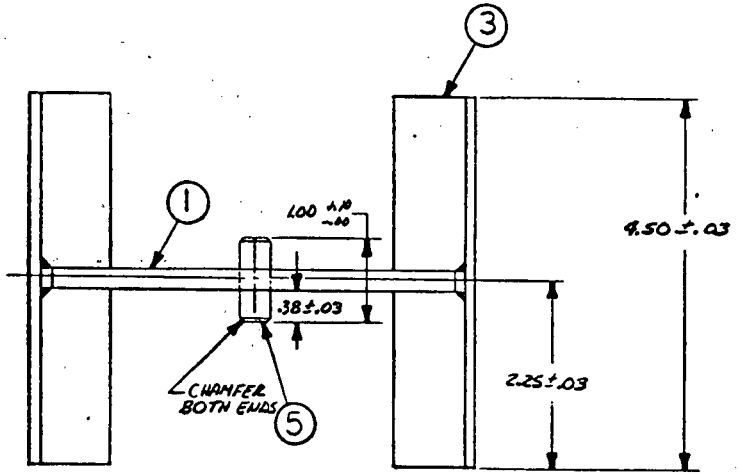

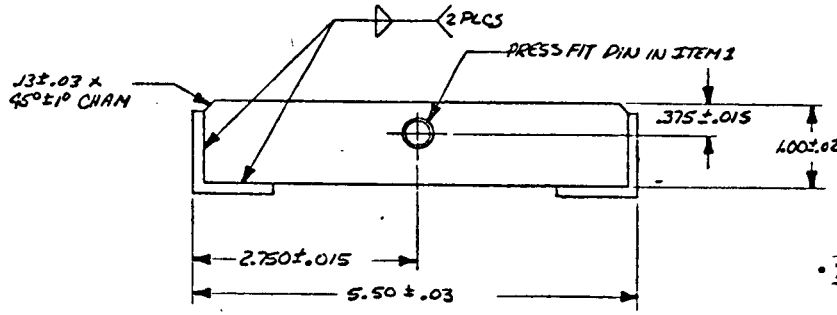

ITEM	DESIGN AGENCY NUMBER	DESCRIPTION	NOTE	SHEET ZONE	ITEM
1		PIN- DRILL ROD, .375 DIA.			5
					4
2		ANGLE, LOW CARBON STEEL, (1 X 1 X .125)			3
					2
1		PLATE, LOW CARBON STEEL, .250 THK.			1
NA	9912119	WELDING, STEEL			
NA	9900000	GENERAL REQUIREMENTS			

LIST OF MATERIAL

AGENCY APPROVALS			SHEET	1
ORG	DATE	INITIALS	SIZE	A4
1342			SHEET INDEX	
			PART CLASSIFICATION	UNCLASSIFIED
			SYMB. CLASSIFICATION LEVEL	UNCLASSIFIED
2453				

TITLE: FRONT SUPPORT BEAM

SIZE	CODE IDENT. NO.	DWG. NUMBER
C	14213	T41744
SCALE FULL		SHEET 1 OF 1

NOTES:

1. GENERAL REQUIREMENTS AS DEFINED IN 9900000.
2. MATERIAL: LOW CARBON STEEL.

DESIGN AGENCY PART IDENTIFYING NO.	REVISIONS ISSUE	DESCRIPTION	PREPARED BY	DATE	CHKD	ENGR
T41746-000	A		VAN THEEMSCHE 9652/HUERTA 1342			

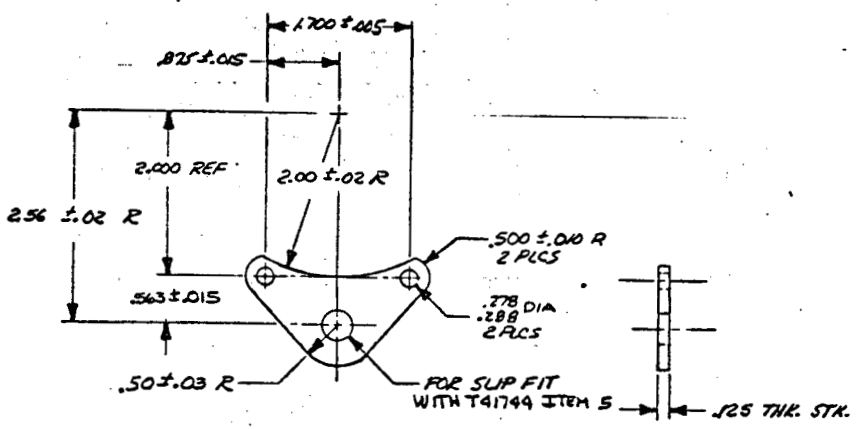

AGENCY APPROVALS			SHEET 1
ORG	DATE	INITIALS	ISSUE A
1342			SHEET NUMBER
			PART CLASSIFICATION: UNCLASSIFIED
			DWG. CLASSIFICATION LEVEL: UNCLASSIFIED
9658			

TITLE: PLATE, SUPPORT BEAM, FRONT

SIZE	CODE IDENT. NO.	DWG. NUMBER
C	14213	T41746
SCALE FULL		SHEET 1 OF 1

DESIGN AGENCY PART IDENTIFYING NO.	REVISIONS ISSUE	DESCRIPTION	PREPARED BY	DATE	CHKD	ENGR
T41745-000	A		VANTHEEMSCHE 9652/HUERTA 1342			

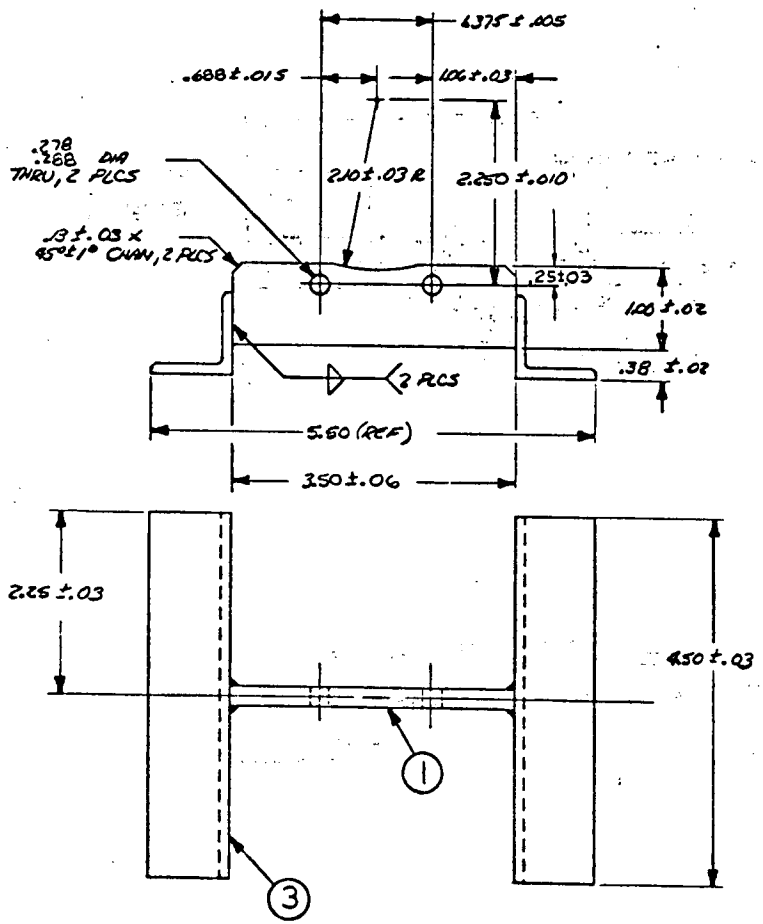

					5
					4
2		ANGLE, LOW CARBON STEEL, (1 X 1 X .125)			3
					2
1		PLATE, LOW CARBON STEEL, .250 THK.			1
NA	9912119	WELDING, STEEL			
NA	9900000	GENERAL REQUIREMENTS			
NO REQD	DESIGN AGENCY NUMBER	DESCRIPTION	NOTE	SHEET ZONE	ITEM

LIST OF MATERIAL

AGENCY APPROVALS			SHEET 1
ORG	DATE	INITIALS	ISSUE A
1342			SHEET INDEX
			PART CLASSIFICATION: UNCLASSIFIED
			DWG. CLASSIFICATION LEVEL: UNCLASSIFIED
DCMS			

TITLE: BACK SUPPORT BEAM

SIZE	CODE IDENT. NO.	DWG. NUMBER
C	14213	T41745

SCALE FULL SHEET 1 OF 1

NOTES:

1. GENERAL REQUIREMENTS AS DEFINED IN 9900000.
2. MATERIAL: LOW CARBON STEEL.

DESIGN AGENCY PART [redacted] NO.	REVISIONS				
	ISSUE	DESCRIPTION / PREPARED BY	DATE	CHKR	ENGR.
T41743-000	A	VAN THEEMSCHE 9652/HUERTA 1342			

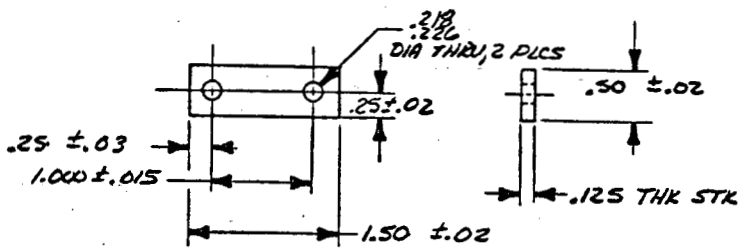

AGENCY APPROVALS			SHEET 1	TITLE
ORG	DATE	INITIALS	ISSUE A	PRESSURE PLATE
1392			SHEET INDEX	
			PART CLASSIFICATION: UNCLASSIFIED	
			DWG CLASSIFICATION LEVEL: UNCLASSIFIED	SIZE B · CODE IDENT NO. 14213 · DWG NUMBER T41743
9652				SCALE FULL · SHEET 1 OF 1

PRINTED IN U.S.A. DIETZGEN AGEPROOF 135-4

OF 9300-010-000

APPENDIX E

SCALE MODEL TEST DATA

R800570 TRUCK-CASK MODEL OPTICAL

BOSCAR

HORIZONTAL DISPL VS TIME

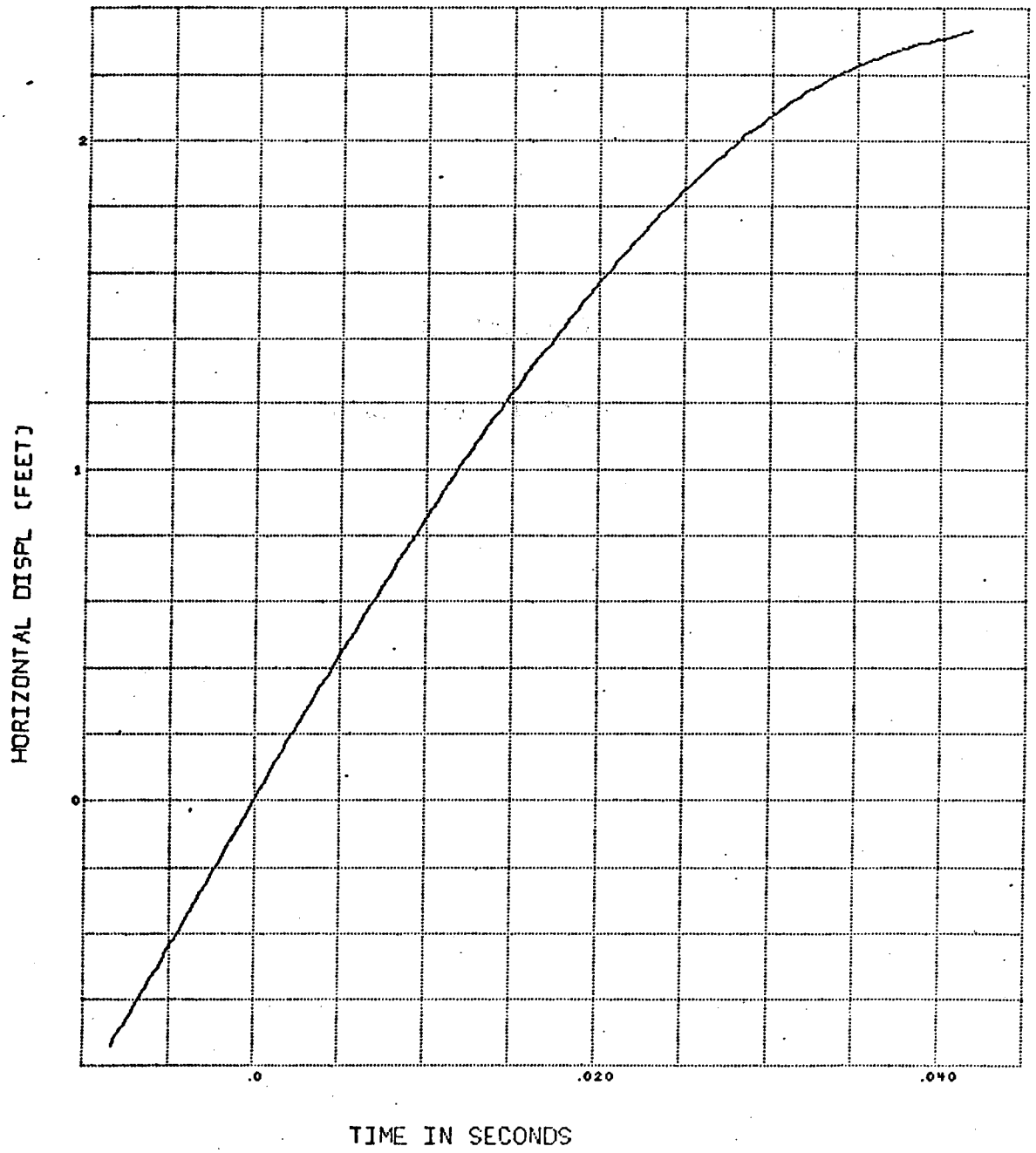

R800570 TRUCK-CASK MODEL OPTICAL

BOSCAR

HORIZONTAL VELOCITY VS TIME

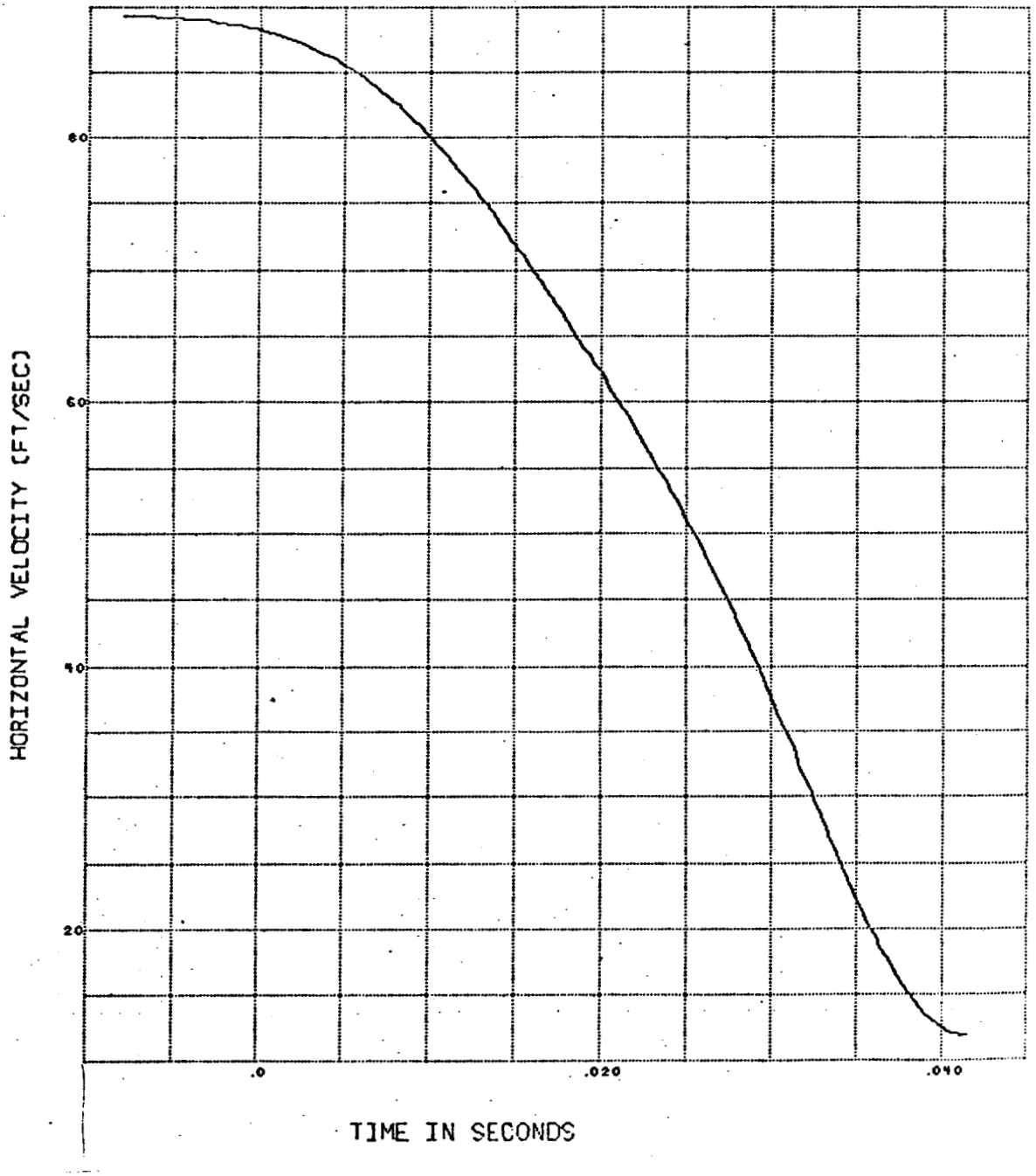

APPENDIX F

Instrumentation for the Full Scale Tests

RS 1282/2008

An Instrumentation Plan for a Truck and Spent-Nuclear-Fuel Shipping Cask Impact Test

M. Huerta, L. M. Ford

Nov. 1976

Abstract

This memorandum describes the instrumentation plan to be used in monitoring a 60 mph impact test of a truck spent-nuclear-fuel shipping system. This full-scale test is scheduled to be run at the Sandia Labs Area III test facility.

Introduction

This memorandum describes the instrumentation for the full scale tractor-trailer test to be conducted in Area III. This is to be a 60 MPH impact into a concrete target which has already been constructed on the North end of the old sled track facility. The instrumentation plan outlined here is consistent with the telemetry package and sensors available to the test program and also with the time frame which has been established for running the test.

The instrumentation plan is designed to monitor items that can be correlated with analysis and also items which may be of interest at a later date. This has been done in view of the fact that this is a very unique test to run and a reasonable amount of instrumentation should be included.

As much detail as possible, without having the hardware available for inspection, has been included. Final details will be discussed with personnel of instrumentation, Division 9483, as soon as the hardware becomes available.

The following items have been established as the desirable parameters to monitor during the test.

1. Rigid body acceleration of the cask body.
2. Attenuation of g-levels through the structure.
3. Permanent strains in the cask body and closure system.
4. Lead motion or slump within the cask body.
5. Dynamics of the cask during the test.
6. Hydrostatic pressure or water hammer effect within the cask cavity.
7. Acceleration response of the fuel elements within the cask cavity.
8. Record of sequence of events during the test. (Fifth wheel connection breaking, tie-downs breaking, etc.)

The instrumentation and photo coverage described here will provide information regarding each of these items.

The instrumentation will include active and passive accelerometers, active and passive pressure transducers, strain gages, and on-off switches which will provide time records of events during the test. Extensive photocoverage will be included. This will include high frame rate motion picture cameras positioned at various angles. Two onboard cameras will be mounted on the trailer structure and will be aimed at the cask tie-down. The target will be instrumented with accelerometers to record target motion. Detail description of various components of the test instrumentation and photo coverage are described in separate sections below.

Equipment

Equipment available for instrumenting this test includes a telemetry package with a capacity of transmitting 12 channels of 2KHZ data. These channels are fixed and cannot, for instance, be combined to form fewer higher frequency channels. This T.M. Package also has four on-off channels which can be used in conjunction with crush switches to record times at which different events happen. This package will be bolted to the back end of the cask. In addition to the large T.M. package just described, a smaller T.M. unit containing 2 accelerometers is available. The smaller T.M. is packaged as a unit with the accelerometers and can be bolted to any part of the structure Different models of piezoresistive accelerometers, as well as active and passive pressure transducers and strain gages are available. All active sensors, except for the accelerometers contained in the small T.M. unit, will operate through the 12 channel telemetry unit. Passive accelerometers which operate on the principle of a ball crushing a thin aluminum disk are also available. Numerous motion picture cameras are available for filming the test.

Photocoverage

By far the most valuable data that will be obtained from this test will be in the form of high speed motion picture films. Numerous cameras will be aimed at the system from various directions. Two onboard cameras viewing the tie-downs will be mounted on the trailer to record tie-down response. Figure 1 illustrates camera locations. This plan has been designed by T. A. Leighley of photometrics, Division 9412, and is based on experience obtained from filming preliminary scale model tests. High speed cameras located on the sides will be surveyed in place to determine their exact location with respect to the target. (This will be necessary information in the data reduction process.) The equipment will be set up on the morning of the test.

In order to have proper lighting, it has been determined that the test be run at approximately 3:00 p.m. It has also been determined that in order to prevent possible disturbances to cables, an absolute minimum number of personnel will be allowed in the immediate test area on the day of the test. Redundant triggering circuits and power sources will be provided for the cameras. (This will minimize the possibility of having a block of cameras malfunction.)

It is expected that a large amount of quantitative data can be obtained from the films. This will include displacement time and velocity-time histories for various points on the structure and on the cask. For purposes of film data reduction, the tractor and trailer frame will be striped. The centers of the wheels will be painted with a bright color. Also, some areas of the cask should be painted with a bright color. Details concerning the painting scheme will be communicated shortly after the equipment arrives.

In conjunction with the photocoverage, a fixed reference as indicated in Figure 2 will be provided by Division 9412.

Active Accelerometers

The active accelerometers will have to operate through the telemetry system which has a 2KHZ frequency response limitation. It has been determined that the predominant frequency response of the cask will probably be below this level. The frequency limitation of the telemetry unit does not present a problem with regard to accelerometer signals. The expected frequency response level of the cask is also within the capability of the accelerometers. The type of accelerometers which will be used to monitor the cask motion are piezoresistive Endevco models 2262-200 and 2261A-2500. The model 2262 is a damped low natural frequency (3000 HZ) accelerometer. It will provide good resolution at low g levels. Its frequency response has been experimentally determined to be reasonably linear up to 2KHZ. The model 2261A-2500 is an undamped accelerometer with a natural frequency of 31KHZ and a peak g capability of 2500 g's. These will be used to capture any possible high g spikes.

A total of five active accelerometers will be mounted on the sides of the cask body monitoring accelerations in the axial direction. Two of these will be near the head end, two near the bottom end, and one located approximately in the middle (see Figure 2). These will be mounted on the sides of the cask. For mounting purposes, there are some large stainless steel blocks on both sides of the cask at each end. These blocks are part of the cask shell and the accelerometers can be mounted in these areas. The middle accelerometer will have to be mounted on a small stainless steel cube welded to the cask shell. (All accelerometers will be mounted with screws and dental cement.)

The front locations will have an Endevco model 2262-200 and one 2261A-2500 accelerometer. These will be calibrated to 200 and 1000 g's respectively.

The middle unit will be a model 2261A-2500 calibrated to 500 g's. The two units in the back will be similar to the front units. These will be calibrated to 200 and 500 g's.

Wiring to the accelerometers from the T.M. Package will be along the sides of the cask. Holes will be drilled in the fins and wires will be routed through these. Wires will be routed along both sides of the cask. This will minimize the possibility of wiping out all the accelerometer signals by having a wire bundle cut by debris.

The small T.M. package containing two accelerometers will be bolted to the trailer structure underneath the cask (see Figure 2).

Passive Accelerometers

Numerous passive accelerometers will be used throughout the structure as indicated on Figure 2. This includes units on the tractor frame, trailer structure, and shipping cask. In addition to these locations, the fuel elements and fuel basket inside the cask will also be instrumented with this type of accelerometer. Exact locations will be determined after the hardware can be inspected.

On the tractor and trailer frame, these passive accelerometers will be mounted on cross-members in areas that are relatively well protected. On the cask body, they will be mounted between fins. These accelerometers should give an indication of the g-level attenuation through the vehicular structure and cask.

The nominal range for these devices using the thinnest disk is 200-1000 g's. Readings lower than this can be obtained with some loss of

accuracy. Although a lower range is desirable, it is felt that meaningful data can be obtained from these. Their response time is fast enough to record any significant peak g levels.

Pressure Transducers

Pressure transducers will be included to monitor hydrostatic pressures generated on the head end of the cavity. Three passive type transducers will be located inside the cask cavity. These have a range of 0-20,000 psi. One active transducer will be located in an overflow pipe near the cask head end. The range of this unit is 0-1200 psi. Hydrostatic pressure readings within the cavity will be used for estimating strains in the head bolts.

Crush Switches

Crush switches are on-off devices which can be used to record the time of an event such as the fifth wheel connection breaking. The telemetry package available for the tests includes provisions for four of these channels. Recommended locations for these are on the front end of the tractor, the front end of the trailer, at the fifth wheel connection, and at the front cask tie-down. These will give indications of when the tractor first impacts the wall, the time when the fifth wheel connection breaks, the time when the front end of the trailer impacts the back end of the cab, and the time when the front tie down breaks if indeed this occurs. These units will be wired to the telemetry package located on the back end of the cask. Wires will be routed along the trailer and tractor structure wherever convenient and well protected.

Strain Gages

Two strain gage rosettes will be mounted on the cask outer shell near the head end. These will be mounted on the sides of the cask. This

is the area of the cask that will probably be strained the most as any lead motion within the shell will tend to bulge out the outer shell. The system will be calibrated to read ± 2000 micro inches per inch of strain at this point. This will record strains well beyond the yield point. Shell strains at this point may be correlated with analytical calculations at a later date.

T.M. Package

The large T.M. package has dimensions of approximately 13" x 13" x 13" and weighs about 80 lbs. It will be bolted to the back end of the cask as illustrated in Figure 2. This allows it to move with the cask should the cask come off the trailer. The instrumentation is very well protected and should remain functional throughout the event.

Target Instrumentation

As a point of interest, the concrete target should be instrumented with accelerometers. The units will be placed on the top of the target as indicated in Figure 2. These units can be hard wired separately. Division 9335 will install and record the output of these units. They will be installed on the face of the target near the top.

Miscellaneous

Precautions will be taken to prevent a dust cloud from obscuring the system from photo coverage during the impact. The tractor and trailer will be cleaned prior to testing and the dirt area in front of the target will be oiled or wetted down.

The system should be extensively still photographed prior to testing. This should include the tractor, trailer, king pin connection, tie downs, and cask. These will be useful in post-test analysis of the structure.

The bolts on the cask closure system will be torqued to a specific value. These torque values and the head area will be carefully checked after the test to detect any changes.

Acknowledgements

In the course of preparing this instrumentation plan extensive consultations were held with W. V. Hereford and M. E. Barnett of Instrumentation, Division 9483. The photography plan is principly the work of T. A. Leighley, photometrics, Division 9412. The authors would like to thank J. T. Foley for carefully reviewing the manuscript. Numerous other individuals were consulted regarding different aspects of this instrumentation plan. Their help is gratefully acknowledged.

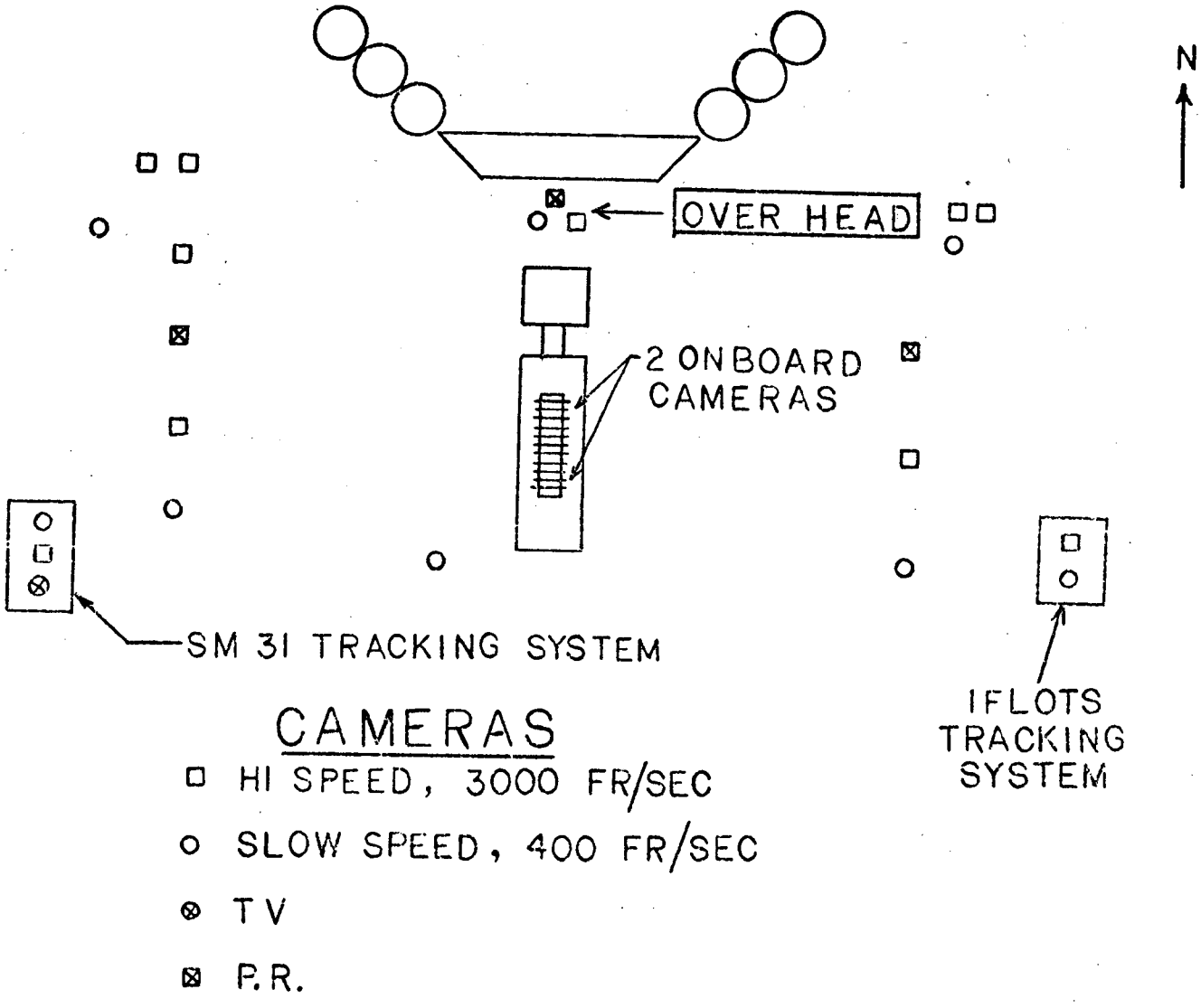

FIGURE 1. PHOTOGRAPHY PLAN

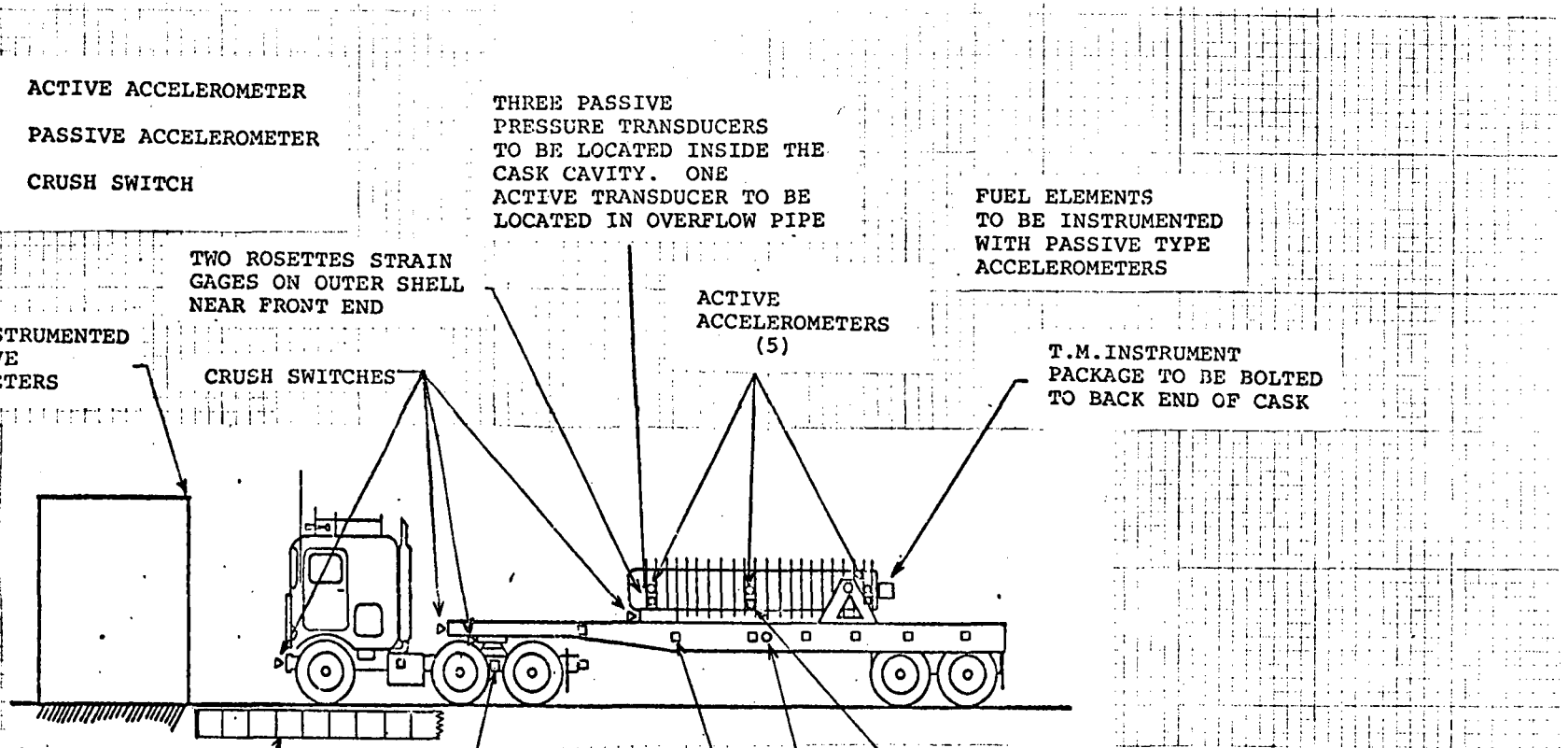

FIGURE 2. INSTRUMENTATION PLAN

APPENDIX G

DATA FROM THE FIRST FULL SCALE TEST

R422247 TRUCK-CASK OPTICAL

BOSCAR

HORIZONTAL DISPL VS TIME

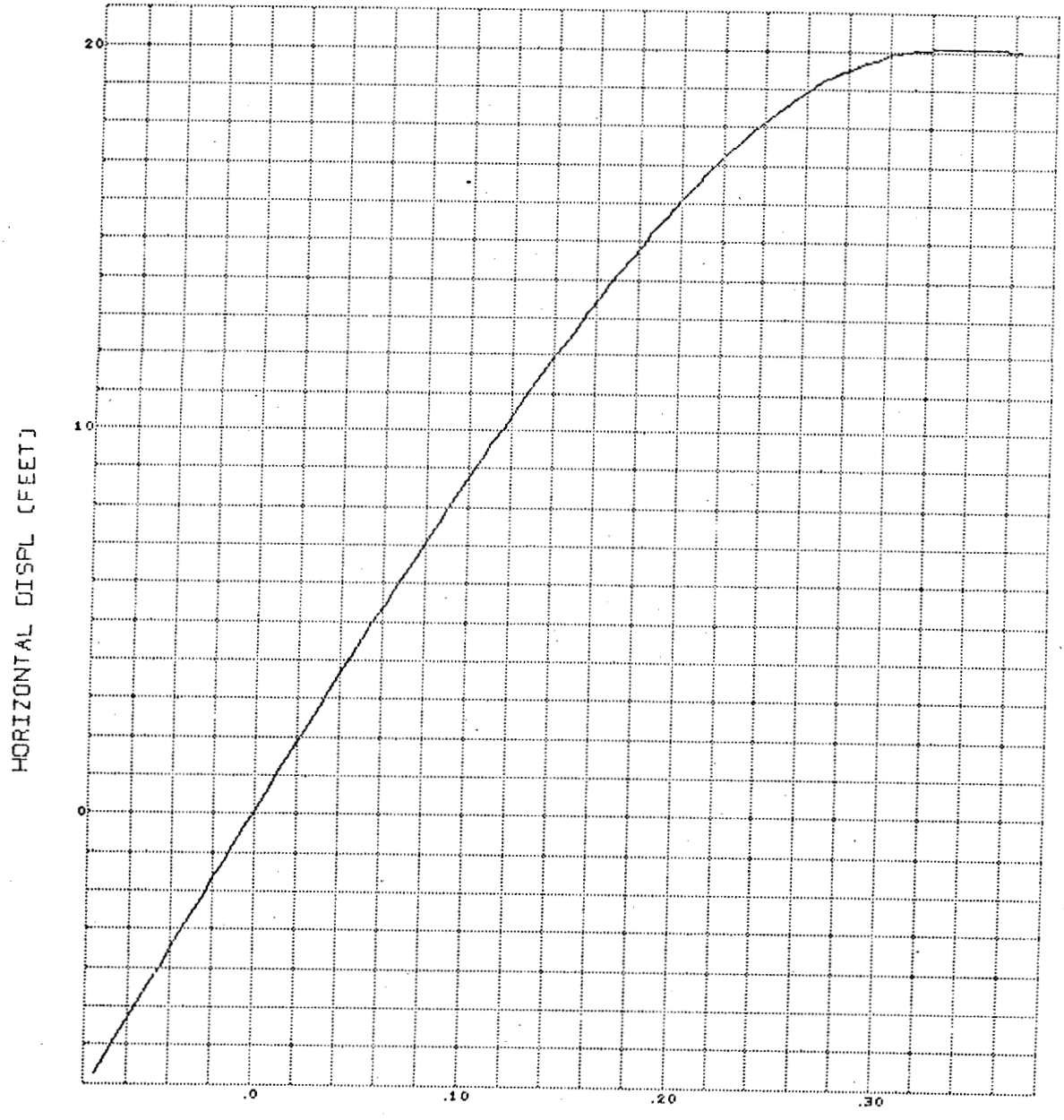

BOSCAR R422247 TRUCK-CASK OPTICAL

HORIZONTAL VELOCITY VS TIME

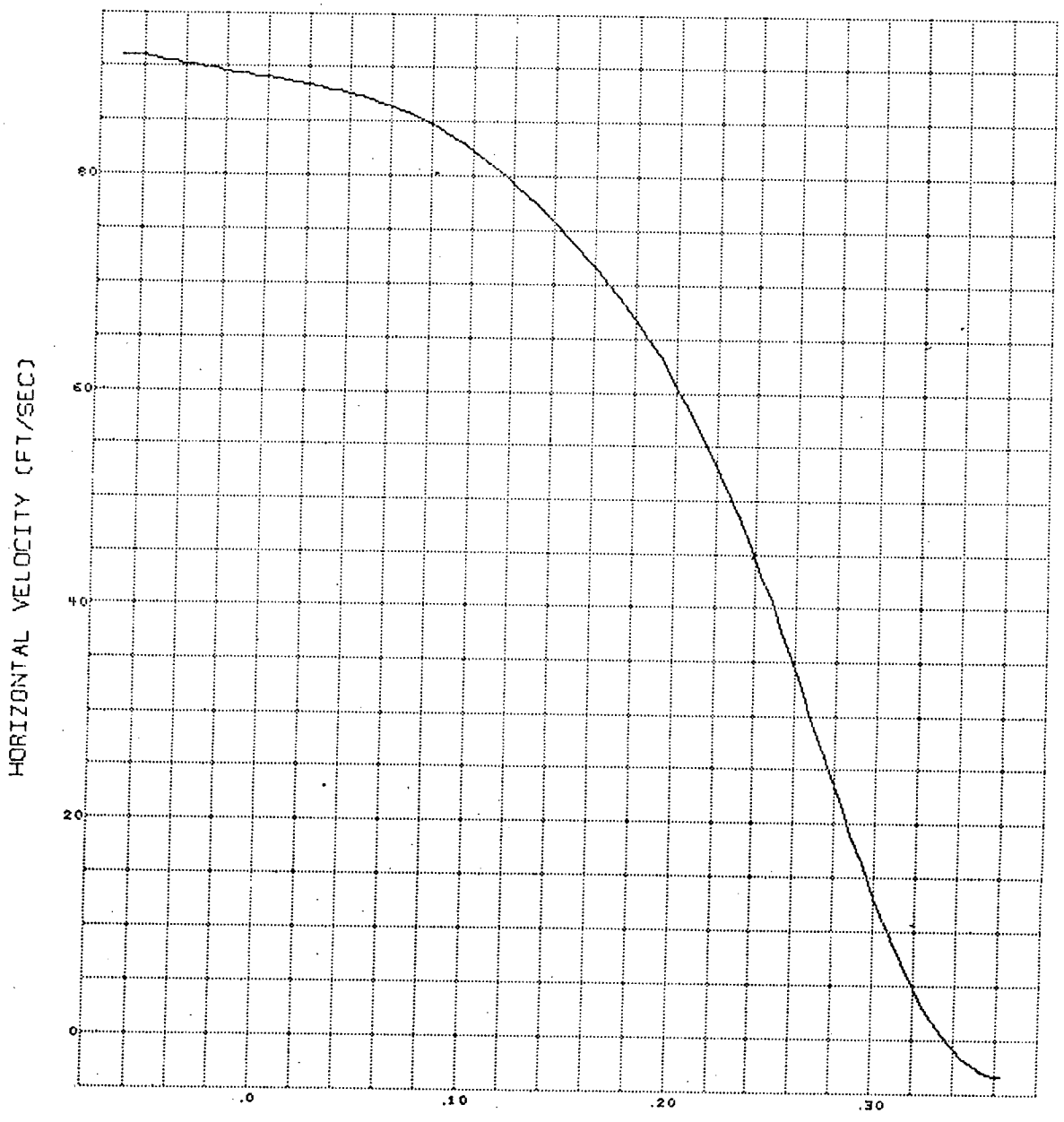

R422247 Truck Cask Attitude

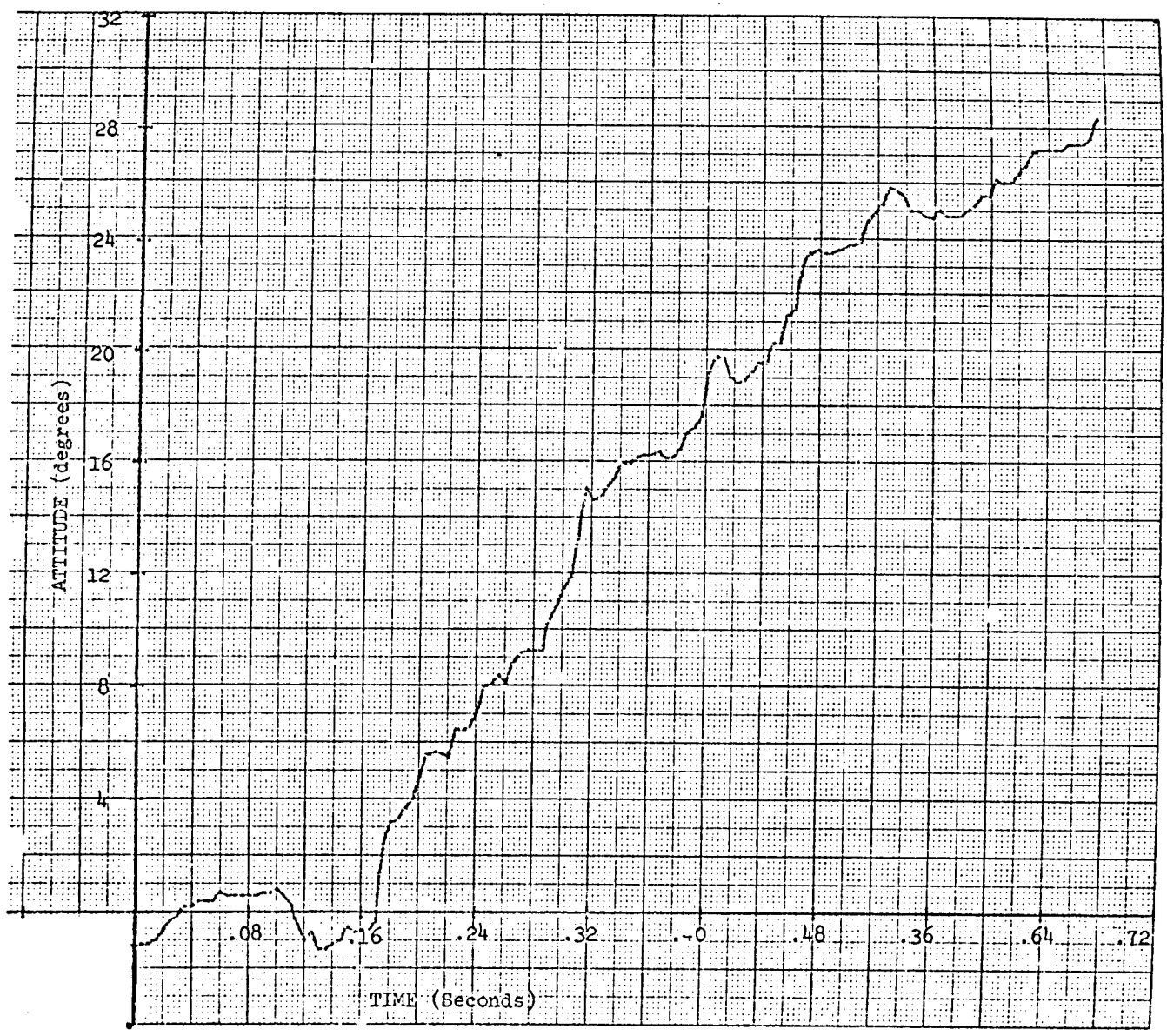

R422247 TRUCK AND SPENT NUCLEAR FUEL SHIPPING CASK
CASK ACCEL FRONT LEFT 50 HZ LPF

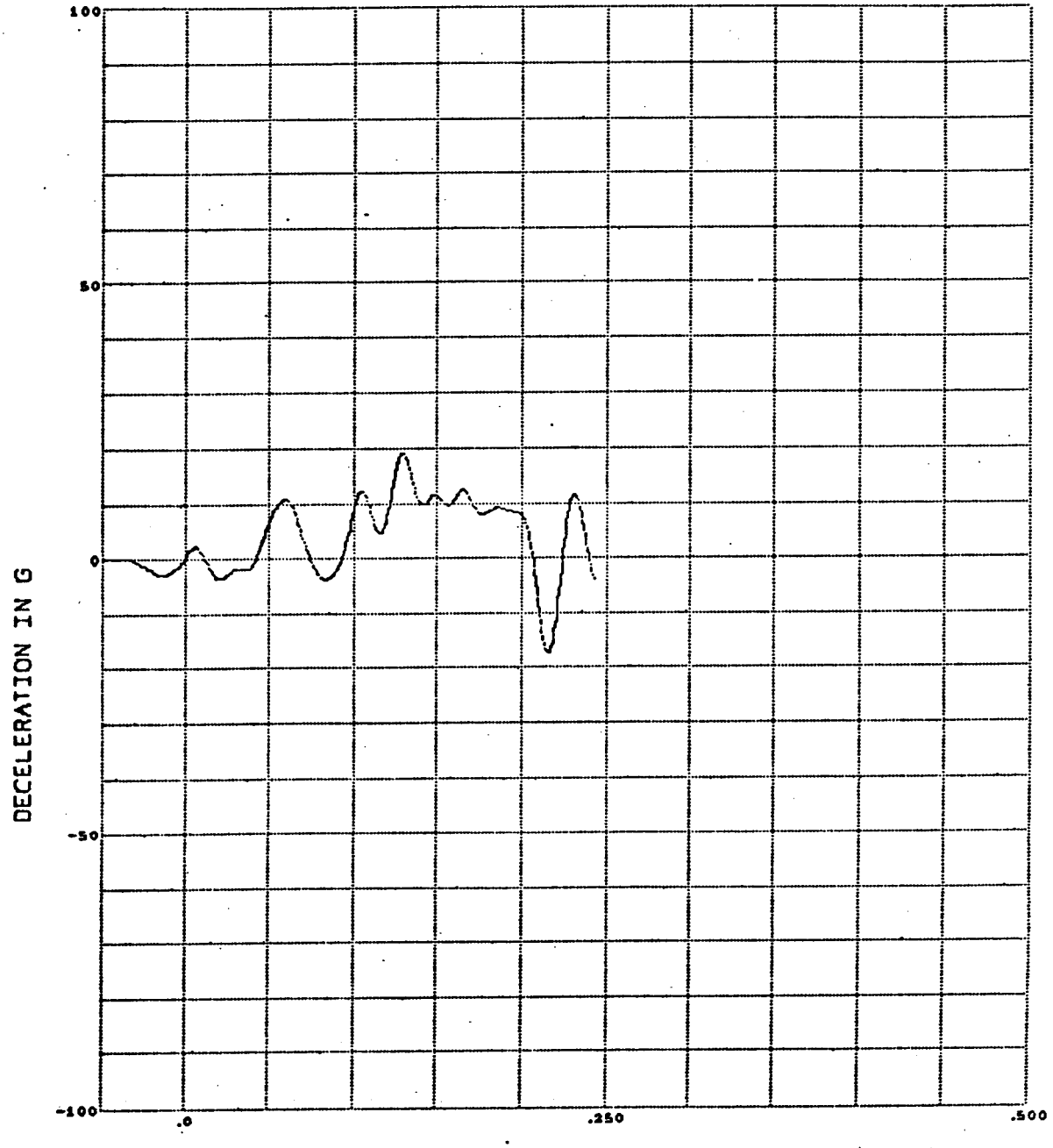

R422247 TRUCK AND SPENT NUCLEAR FUEL SHIPPING CASK
CASK ACCEL CENTER LEFT 50 HZ LPF

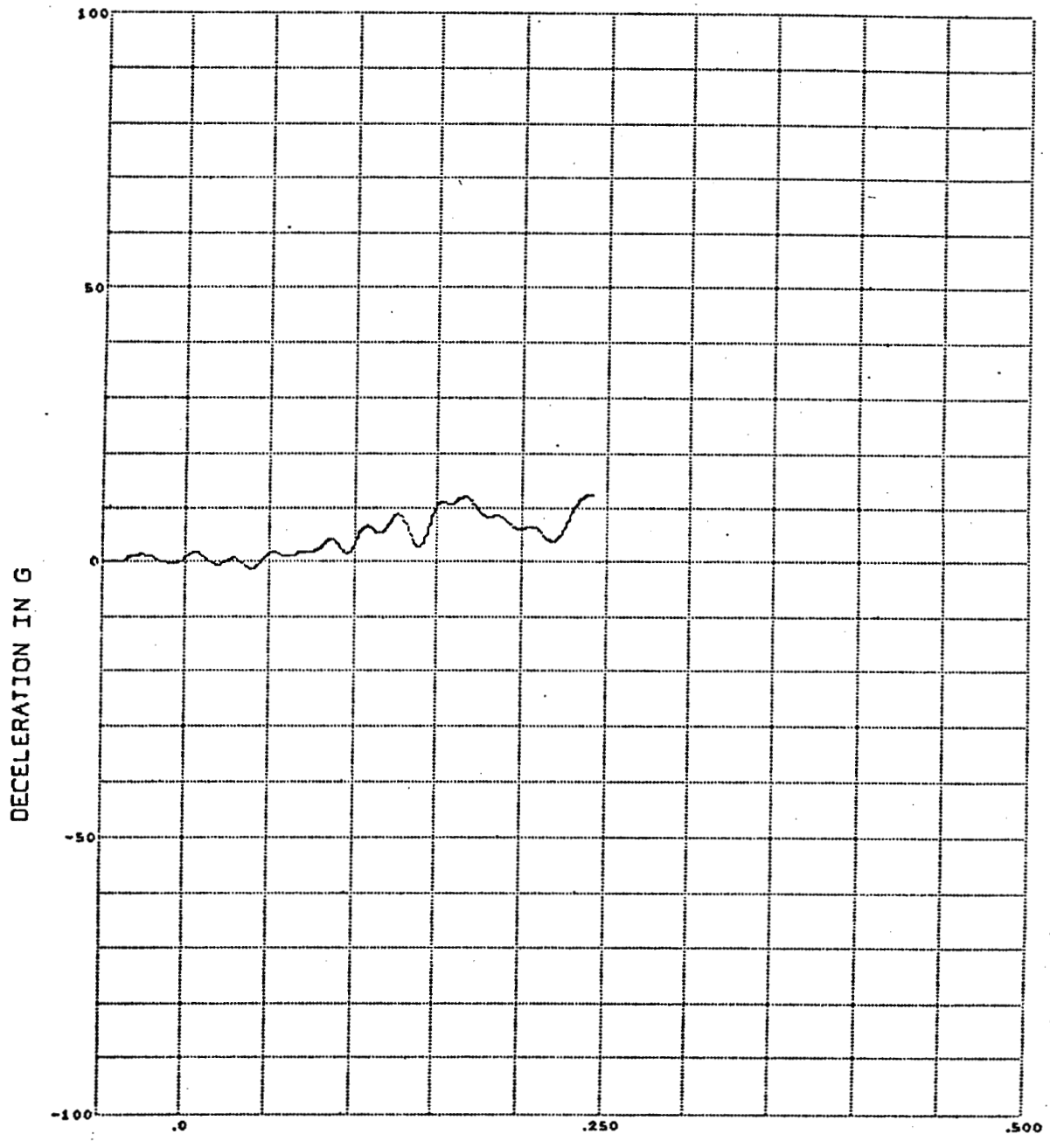

R422247 TRUCK AND SPENT NUCLEAR FUEL SHIPPING CASK

CASK ACCEL BACK LEFT 50 HZ LPF

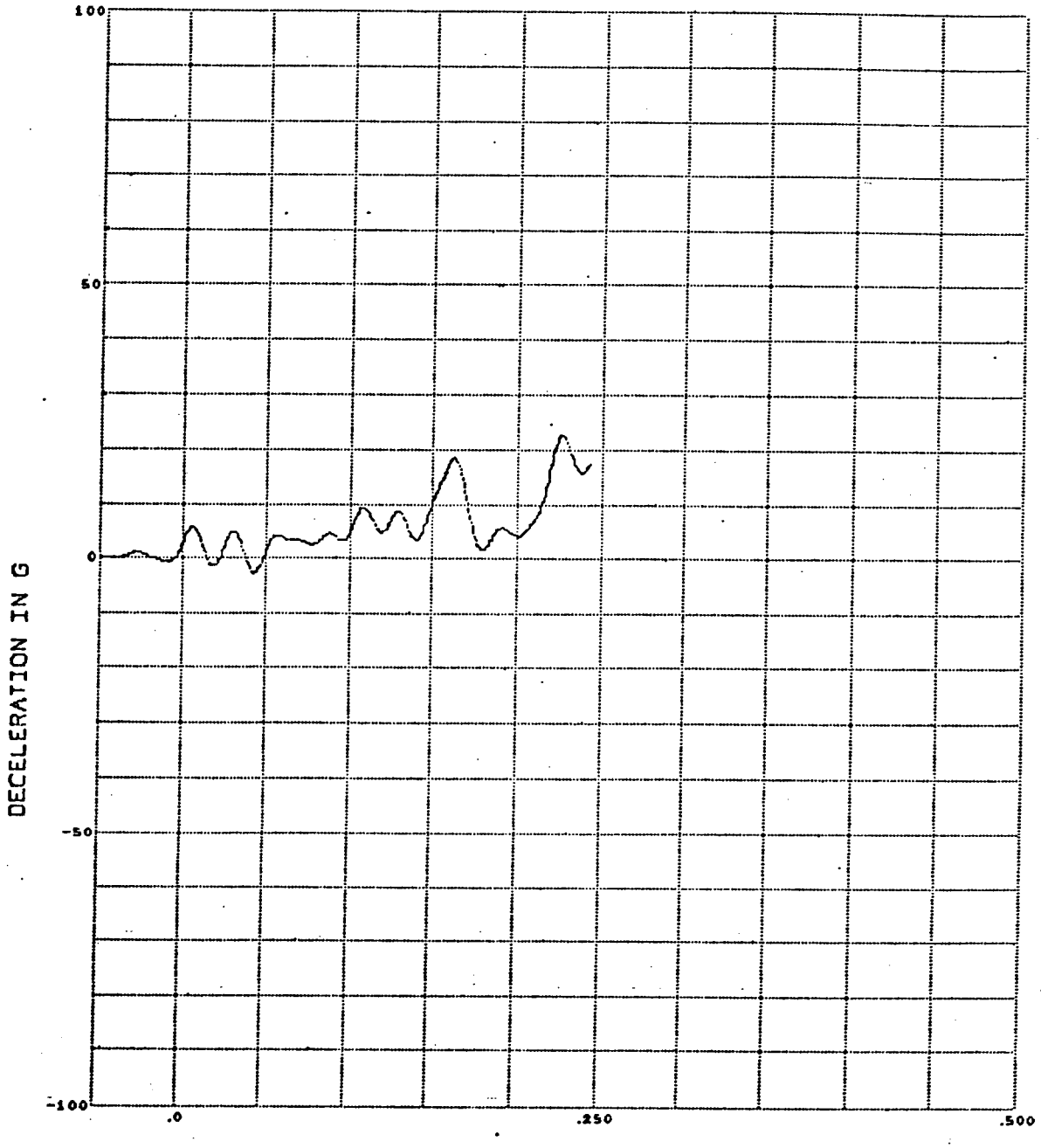

R422247 TRUCK AND SPENT NUCLEAR FUEL SHIPPING CASK
CASK ACCEL BACK RIGHT 50 HZ LPF

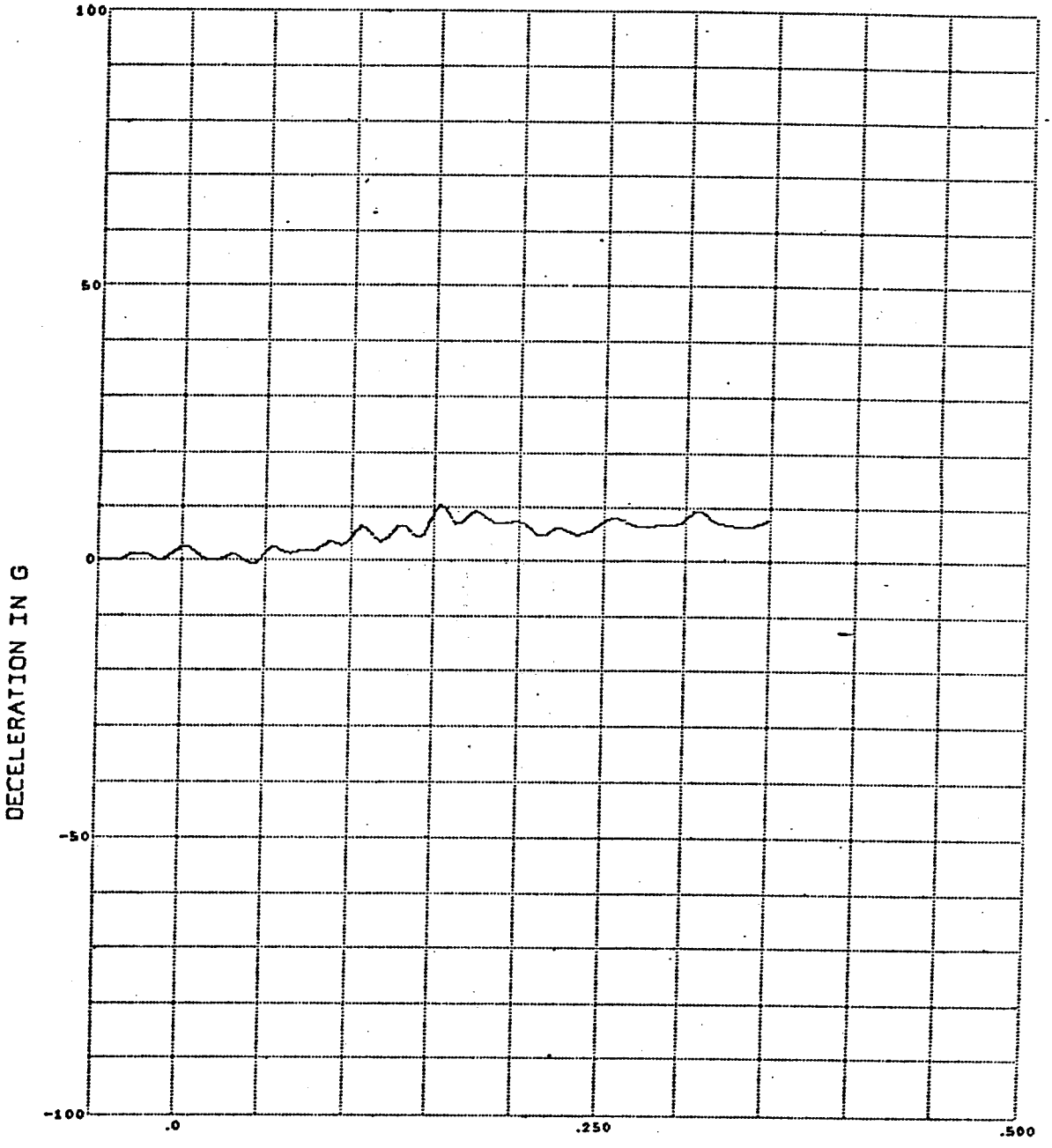

R422247 TRUCK AND SPENT NUCLEAR FUEL SHIPPING CASK

CASK ACCEL BACK LEFT

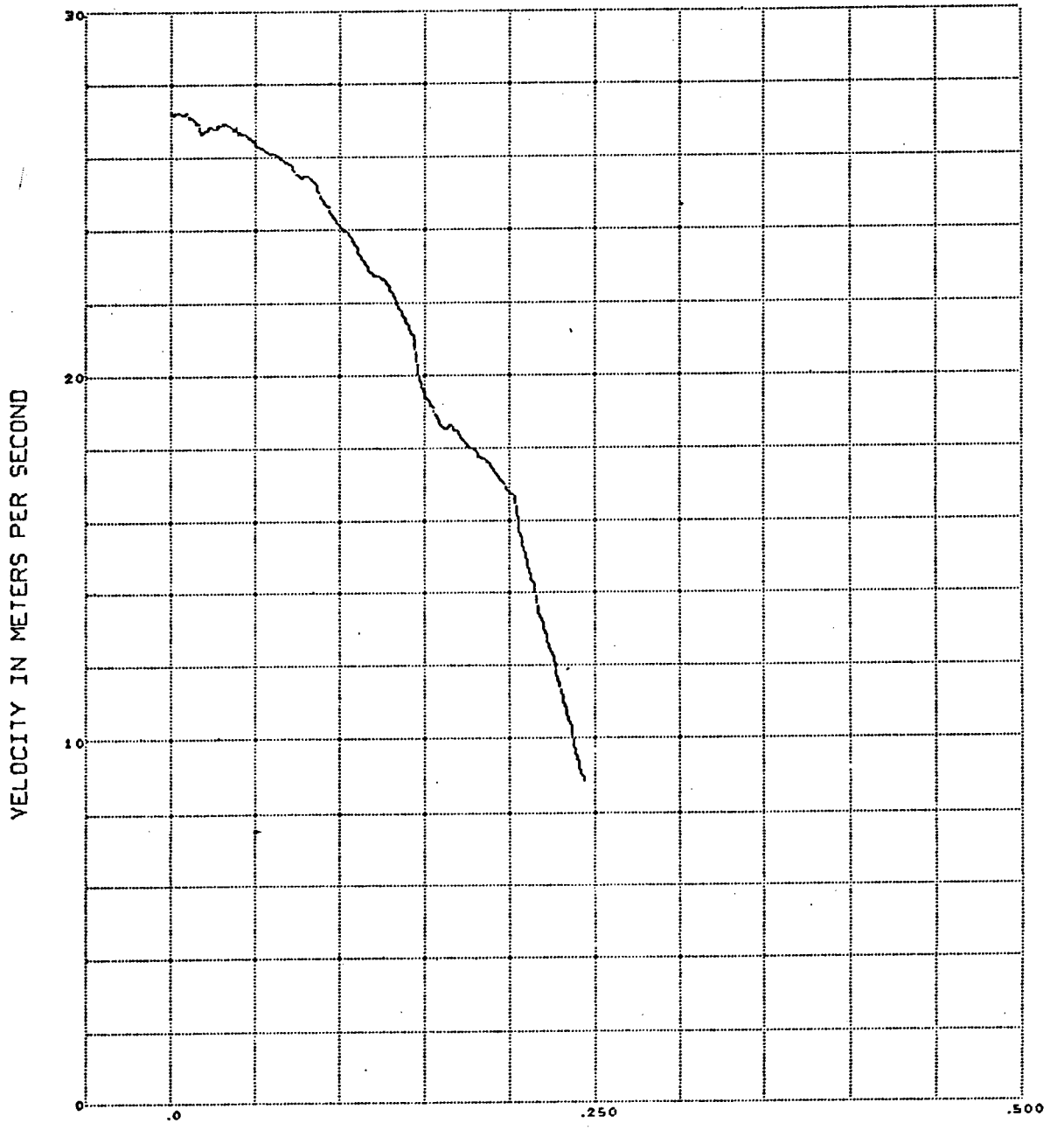

R422247 TRUCK AND SPENT NUCLEAR FUEL SHIPPING CASK

CASK ACCEL BACK LEFT

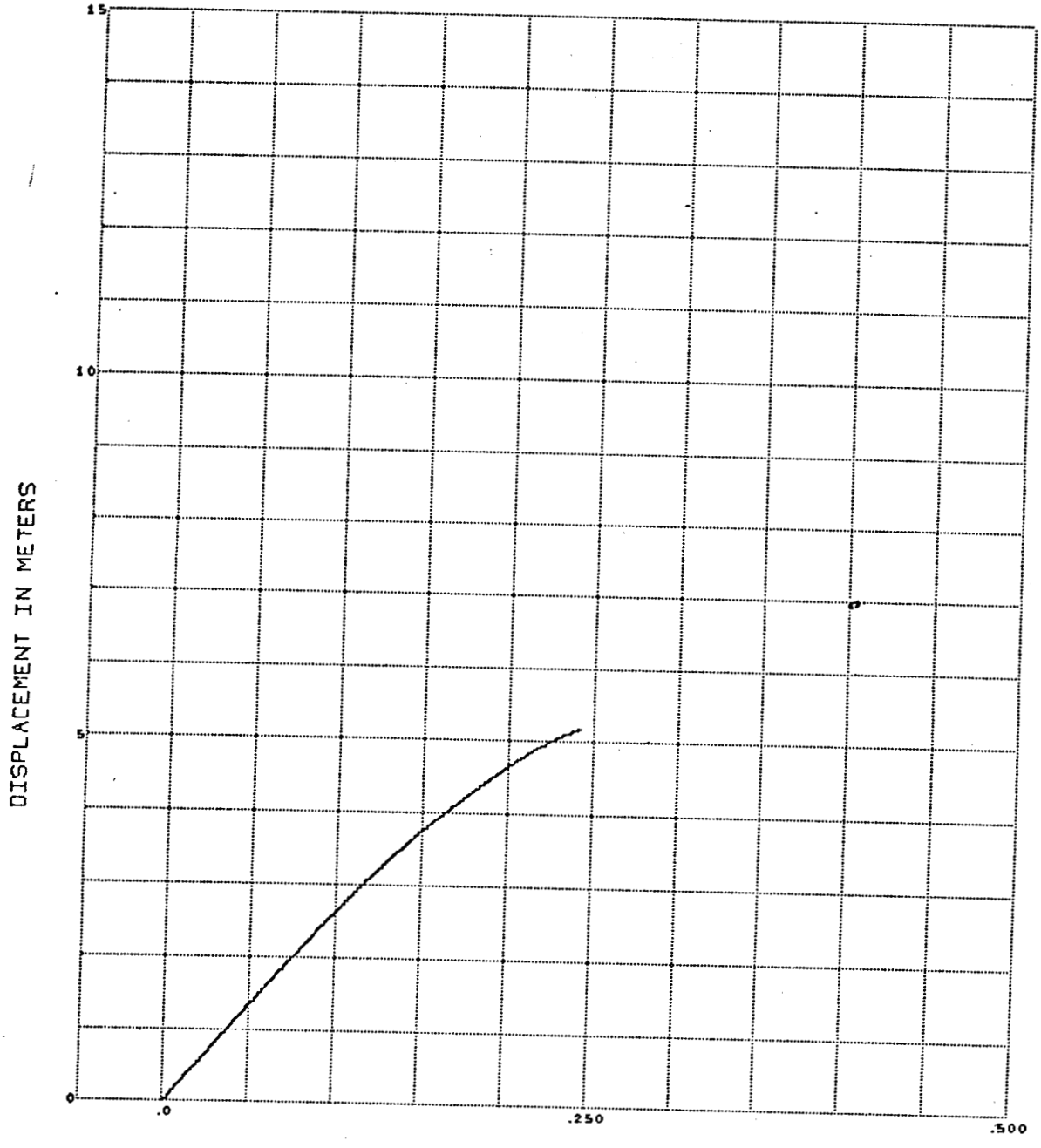

R422247 TRUCK AND SPENT NUCLEAR FUEL SHIPPING CASK
STRAIN 6 RIGHT FRONT CASK 45 DEGREES AFT

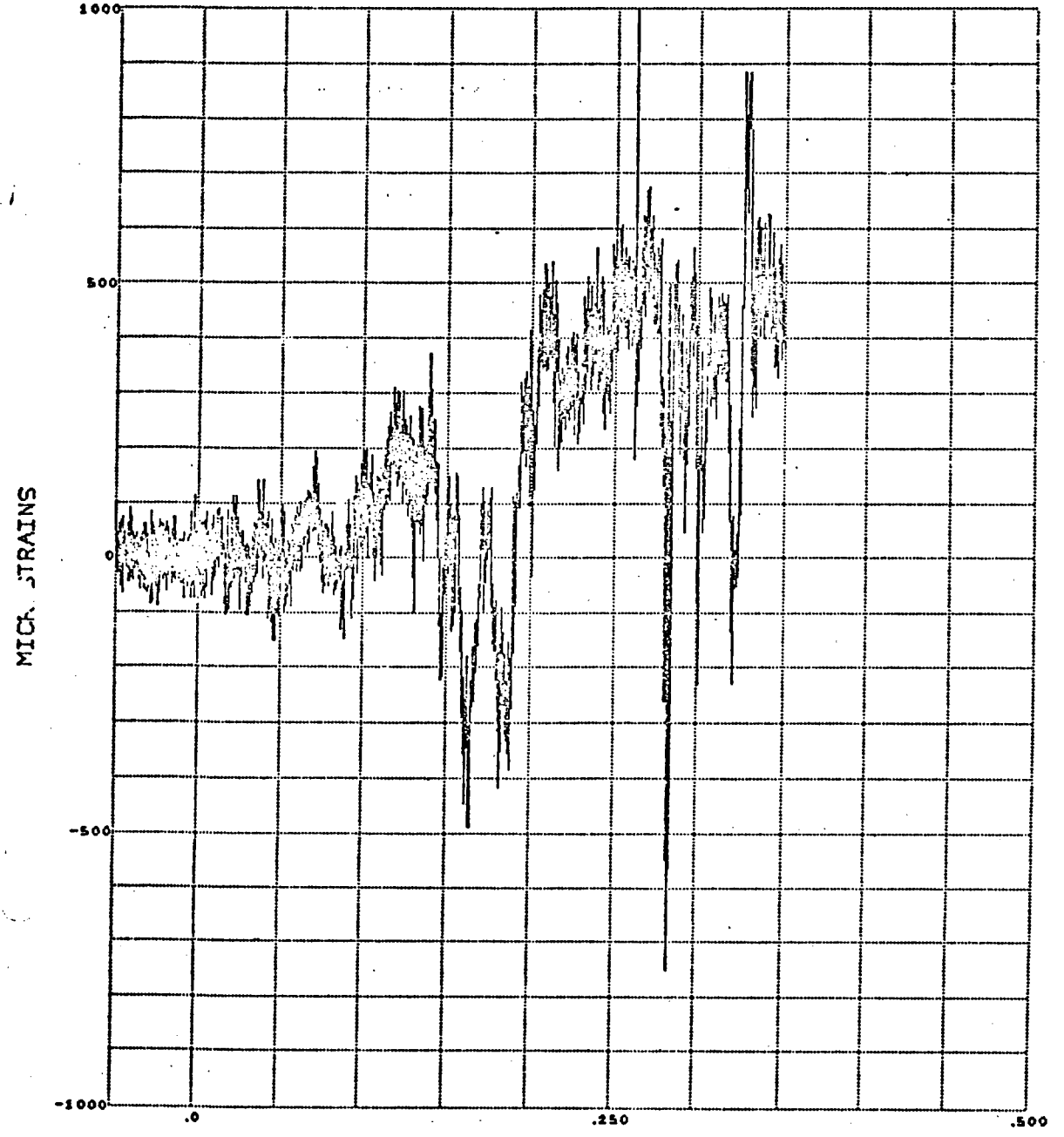

R422247 TRUCK AND SPENT NUCLEAR FUEL SHIPPING CASK
STRAIN 5 RIGHT FRONT CASK 0 DEGREES

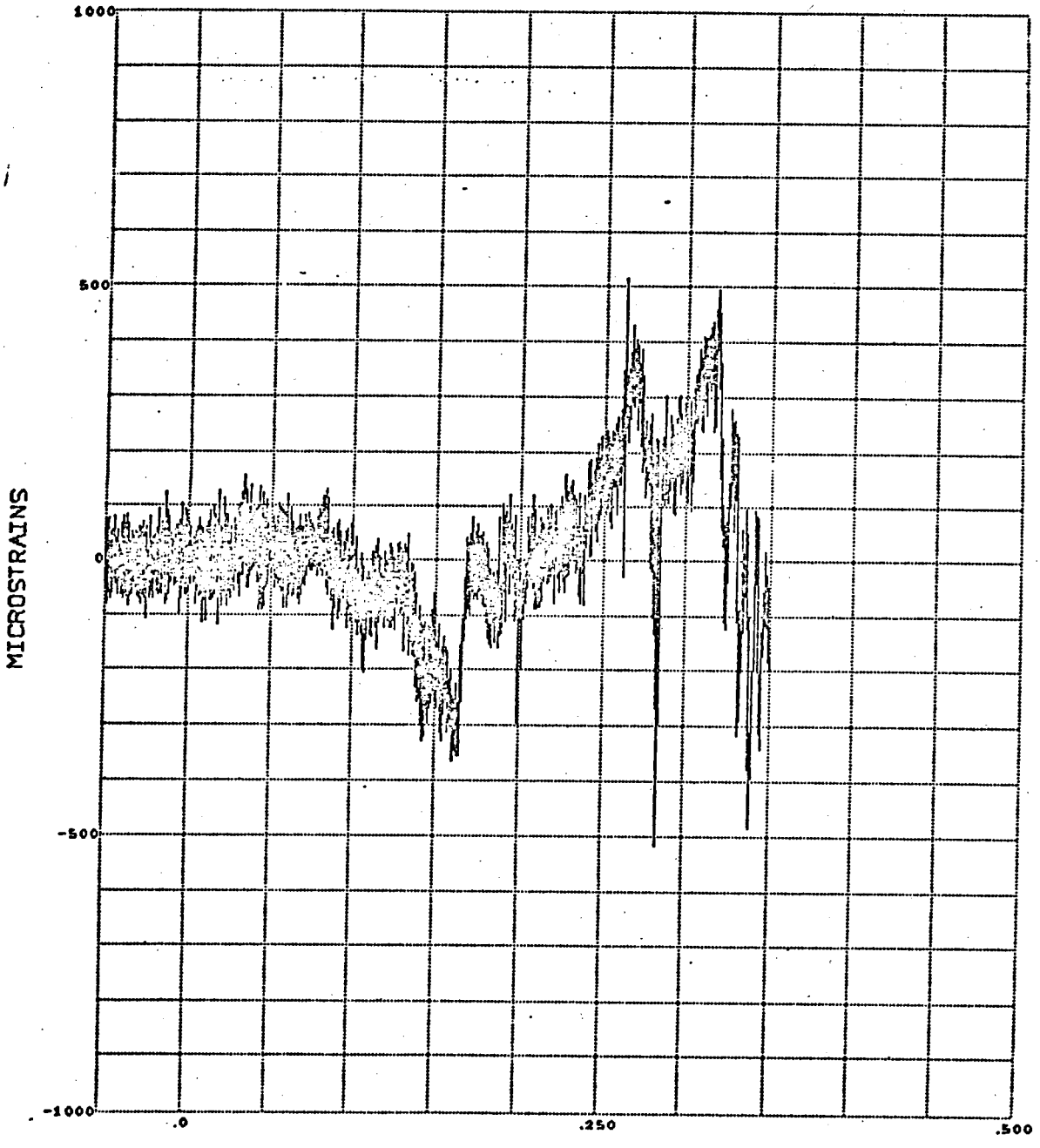

R422247 TRUCK AND SPENT NUCLEAR FUEL SHIPPING CASK
STRAIN 4 RIGHT FRONT CASK 45 DEGREES FRONT

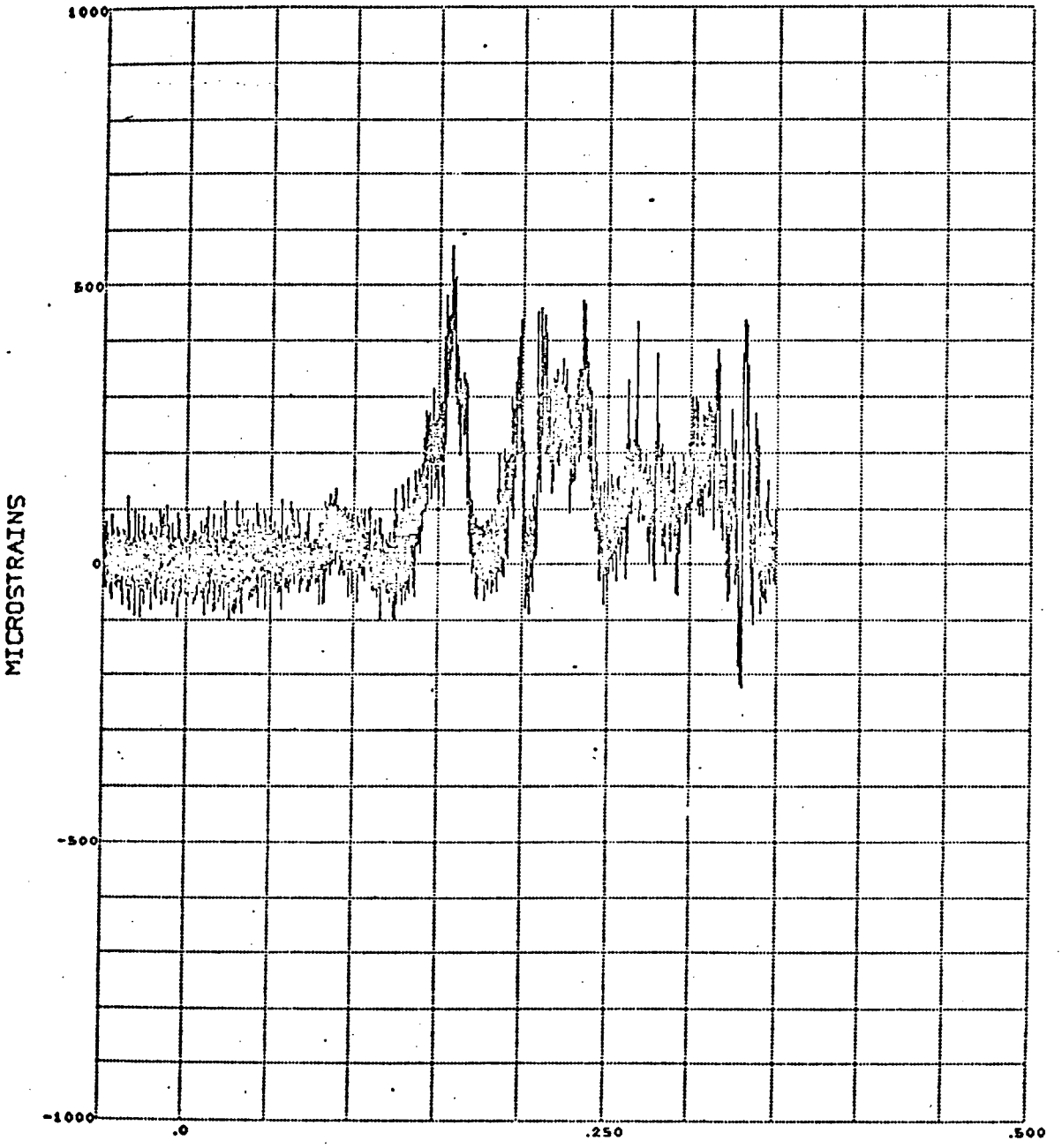

APPENDIX H

DATA FROM THE SECOND FULL SCALE TEST

R422259 TRUCK-CASK IMPACT HY-CAM WEST OPTICAL

HORIZONTAL DISPL VS TIME

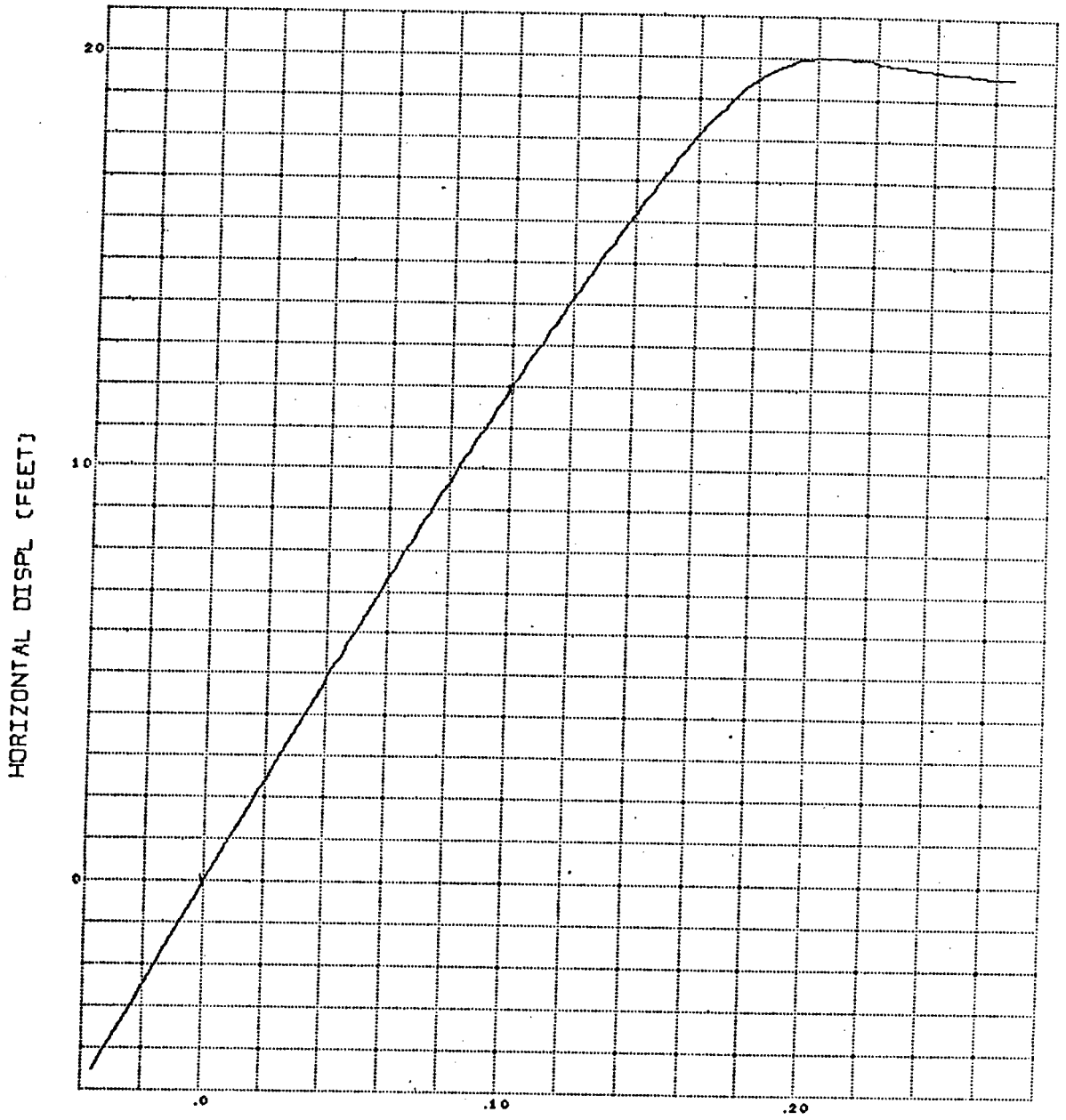

R422259 TRUCK-CASK IMPACT HY-CAM WEST OPTICAL

HORIZONTAL VELOCITY VS TIME

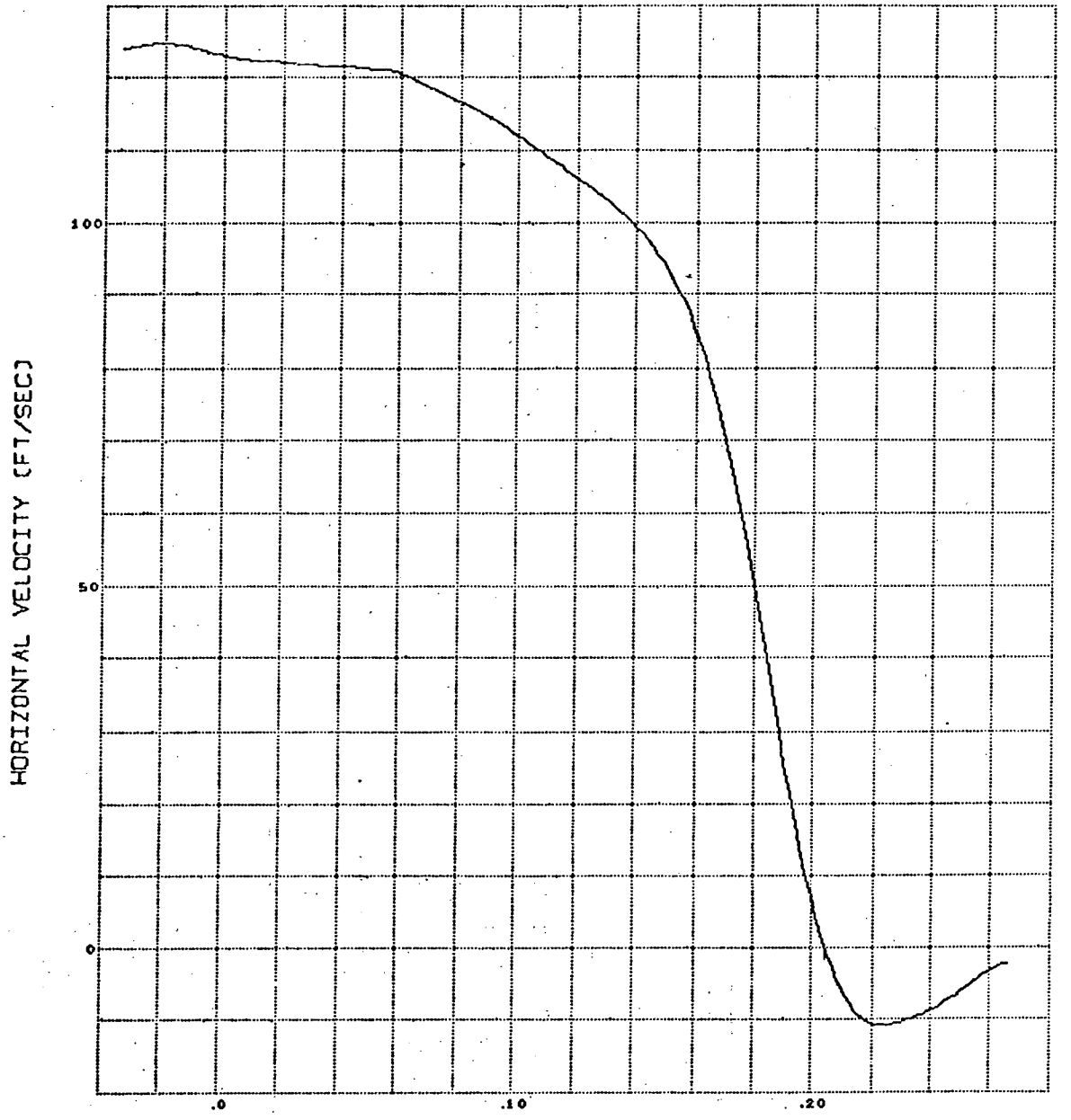

R422259 TRUCK-CASK IMPACT HY-CAM WEST OPTICAL

ATTITUDE VS TIME

R422259 TRUCK AND SPENT NUCLEAR FUEL SHIPPING CASK (84 MPH)
CASK ACCEL FRONT RIGHT 50 HZ LPF

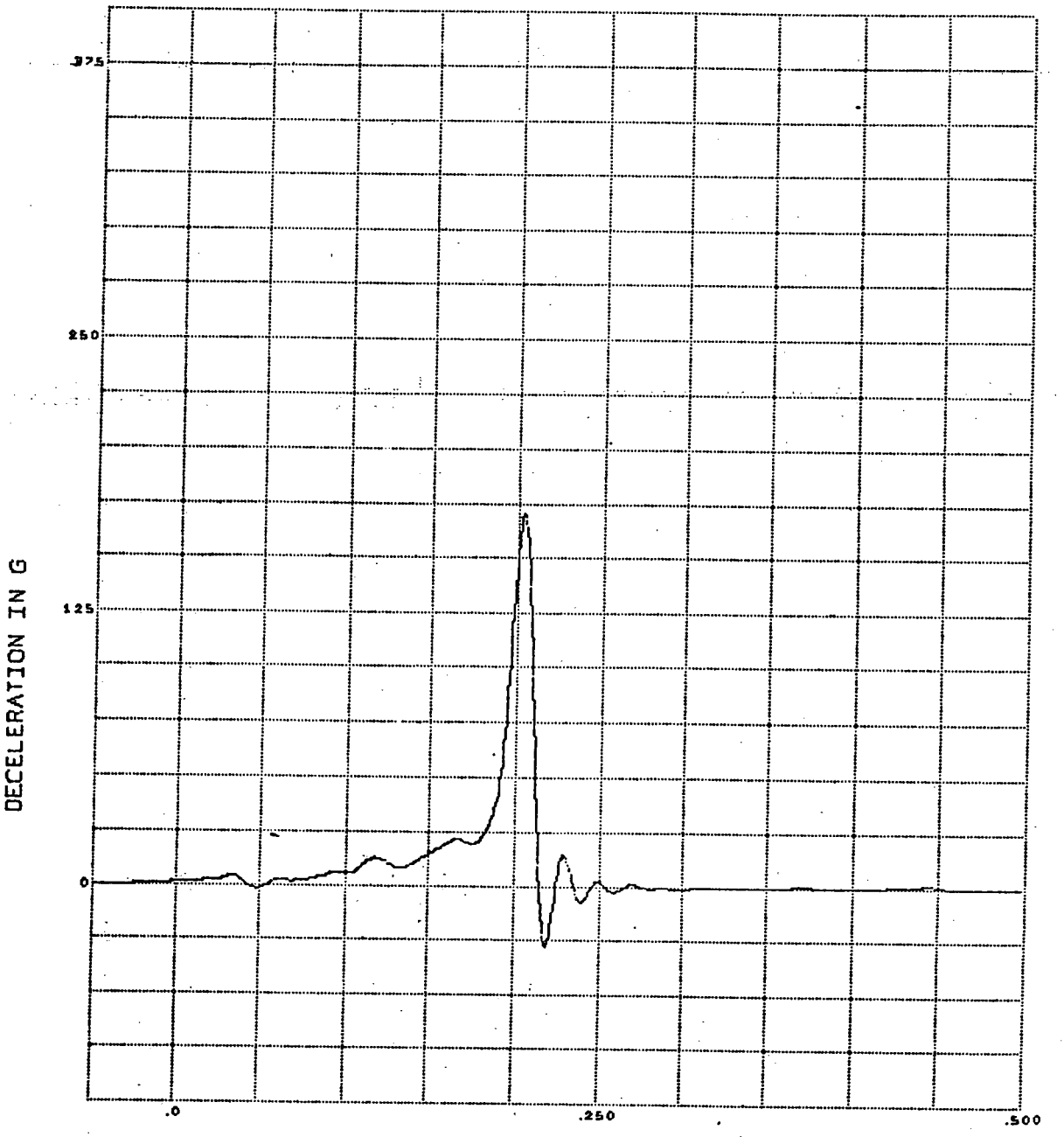

R422259 TRUCK AND SPENT NUCLEAR FUEL SHIPPING CASK (84 MPH)
CASK ACCEL FRONT LEFT 50 HZ LPF

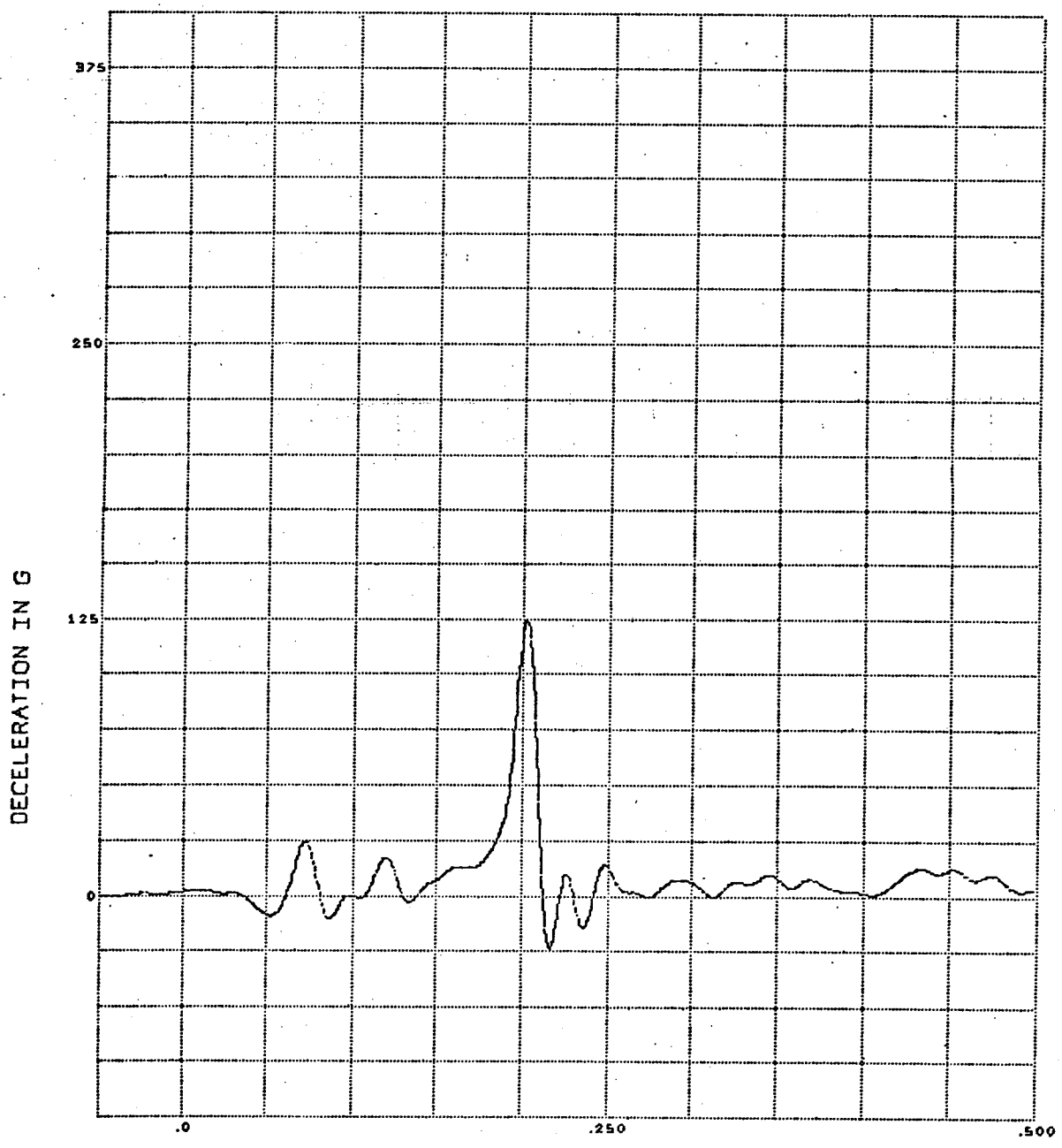

R422259 TRUCK AND SPENT NUCLEAR FUEL SHIPPING CASK (84 MPH)
CASK ACCEL CENTER LEFT 50 HZ LPF

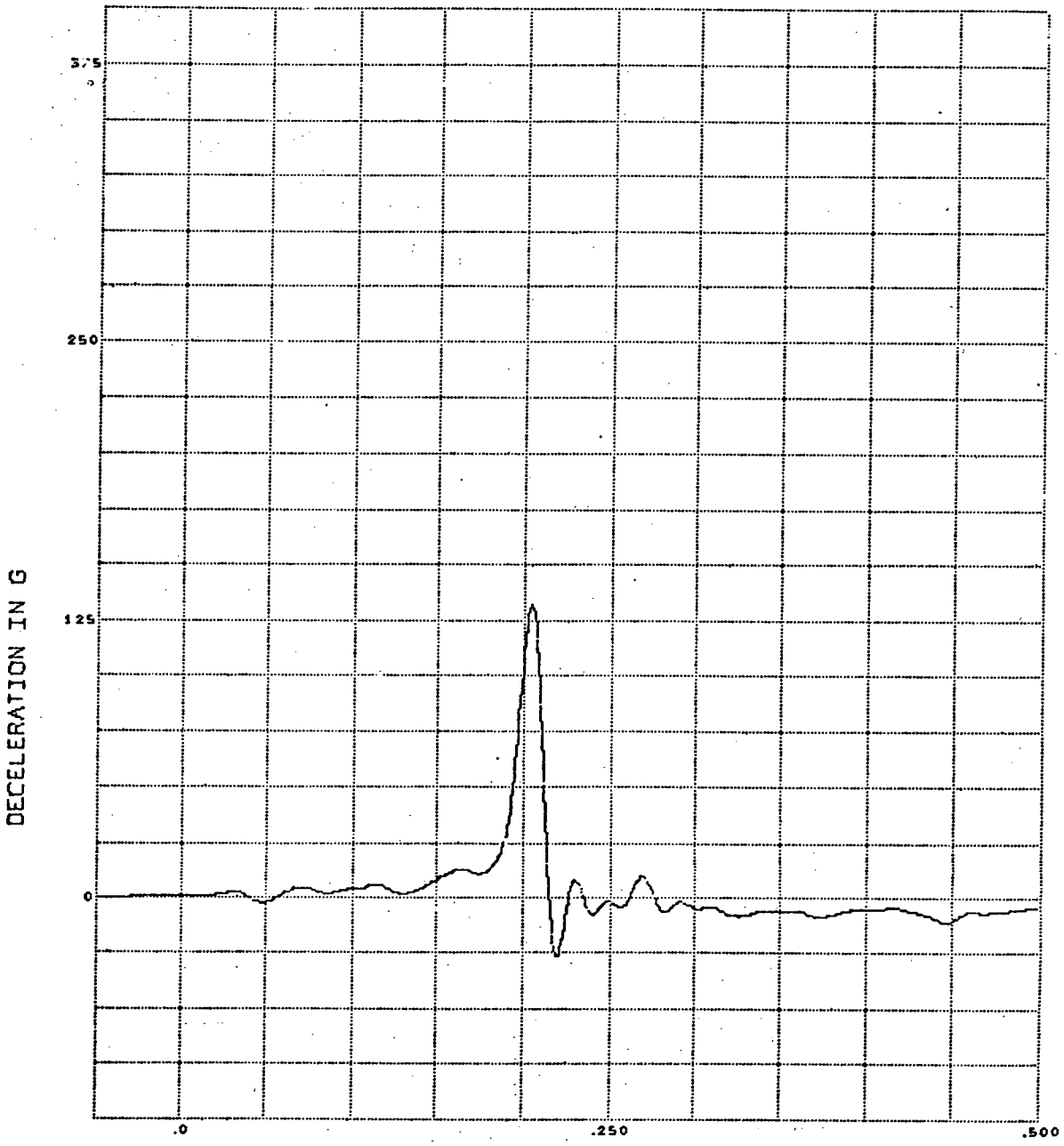

R422259 TRUCK AND SPENT NUCLEAR FUEL SHIPPING CASK (84 MPH)
CASK ACCEL BACK LEFT 50 HZ LPF

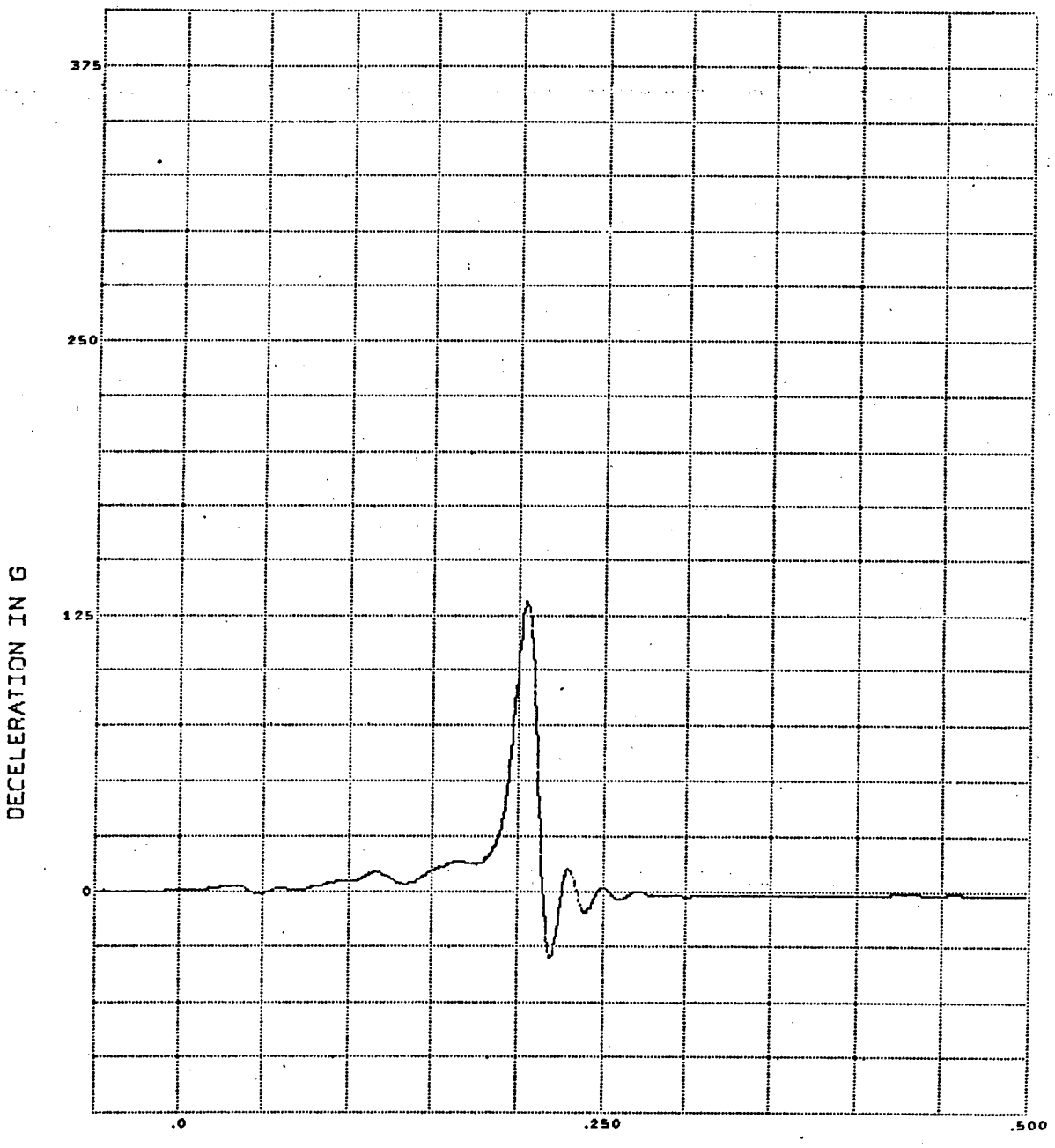

R422259 TRUCK AND SPENT NUCLEAR FUEL SHIPPING CASK (84 MPH)
CASK ACCEL AFT RIGHT 50 HZ LPF

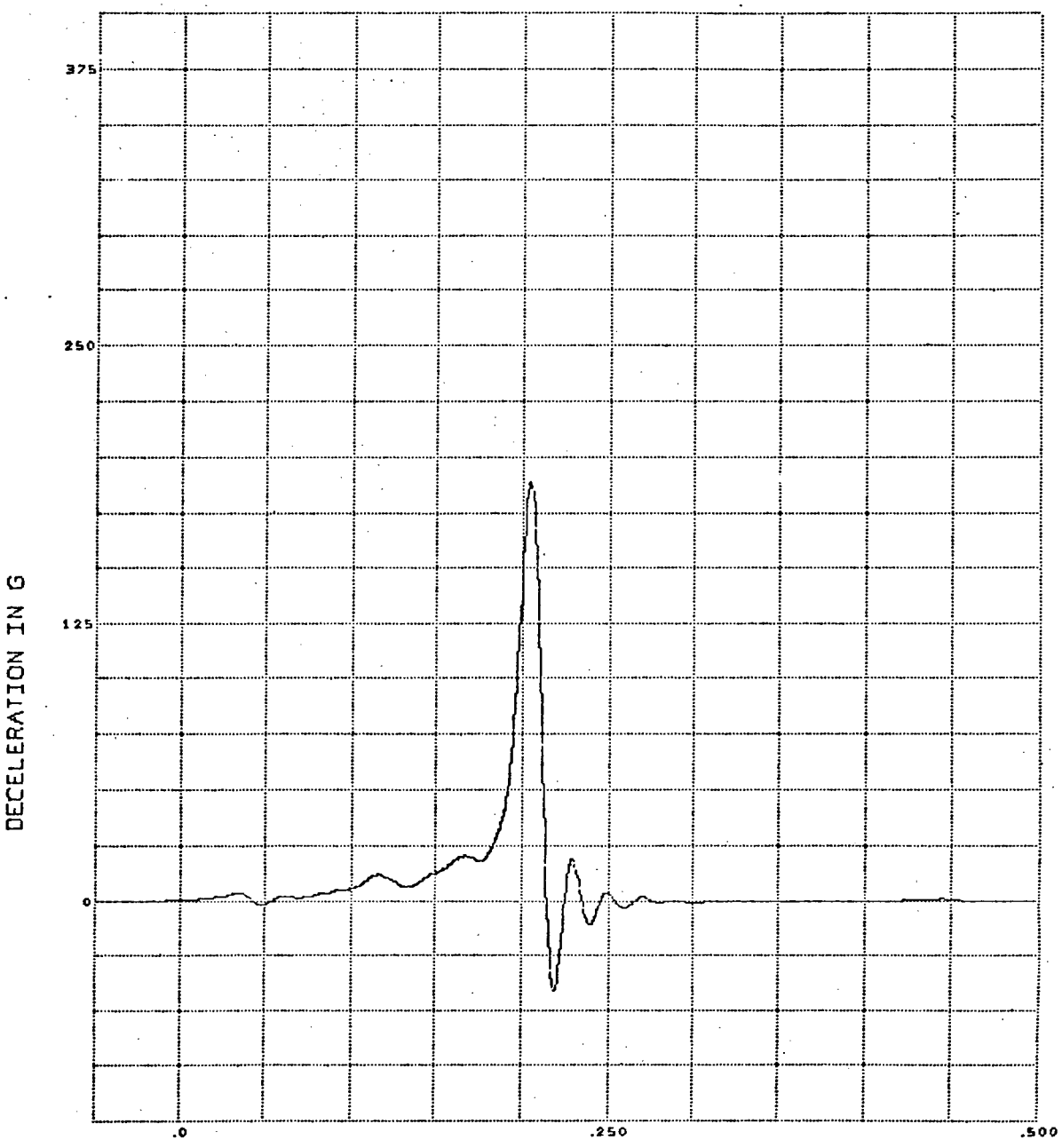

R422259 TRUCK AND SPENT NUCLEAR FUEL SHIPPING CASK (84 MPH)
CASK ACCEL BACK LEFT 800 HZ LPF

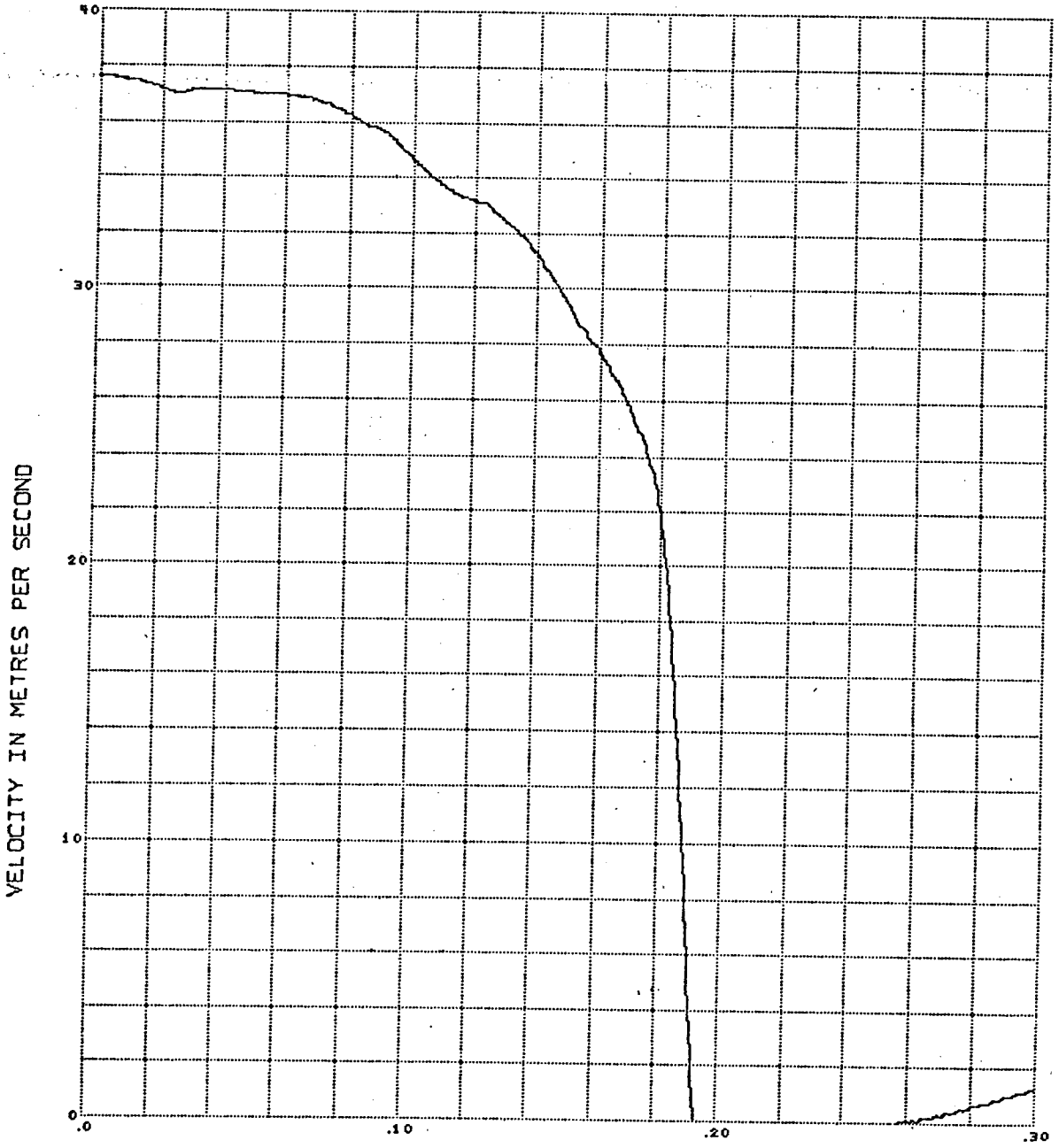

R422259 TRUCK AND SPENT NUCLEAR FUEL SHIPPING CASK (84 MPH)
CASK ACCEL BACK LEFT 800 HZ LPF

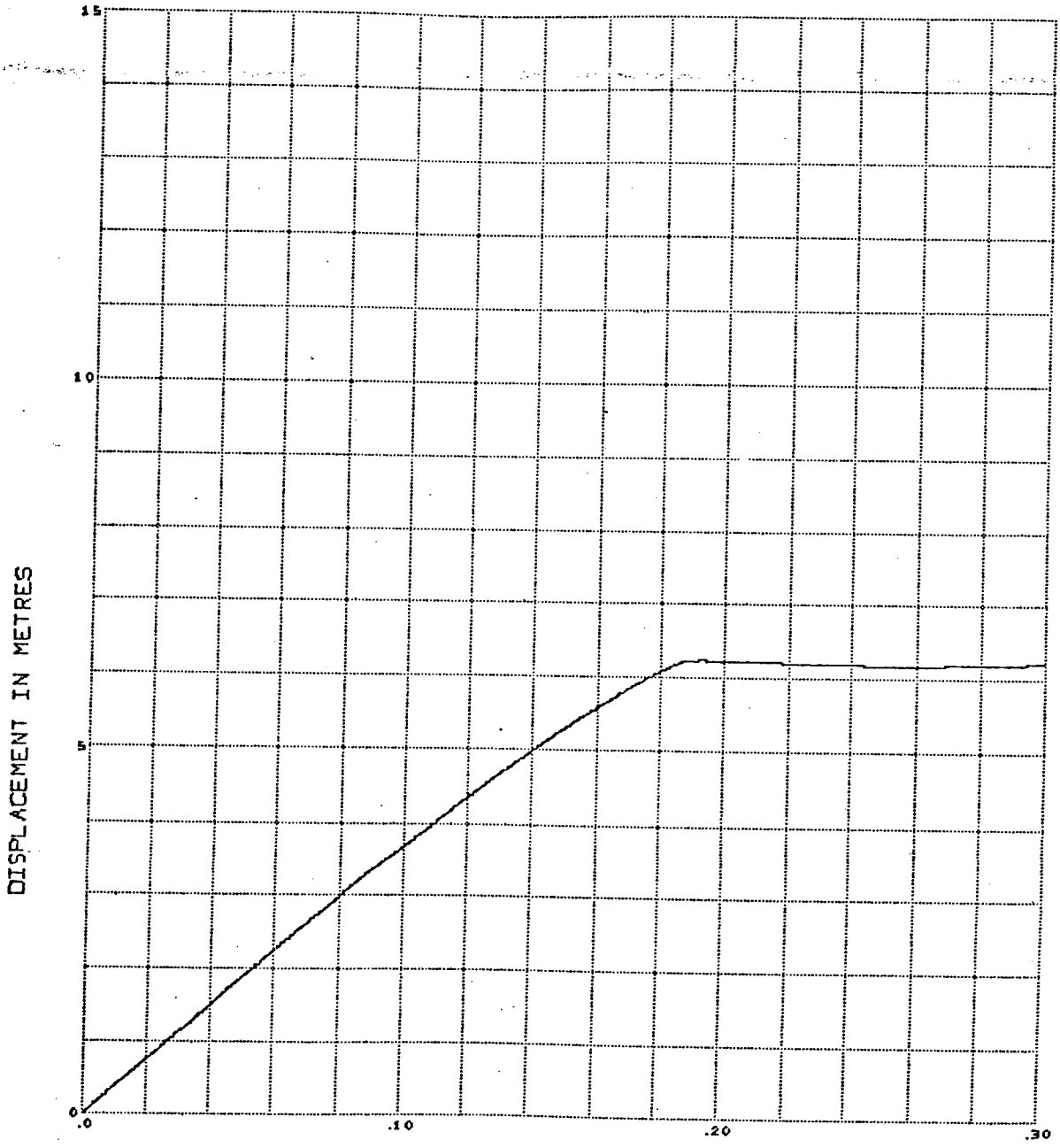

R422259 TRUCK AND SPENT NUCLEAR FUEL SHIPPING CASK (84 MPH)
STRAIN 6 RIGHT FRONT CASK 45 DEGREES AFT
(EXCEEDED RANGE OF GAGE)

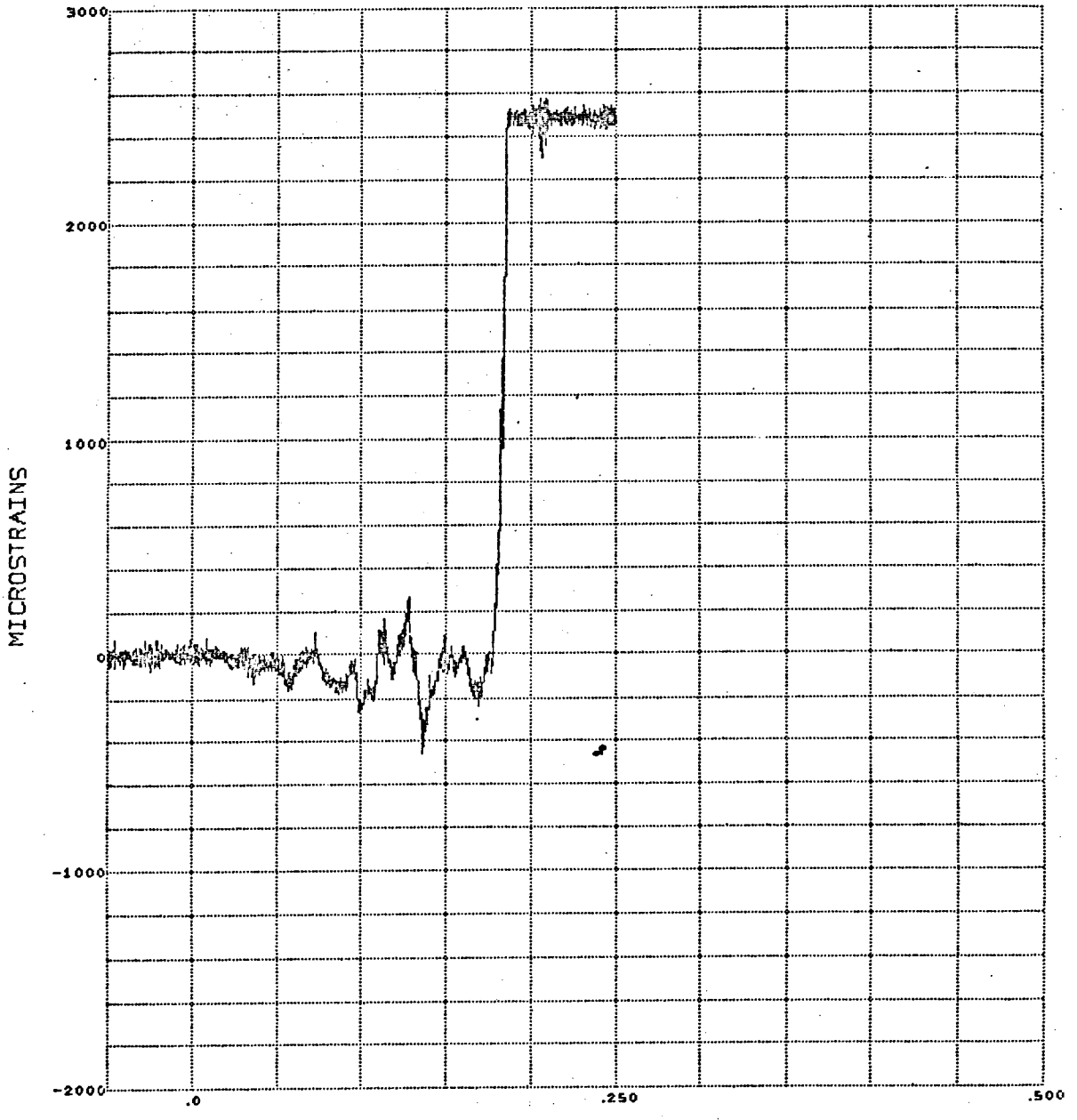

R422259 TRUCK AND SPENT NUCLEAR FUEL SHIPPING CASK (84 MPH)
STRAIN 5 RIGHT FRONT CASK 0 DEGREES
(EXCEEDED RANGE OF GAGE)

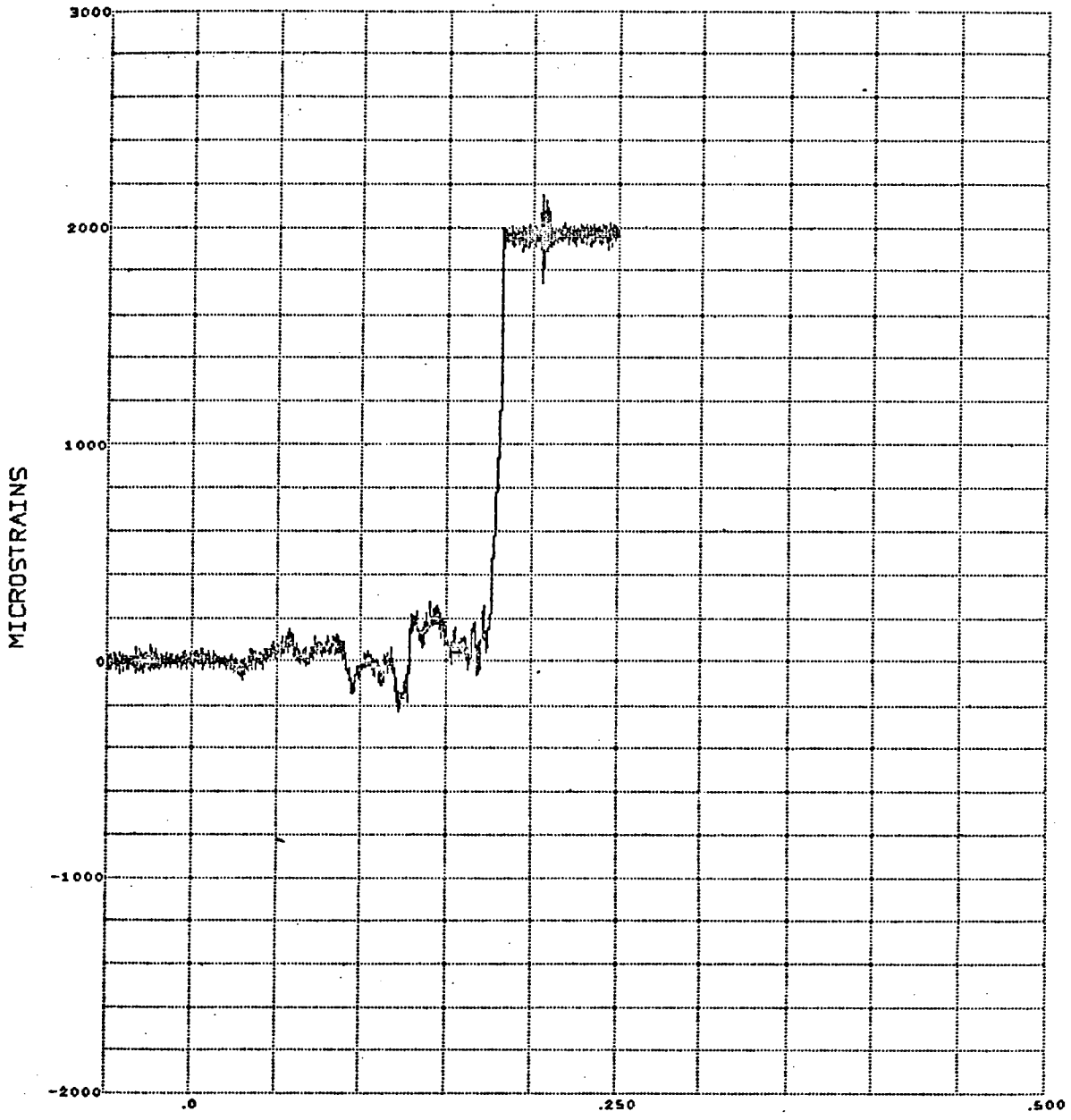

R422259 TRUCK AND SPENT NUCLEAR FUEL SHIPPING CASK (84 MPH)
STRAIN 4 RIGHT FRONT CASK 45 DEGREES FRONT
(EXCEEDED RANGE OF GAGE)

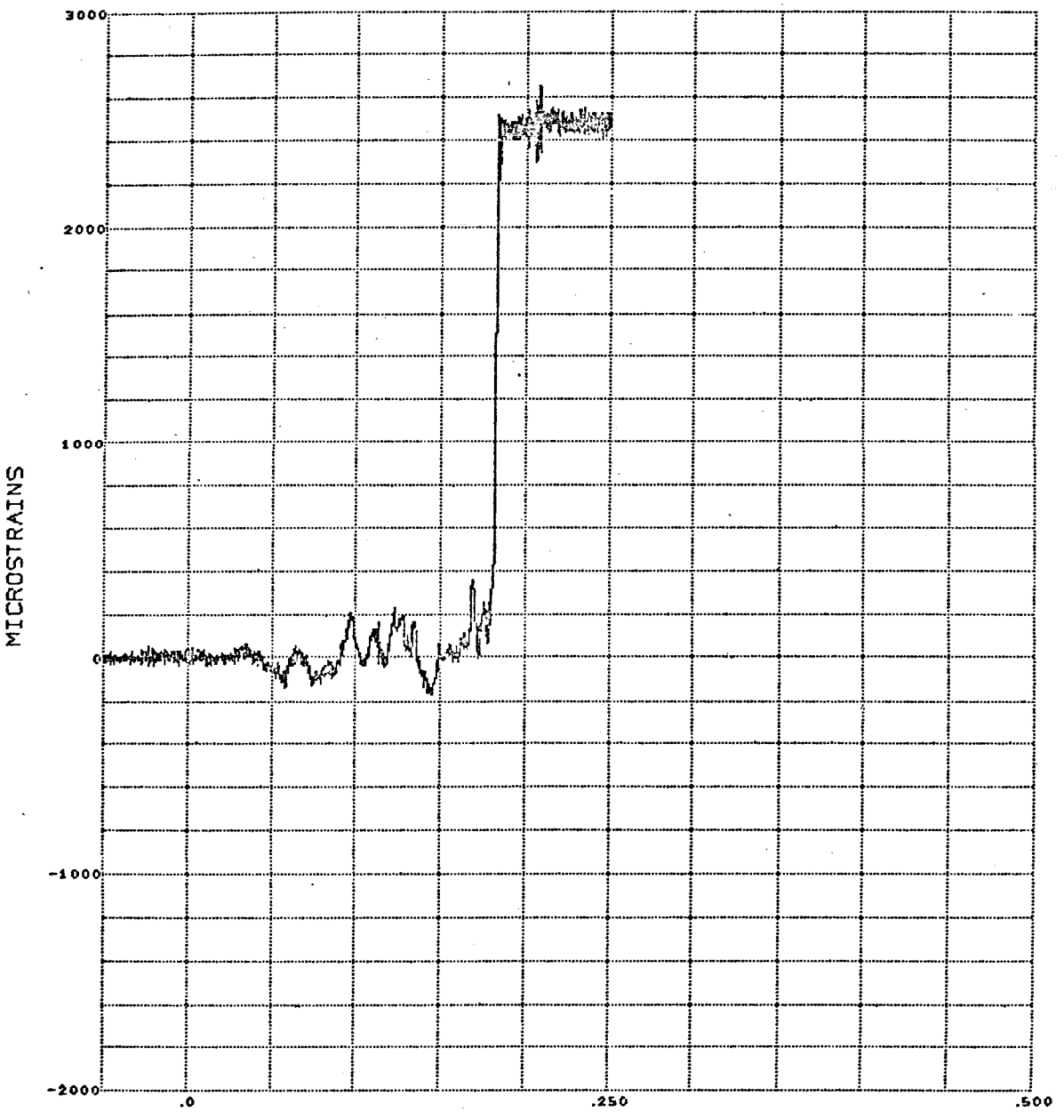

Distribution:

Environmental Control Technology (2)
U. S. Department of Energy
Washington, D.C. 20545
Attn: W. A. Brobst
J. A. Sisler

Battelle Columbus Laboratories (2)
505 King Avenue
Columbus, OH 43201
Attn: E. C. Lusk

Oak Ridge National Laboratory (2)
P. O. Box X
Oak Ridge, TN 37830
Attn: J. H. Evans
L. B. Shappert

R. W. Peterson
Allied - General Nuclear Services
P. O. Box 847
Barnwell, SC 29812

General Electric Co.
175 Curtner Avenue
San Jose, CA 95125
Attn: R. H. Jones

J. L. Ridihalgh
Ridihalgh & Associates
2112 Iuka Avenue
Columbus, OH 43201

R. E. Best
Nuclear Assurance Corporation
24 Executive Park West
Atlanta, GA 30329

M. J. Clemens
Engineering Mechanics
General Motors Research Laboratories
Warren, MI 48090

Professor Emit Witmer
Aeroelastic and Structures Research Lab
Massachusetts Institute of Technology
Cambridge, MA 02139

Professor O. Buyukozturk
Civil Engineering Department
Massachusetts Institute of Technology
Cambridge, MA 02139

Professor D. T. Tang
Civil Engineering Department
State University of New York at Buffalo
Buffalo, NY 14214

C. Fry
TVA
Division of Purchasing
630 Commerce Union Bank Building
Chattanooga, TN 37401

Battelle Pacific Northwest Laboratories (2)
Battelle Boulevard
Richmond, WA 99352
Attn: H. K. Elders
B. Andrews

L. Macklin
Transnuclear, Inc.
One North Broadway
White Plains, NY 10601

F. Janucik
Knoles Atomic Power Laboratory
Box 1072
Schenectady, NY 12309

Professor T. A. Duffey
Mechanical Engineering Department
University of New Mexico
Albuquerque, NM 87131

1200 L. D. Smith
1280 T. B. Lane
1281 S. W. Key
1281 Z. E. Beisinger
1282 T. G. Priddy
1282 W. F. Hartman
1282 J. T. Foley
1284 R. T. Othmer
1284 L. T. Wilson
1336 J. K. Cole
3135 W. W. Gravning
5400 A. W. Snyder
5430 R. M. Jefferson
5433 R. B. Pope
5433 H. R. Yoshimura (10)
5433 D. R. Stenberg
8120 W. E. Alzheimer
8122 C. S. Hoyle
9335 D. C. Bickle
9335 R. L. Lucas
9412 T. L. Leighley
9422 J. E. C. De Baca
9483 W. V. Hereford
9483 M. E. Barnett
9573 G. M. Haines
9573 C. C. Bates
9652 J. Puhara
1282 M. Huerta
3141 C. A. Pepmueller (Actg) (5)
3151 W. L. Garner (3)
For DOE/TIC (Unlimited Release)
DOE/TIC (25)
R. P. Campbell, 3171-1